獸醫學博士 學位論文

Analysis of host gene expression profiles for identification of diagnostic biomarker in subclinical infection with *Mycobacterium avium* subspecies *paratuberculosis* in cattle

Mycobacterium avium subspecies *paratuberculosis*에 의한 소의 준임상형 감염 단계에서의 숙주 유전자 발현 분석을 통한 진단용 생물학적 표지자의 규명

2018 年 8 月

서울대학교 대학원

수의학과 수의병인생물학및예방수의학 전공

박 현 의

Analysis of host gene expression profiles for identification of diagnostic biomarker in subclinical infection with *Mycobacterium avium* subspecies *paratuberculosis* in cattle

A Dissertation
Submitted to the Graduate School in Partial Fulfillment of the Requirements for the Degree of Doctor of Philosophy

To the Faculty of College of Veterinary Medicine
Department of Veterinary Medicine
The Graduate School
Seoul National University

By

Hyun Eui Park

2018

Abstract

Analysis of host gene expression profiles for identification of diagnostic biomarker in subclinical infection with *Mycobacterium avium* subspecies *paratuberculosis* in cattle

Hyun Eui Park

(Supervisor: Han Sang Yoo, D.V.M., Ph.D)

Department of Veterinary Medicine
The Graduate School
Seoul National University

Johne's disease (JD) is the chronic wasting disease of the ruminants caused by *Mycobacterium avium* subsp. *paratuberculosis* (MAP) which cause major economic losses for dairy industry worldwide. JD is mainly distributed by fecal-oral route through contaminated materials such as feed, water, and milk with MAP. During the early stage of infection, infected cattle do not show clinical symptoms however, they shed low numbers of MAP into environment and MAP can be circulated in the herd and infect other cattle. Therefore, it is very important to detect infected cattle at early stage for successful eradication of the disease. However, current diagnostic methods, including fecal culture, fecal PCR, and ELISA are insufficient for diagnosis of subclinical stages of disease. Therefore, alternative diagnostic methods which enable

to detect subclinical cattle have been requested.

First, we described the gene expression profiles of MAP-infected cattle which were classified by the results of ELISA and fecal PCR. Six genes (*LTF, HGF, HP, CXCR3*, *GBP6*, and *TFRC*) were significantly up-regulated in subclinical cattle. These genes should be further evaluated to determine their suitability for diagnosis of subclinical infection of MAP. Various factors including infection dose, infected age, animal species, and coexistence of other disease might affect the accuracy of these prognostic biomarkers. Accordingly, field studies need to be conducted to determine the adequacy of these prognostic biomarkers for use as a diagnostic tool of subclinical stage of JD.

Second, we demonstrated that manipulation of host responses for the survival of MAP that occurs during the subclinical phases of JD in cattle. Downregulation of *IL-17A, IL-17F, IL-22, IL-26, HMGB1*, and *IRF4* and upregulation of *PIP5K1C* indicate suppression of the Th1 response due to MAP infection and loss of granuloma integrity. In addition, increased expression of *IRF5* and *IRF7* suggest activation of IFN-α/β signaling during subclinical stages, which induced indoleamine 2,3-dioxygenase mediated depletion of tryptophan metabolism. Increased expression of *CORO1A* indicate modulation of calcium signaling, which enhanced the survival of MAP. Taken together, distinct host gene expression induced by MAP infection indicates enhanced survival of MAP during subclinical stages.

Third, we describes the response of eight host biomarkers (*HP, TIMP1, MMP9, SERPINE1, TFRC, S100A8, DEFB1*, and *DEFB10*) significantly discriminated

MAP-infected and non-infected cattle. Moreover, these eight biomarkers showed good accuracy (AUC $\geq$ 0.7) for diagnosis of subclinical animals. Additionally, four genes (*TIMP1, S100A8, DEFB1*, and *DEFB10*) showed sensitivity over 80% and specificity over 90%. Taken together, a real-time PCR method was developed based on eight biomarkers that can be used as a new diagnostic tool for JD with good diagnostic performance.

In conclusion, these results demonstrate the possibility of diagnosing subclinical cases of paratuberculosis using biomarker-based diagnostic techniques and expected to contribute to the development of biomarker based diagnostic methods to replace the currently used diagnostic methods.

Keywords: *Mycobacterium avium* subsp. *paratuberculosis*, biomarker, subclinical stage, diagnosis

Student Number : 2013-21548

Contents

List of figures

List of tables

List of abbreviations

ANOVA	Analysis of variance
CCL4	C-C motif chemokine 4
CCL5	C-C motif chemokine 5
CD	Cluster of differentiation
CFU	Colony forming unit
CHI3L1	Chitinase-3-like protein 1
CORO1A	Coronin 1A
CXCL9	C-X-C motif chemokine 9
CXCL10	C-X-C motif chemokine 9
CXCR3	C-X-C chemokine receptor type 3
CSF	Cerebral spinal fluid
DMEM	Dulbecco’s modified eagle’s medium
ELANE	Neutrophil elastase
ELISA	Enzyme-linked immunosorbent assay
FAP	Fibronectin attached protein
GBP6	Guanylate-binding protein 6
HGF	Hepatocyte growth factor
HMGB1	High mobility group box 1
HP	Haptoglobin

IDO	Indoleamine 2,3-dioxygenase
IFN- γ	Interferon-gamma
IL-10	Interleukin 10
IL-17A	Interleukin 17A
IL-17F	Interleukin 17F
IL-22	Interleukin 22
IL-26	Interleukin 26
IRF3	Interferon regulatory factor 3
IRF4	Interferon regulatory factor 4
IRF5	Interferon regulatory factor 5
IRF7	Interferon regulatory factor 7
IS900	Insertion sequence 900
JD	Johne's disease
KLRB1	Killer cell lectin-like receptor subfamily B member 1
KLRC1	Killer cell lectin-like receptor subfamily C, member 1
LTF	Lactotransferrin
MAP	*Mycobacterium avium* subsp. *paratuberculosis*
M-cell	Microfold cell
MDM	Monocyte-derived macrophages
MMP9	Matrix metalloproteinase-9
MPO	Myeloperoxidase

NAHMS	National Animal Health Monitoring System
PCR	Polymerase chain reaction
PBMC	Peripheral blood mononuclear cells
PIGR	Polymeric immunoglobulin receptor
PIP5K1C	Phosphatidylinositol 4-phosphate 5-kinase type-1 gamma
ROC	Receiver operating characteristic
S100A8	Protein S100-A8
S100A9	Protein S100-A9
SERPINE1	Serine protease inhibitor 1
SD	Standard deviation
SPSS	Statistical Package for Social Sciences software
TACO	Tryptophan-aspartate containing coat protein
TFRC	Transferrin receptor
TNF- α	Tumor necrosis factor-α
TLR	Toll-like receptor
TRAIL	Tumor necrosis factor related apoptosis-inducing ligand

General introduction

Mycobacterium avium subsp. *paratuberculosis* (MAP) is a causative agent of bovine paratuberculosis which known as a chronic intestinal inflammatory disease of ruminants worldwide, inducing significant economic losses in the dairy industry (Garcia and Shalloo, 2015; Ott *et al.,* 1999; Wolf *et al.,* 2014). Bovine paratuberculosis is mainly transmitted by fecal-oral route with fecal-contaminated materials such as feed, water, and soil (Stabel, 1998; Whitlock and Buergelt, 1996). Paratuberculosis is characterized with long subclinical stages which have no clinical signs, but excrete MAP into the environment through feces (Arsenault *et al.,* 2014; Koets *et al.,* 2015). Progression of paratuberculosis divided into 4 stages based on immunological status and severity of clinical signs (Tiwari *et al.,* 2006; Whitlock and Buergelt, 1996). In the early stage of infection, there is no clinical symptom for a long time and the condition that does not shed the bacteria through feces persists and is called 'silent stage' (Tiwari *et al.,* 2006; Whitlock and Buergelt, 1996). Since the disease progresses, it still does not show clinical symptoms, but it progresses to intermittent excretion of MAP through the feces, which is called 'subclinical stage' (Tiwari *et al.,* 2006; Whitlock and Buergelt, 1996). After that, the clinical stage begins with initial clinical symptoms such as progressive weight loss with normal appetite (Tiwari *et al.,* 2006; Whitlock and Buergelt, 1996). With the progression of the disease, weight loss is getting worse and the feces gradually turns into diarrhea.

Diarrhea is intermittent at first, but gradually becomes constant, and a large amount of MAP is released through the feces. In an advanced clinical stage, animals become weak, lethargic, cachetic, and eventually dead (Tiwari *et al.,* 2006; Whitlock and Buergelt, 1996). Currently, the diagnosis of paratuberculosis is based on clinical symptoms, histopathological examination, bacterial culture, interferon-gamma (IFN-γ) assay, and the PCR to detect the *IS900* and *ISMAP02* gene from feces (Britton *et al.,* 2016). However, current diagnostic methods have a disadvantage that it is difficult to detect MAP-infected animals during the subclinical stage. Therefore, development of a new diagnostic method capable of detecting subclinically infected animals is required.

The biomarker is the material that measurable in the biological fluid such including nucleic acids (DNA, mRNA, microRNA, and small non-coding RNA), metabolites, and protein which reflect the physiological change of healthy or diseased individual (Strimbu and Tavel, 2010). Because biomarkers appear differently depending on the occurrence and progress of the specific diseases, it can be used for indicator substance in blood or body fluids that allows measurement of physiological change during the progress of the disease (Mayeux, 2004). Therefore, biomarkers have been used for various purposes such as early diagnosis of disease, evaluation of prognosis, and prediction of response to therapy (Chen *et al.,* 2008). Especially, biomarkers considered as a non-invasive diagnostic tool for diverse diseases such as cancers, autoimmune diseases, and infectious diseases (Chen *et al.,* 2008; Doecke *et al.,* 2012; Keane *et al.,* 2018; Stanescu *et al.,* 2018; Unver and McAllister, 2018; Yan *et al.,*

2018).

The purpose of this study was to analyze host gene expression in whole blood of MAP-infected cattle during the subclinical stage to identify the diagnostic biomarker for paratuberculosis. This is organized into three chapters. The gene expression profiles of selected host biomarkers which have diagnostic potential were investigated in chapter I. Gene expression profiles of immune-regulatory genes which can enhance survival of MAP during subclinical stage was analyzed in chapter II. In chapter III, a real-time PCR method based on eight biomarkers was described that can be used as a new diagnostic tool for bovine paratuberculosis with good diagnostic performance.

Literature Review

Paratuberculosis

Bovine paratuberculosis is a chronic, wasting disease of wild and domestic ruminants caused by *Mycobacterium avium* subsp. *paratuberculosis*. Paratubercuolsis is characterized with a very long incubation period (Whitlock and Buergelt, 1996). In general, young calves within 4 months of age are most susceptible to infection, but clinical symptoms usually appear 2-4 years after infection. Due to the long incubation period, most of the infected animals maintain subclinical state which shows no apparent clinical symptoms but excretes MAP into the environment through feces (Whitlock and Buergelt, 1996). Transmission of the disease mainly occurs in the neonatal period by oral ingestion of MAP through the teat contaminated with feces (Whitlock and Buergelt, 1996). Also, contaminated feed, water, and soil can also be a source of transmission. Moreover, vertical transmission can occur through various ways such as placental infection in infected dams, mating with infected bulls (Adaska and Whitlock, 2012; Mercier *et al.*, 2016; Nielsen *et al.*, 2016; Thompson *et al.*, 2007). In the initial stage of infection, infected animals do not show clinical symptoms and do not shed MAP through the feces (Koets *et al.*, 2015). After that, as the disease progresses, infected animals begin to excrete MAP through the feces, but most animals do not show any clinical symptoms

(Whitlock and Buergelt, 1996). At the beginning of the clinical stage, progressive weight loss and normal or increased appetite can be seen in infected animals (Whitlock and Buergelt, 1996). The clinical symptoms that are mainly observed are diarrhea, which is intermittent at first but gradually becomes constant. In clinical stage, animals excrete a large amount of MAP through the feces and show strong antibody response (Whitlock and Buergelt, 1996). Subsequent diarrhea leads to hypoproteinemia and dehydration. Infected animals become very weak and sometimes unable to stand, finally, cachexia and dehydration lead to the death of debilitated cattle (Whitlock and Buergelt, 1996).

Paratuberculosis causes huge economic loss to dairy industry by decreasing milk production, decreasing growth rate and culling of infected animals (Bates *et al.,* 2018; Garcia and Shalloo, 2015). In the USA, approximately 68% of dairy herds are positive for paratuberculosis, and less than 10% of beef cattle herds are infected (Carter, 2012). According to the National Animal Health Monitoring System in the United States, economic losses from infected herds are estimated at $ 40 per year per infected cattle, with an overall estimated loss of $ 200 to $ 250 per year (Garcia and Shalloo, 2015).

1. Etiologic agent

Mycobacterium avium subsp. *paratuberculosis* is a small, gram-positive, acid-fast, rod that is facultative intracellular bacterium (Salem *et al.,* 2013). The primary host

of MAP is the ruminant such as cattle, goat, sheep, and deer (Stabel, 1998). However, non-ruminant animals can also be affected and act as a source of infection to herd (Florou *et al.,* 2008; Münster *et al.,* 2013). MAP contains a lipid component called mycolic acid in the cell wall, which is resistant to low pH, high temperature, drying and various chemical compounds (Minnikin *et al.,* 1984). Because of these properties, MAP can survive for many years in the environment such as water and soil (Raizman *et al.,* 2011; Rhodes *et al.,* 2013). MAP is considered to be an important pathogen in public health because it can survive during the pasteurization of milk due to heat resistance (Donaghy *et al.,* 2007; Stabel, 2008). Recently, MAP has been isolated from patients with Crohn's disease, an immune-mediated inflammatory bowel disease, and it has been argued that MAP is involved in the pathogenesis of Crohn's disease (Bull *et al.,* 2003; Feller *et al.,* 2007; Timms *et al.,* 2016).

2. Epidemiology

Mycobacterium avium subsp. *paratuberculosis* classified into three groups based on genetic polymorphism of *IS900* and *IS1311* genes, characteristics of growth, and host species (Sevilla *et al.,* 2005). Sheep types are mostly isolated from sheep and goats, whereas cattle types are isolated from relatively broad host species including domestic and wild ruminants, non-ruminants, and humans (Singh *et al.,* 2009). The Bison type also has been reported to be isolated from livestock, wild ruminants, and

humans (Kaur *et al.,* 2011; Sonawane *et al.,* 2016). Recent studies have shown that the bison type is widely distributed in India and has also been isolated in Korea and Uganda (Kim *et al.,* 2013; Okuni *et al.,* 2012; Singh *et al.,* 2009). Despite a lot of preventive measures, paratuberculosis occurs globally in North America, South America, Europe, Asia and Australia (Stabel, 1998). A national level of the test was conducted for detection of paratuberculosis by the National Animal Health Monitoring System (NAHMS) of USA in 1996. As a result, 21.6% of the cattle were confirmed as positive (Lombard, 2011). In 2007, 68.1% of the dairy herds were positive for paratuberculosis with the environment fecal sample (Lombard *et al.,* 2013). Also, 95% of the dairy herd which breeds more than 500 cattle were positive for paratuberculosis (Carter, 2012). In the case of the beef cattle herd, nationwide surveys were conducted by NAHMS of the the USA in 1997. In all 21 provinces, 10,372 beef cattle in 380 herds were selected for the survey, and only 0.4% of the beef cattle and 7.9% of the herd were positive (Dargatz *et al.,* 2001). Between 2003 and 2010, more than 3,100,000 dairy cattle and over 692,000 beef cattle were tested for paratuberculosis by serum ELISA. As a result, 5 to 6.6% of dairy cattle and 2.1 to 3.6% of beef cattle were positive (Carter, 2012). Between 2003 and 2010, approximately 514,000 dairy cattle and 67,000 beef cattle were tested for fecal PCR and culture tests. The results showed that 7.2 to 14.1% of dairy cattle and 2.8 to 16.9% of beef cattle were positive (Carter, 2012). Also, ELISA test for 4,990 cattle in 158 dairy herds in Wisconsin showed that 50% of the herd and 7.29% of dairy cattle were positive (Collins *et al.,* 1994). In the European countries, the prevalence of

paratuberculosis was examined by ELISA. Prevalence of paratuberculosis was 14.7 to 24.1% in Germany, 19.0% in Austria, 7.7% in Norway, 2.4 to 6.8% in Italy suggesting that there is an endemic state of paratubercuosis in Europe, except Sweden (Nielsen and Toft, 2009). In Switzerland, 19.8% of dairy cattle were positive for fecal PCR and 5% of dairy cattle were positive by PCR with milk sample in Turkey (Corti and Stephan, 2002; Ozturk *et al.*, 2010). In Japan, paratuberculosis was first confirmed in cattle which imported from the United States in 1959 (Momotani, 2012). However, until the 1980s, the outbreak of paratuberculosis was limited in imported animals, but since the 1980s, paratuberculosis occurred in Hokkaido, Tohoku, and Kanto regions and begin to spread entire Japan (Momotani, 2012). In the South Korea, prevalence of paratuberculosis was 0.96% in 1968, 6.7% in 1994 and 6.7% to 7.1% in 2003 (Kim *et al.*, 1994; Pak *et al.*, 2003). In 2009, 13.8% of herds and 3.3% of cattle were infected with MAP in the Gyeongnam area (Lee and Jung, 2009). Especially, the prevalence of paratuberculosis in black goats is estimated to be 4.6 to 15.3% according to animal level and 18.2 to 38.2% according to herd level (Lee *et al.*, 2006).

Taken together, paratuberculosis is occurring in many countries around the world especially in nations where dairy industries have developed, and the number of infected animals and herds is steadily increasing.

3. Transmission

The transmission of paratuberculosis is mostly occurring through the fecal-oral route, and it is also possible to be spread with other pathways (Whitlock and Buergelt, 1996). Infected cattle release MAP through the feces during disease progression, which causes contamination of solid feed, water, grass and soil (Rhodes *et al.*, 2013). MAP can survive for more than a year in the pasture and survive for longer periods of time in water which induces circulation of disease within the herd (Sweeney, 1996). The susceptibility to infections is the highest in young calves and the susceptibility to infection decreases with increases with age (Mortier *et al.*, 2015). Although the relationship between the age of calves and susceptibility to infection has not been fully elucidated, several hypotheses have been suggested by various studies. In newborn calves, intestinal permeability is increased to accept large-sized substances such as antibodies in colostrum. Therefore, the calf is vulnerable to infection because MAP can easily entry the mucosa (Sweeney, 2011). High susceptibility in calf stage is can be related to the immunological changes that occur during the process of growing from calf to adult cattle. In the newborn period, innate and acquired immune mechanisms are not enough to protect the host from pathogens (Chase *et al.*, 2008). With the growth of newborn calves, activation of innate and acquired immune mechanisms occurs and subsequently induces increase the resistance to disease (Chase *et al.*, 2008). Due to the high susceptibility of calf stage, most of the infections occur when the calves are exposed to fecally contaminated

environment (Whitlock and Buergelt, 1996). It is also possible that direct intrauterine infection through the infected dam. For example, MAP was isolated in the uterine flush fluid of infected cattle which show clinical signs (Rohde and Shulaw, 1990). In addition, MAP can adhere to bovine ova was cultured in MAP-containing media (Rohde *et al.,* 1990). Therefore, it is highly probable that infected calves born from the infected dam are infected. Also, semen of infected bulls can be the source of infection. In detail, MAP was detected in the semen, testes, epididymides and seminal vesicles of MAP-infected bulls including cattle with no clinical symptoms (Ayele *et al.,* 2004).

4. Infection and Disease

Primary infection site of *Mycobacterium avium* subsp. *paratuberculosis* is the ileum and ileocecal valve (Sigurethardóttir *et al.,* 2004). Transmission of the disease mainly occurs by fecal-oral route with contaminated materials such as feed, water, and teat (Sweeney, 1996). Paratuberculosis is characterized by weight loss and persistent diarrhea in the terminal stage of infection. In silent or subclinical stage, cattle may healthy for several months or years (Tiwari *et al.,* 2006). In clinical stage, diarrhea may be constant or intermittent. With the progression of disease becomes more severe, show some of the following clinical signs: weight loss, normal or increased appetites, hypoproteinemia, intermandibular edema, chronic diarrhea and cachexia (Tiwari *et al.,* 2006; Whitlock and Buergelt, 1996).

In general, intestinal lesions develop with severity and progression of the disease. Lesions are characterized by corrugated intestine walls, enlarged mesenteric lymph nodes, and formation of granulomas (Plattner *et al.*, 2009; Tiwari *et al.*, 2006; Whitlock and Buergelt, 1996). Sometimes, there is no correlate on between clinical symptoms and the severity of the lesion and mild intestinal lesions characterized by infiltration with a large number of lymphocytes, few macrophages, and no epithelioid macrophages in the submucosa (Sweeney, 2011). On the other hand, severe intestinal lesions consist of diffuse granulomatous lesions which contain epithelioid macrophages and giant cells in the mucosa and submucosa of the intestine (Sweeney, 2011). Infection of MAP induces the immunological change of host animal with the progression of the disease. In experimentally infected calves, proliferative response to MAP was observed in 6 months after infection (Koo *et al.*, 2004). In detail, CD4+ memory T cell expressing CD25 and CD26 were predominant and CD8+ T cells proliferated due to MAP infection until 18 months after infection. Also, γδ T cells did not proliferate until 18 months after infection. However, after 18 months, γδ T cells which express CD25, ACT2, and CD26 were proliferated presence of the MAP antigens (Koo *et al.*, 2004).

5. Pathogenesis

Macrophages and M cells are important in the pathogenesis and/or defense system of the gut against *Mycobacterium avium* subsp. *paratuberculosis* (Coussens, 2004).

Researches on the pathogenesis of paratuberculosis have been conducted through various in vivo and in vitro methods. In the beginning, many researchers started to study the invasion path of the MAP and classified the invasion path of the MAP into two categories based on infection dose (Buergelt *et al.,* 1978; Gilmour and Gardiner, 1968; Sweeney *et al.,* 2006). The identified invasion paths are as follows (Figure 1). When a large number of MAP enter the lymph node after infiltration through the tonsil and spread to the mesenteric lymph nodes and ileum through the blood vessels or the lymphatic vessels (Buergelt *et al.,* 1978; Payne and Rankin, 1961). On the other hand, when a small amount of MAP invades, the microorganism invades through the intestinal mucosa of the ileum (Sweeney *et al.,* 2006). When MAP is ingested and enters the ileum of the intestine, MAP is phagocytized by M cells and transported into the submucosal tissue where they survived and proliferated in macrophages after being phagocytosed (Arsenault *et al.,* 2014; Koets *et al.,* 2015). MAP can survive within macrophages after phagocytosed by manipulation of the host immune response in various ways (Arsenault *et al.,* 2014). One of the surviving strategies is the inhibition of phagolysosomal maturation, which involved in the destruction of internalized pathogens (Arsenault *et al.,* 2014). As shown in Figure 2, MAP can block responsiveness of macrophage through inhibition of toll-like receptor signaling and IFN-γ signaling which plays a central role in immune response to intracellular pathogens (Coussens *et al.,* 2004). Previous studies using infection models for identification of invasion route have been conducted. Stabel *et al.,* analyzed pathologic changes and fecal shedding of MAP when oral and

intraperitoneal infections occurred in newborn calves (Stabel *et al.,* 2009). When oral infection occurs, colonization of MAP in intestinal tissues and associated lymph nodes is well established compared to intraperitoneal infection (Stabel *et al.,* 2009). Primary colonization sites of MAP are the ileal and jejunal region of the small intestine and nearby lymphoid tissues (Sigurethardóttir *et al.,* 2004). After ingestion of MAP through the fecal-oral route, it penetrates through the tonsil mucosa and then spreads through the bloodstream to the mesenteric lymph nodes and the ileum (Payne and Rankin, 1961; Sweeney *et al.,* 2006). However, it is known that when a relatively small amount of oral infection occurs, it penetrates primarily into the mucosa of the ileum and spreads to adjacent lymph nodes (Sweeney *et al.,* 2006). MAP-specific T cell proliferative responses were also observed in the gut surgical loop-infected model, confirming the increase of CD8+ and γδ-T cells in the lamina propria of infected areas and significant increase of TNF-α and IFN-γ was confirmed (Charavaryamath *et al.,* 2013). Penetration of MAP in tonsil and the ileum occurs via microfold (M) cells of Peyer's patch (Bermudez *et al.,* 2010; Momotani *et al.,* 1988). As shown in Figure 1, activation of bacterial cell wall protein fibronectin attachment protein (FAP) occurs during the passing of the digestive tract of ruminants (Bannantine and Bermudez, 2013). This promotes opsonization by fibronectin and penetrates into the cell by the fibronectin receptor abundant on the surface of M cell. The penetration of MAP into M cells occurs very rapidly within 30 minutes of contact, and the MAP is then transferred to the submucosal layer (Lamont *et al.,* 2012). In the submucosal layer, MAP is phagocytosed by the

macrophage and spread to nearby tissues and lymph nodes. Effective host defense against bacterial infections in the intestine depends on rapid clearance of bacteria from the intestinal tract. After infiltrating the intestinal mucosa, MAP phagocytosed by macrophages express several receptors (complement receptors (CR1, CR3, and CR4), immunoglobulin receptors (FcR), mannose receptors and scavenger receptors) which involved in the elimination of mycobacterial pathogens (Guirado *et al.*, 2013). In particular, MAP invades to macrophages via complement receptors which induce inhibition of the activation of macrophages, thereby enhancing survival in macrophages by avoiding host immune response (Premanandan *et al.*, 2009).

After the MAP enters the phagosome of the macrophage, the phagosome changes to a late endosome and binds to the lysosome for destroying of internalized pathogens (Koul *et al.*, 2004). Thus, survival of internalized pathogen depends on its ability to inhibit the formation of mature phagolysosomes. As shown in Figure 2, MAP can survive inside the macrophage through inhibition of acidification and phagolysosome fusion inside the phagosome (Cheville *et al.*, 2001). In the phagosome internalizing with MAP, the expression of transferrin receptor, which is an early phagosome marker, is increased and the expression of Lamp-1, which is a marker of the mature phagosome, is decreased (Hostetter *et al.*, 2003). Rab GTPase, another late phagosome marker, was also decreased in the only living MAP containing phagosome. Thus, the living MAP is essential for inhibition of phagosomal maturation (Keown *et al.*, 2012). Formation of the phagolysosome occurs with merging of the phagosome with the lysosome. MAP sulpholipids can

inhibit this mechanism and subsequently induce inhibition of maturation of phagolysosome (Arsenault *et al.,* 2014). Also, membrane trafficking regulation of phagolysosome is inhibited by dephosphorylation of phosphatidylinositol phosphates with MAP SapM (Arsenault *et al.,* 2014). Up-regulation of V-ATPase by MAP inhibits acidification of vacuole which subsequently induces phagolysosomal fusion (Weiss *et al.,* 2002). Also, PtpA protein binds subunit of V-ATPase of macrophage and induce exclusion of V-ATPase from phagosome which subsequently inhibits phagolysosomal fusion (Wong *et al.,* 2011). Fusion of lysosome and phagosome is induced by release of tryptophan–aspartate containing coat (TACO) from phagosome. However, as shown in Figure 2, MAP can inhibit releasing of TACO from phagosome. Also, MAP can manipulate MAPK-p38 pathway through LAM activation of TLR2 (Fratti *et al.,* 2003). Activation of TLR2 also induces up-regulation of IL-10 which suppressing the Th1 immune response (Arsenault *et al.,* 2014).

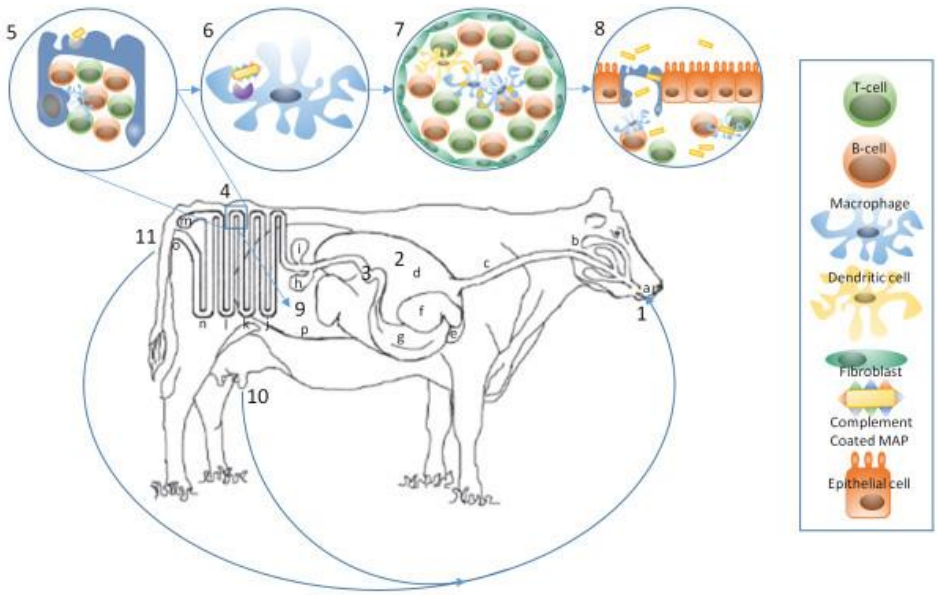

Figure 1. Invasion pathway of the orally ingested MAP**.**

After ingestion with oral route, (1) MAP pass through the GI tract. The ingested MAP also invades to the epithelium of tonsil and transferred to the ileum. Fibronectin attached protein of MAP is activated in the rumen (2) and opsonized by fibronectin during passing the lower digestive tract (3). In the ileum, M cell (4) uptake MAP and subsequently recognition of MAP with the fibronectin receptor occurs (5). Up-taken MAP moves from the epithelium to intra-epithelial macrophages, which recognize complement-coated MAP via complement receptors (6). Formation of granulomas (7) occurs with infected macrophages which internalize MAP but fail to remove. During the progression of JD (8), MAP can transfer to the unborn calf (9) and neonatal calf with milk (10) or fecal to oral route (11). (a) Mouth (b) Salivary Glands (c) Esophagus (d) Rumen (e) Reticulum (f) Omasum (g) Abomasum (h) Gallbladder (i) Pancreas (j) Duodenum (k) Jejunum (l) Ileum (m) Cecum (n) Large Intestine (o) Anus (p) Uterus (Arsenault *et al.*, 2014).

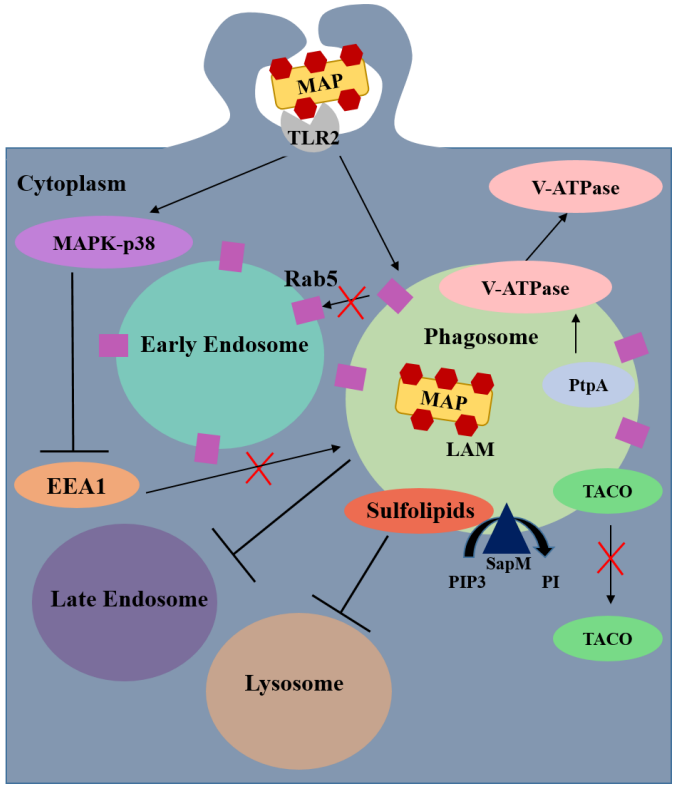

Figure 2. Inhibition of phagolysosomal maturation by MAP.

Phagolysosome formation after ingestion of MAP is inhibited in various ways. First, sulpholipids in MAP inhibit the formation of the phagolysosome by inhibiting the fusion of the phagosome with the lysosome. SapM induces dephosphorylation of phosphatidylinositol phosphates which subsequently disrupting vesicle translocation between phagosome and lysosome. V-ATPase is an important factor in phagosome-lysosome fusion. PtpA induces exclusion of V-ATPase from the phagosome and subsequently induces failure of phagolysosome fusion. MAP inhibits Rab5 and subsequently induces insufficient recruitment of early endosome. TACO is the critical factor for phagolysosome fusion. MAP can interfere with releasing of TACO thereby inhibition of phagolysosome fusion occurs. MAP can affect MAPK-p38 signaling through the activation of TLR2. Activation of TLR2 induces suppression of the various innate immune responses (adapted from Arsenault *et al.*, 2014).

6. Clinical manifestation

Paratuberculosis can be classified into four stages according to the degree of clinical symptoms, shedding level of MAP through the feces, and the degree of MAP-specific antibody in the serum (Whitlock and Buergelt, 1996).

6.1 Silent stage

In the silent infection state, it has the following characteristics; there are no clinical symptoms, and shedding of MAP through the feces is not observed. Also, there is no effective diagnostic method to detect infection. This stage can last for at least 2 to 10 years and animals in silent infections do not show any reduction in body weight or milk production. Animals in the silent stage do not have antibodies to MAP in the serum and may release MAP through the feces, but it cannot be detected by PCR. Therefore, it is very likely that the disease will be transmitted by animals in the silent stage.

6.2 Subclinical stage

In a subclinical infection, there is no clinical sign of infection yet, but the shedding of the MAP through the feces begins to be detected by PCR and may be confirmed through fecal culture. However, shedding of the MAP through the feces is mostly intermittent, and antibodies to MAP are not yet formed, so it is very difficult to make an accurate diagnosis with subclinically infected animals. Animals in the subclinical

stage are able to contaminate the environment and infect other animals in the herd because they release the MAP through the feces for a long time.

6.3 Clinical stage

Depending on the infection dose and the condition of the infected animal, initial clinical symptoms begin to appear after an incubation period of 2 to 10 years. The first clinical sign is a gradual loss of weight despite normal or increased appetite. Diarrhea starts with weight loss for about 3 to 6 months and occurs constantly or intermittently. Most of the animals in this stage have antibodies to MAP in the serum, which can be diagnosed by ELISA and the shedding of the MAP through the feces.

6.4 Advanced clinical stage

Animals entering the advanced clinical stage become more and more debilitated. Main clinical manifestations include chronic diarrhea, hypoproteinemia, and submandibular edema (bottle jaw). Animals at this stage can become dehydrated and lethargic due to chronic diarrhea. Also, infected animals excrete a large amount of MAP into the environment and have a strong MAP-specific antibody titer in the serum, but in many cases, it is often culled before this stage is reached.

7. Prevention and Control

Many countries have been developed about the programs for the prevention and control of paratuberculosis (Benedictus and Kalis, 2003; Groenendaal and Galligan, 2003; Rossiter and Burhans, 1996). Common point of control strategies for paratuberculosis is as follows; (1) regular screening for paratuberculosis in national level, (2) immediate separation between calf and dam after birth, (3) using safe colostrum obtained from cattle identified as negative for paratuberculosis to prevent vertical infection, (4) management of hygiene in the herd, especially the area of the neonatal calves. In particular, the equipment which contacts with the feces of infected animals should not be introduced to the calf area.

For successful eradication of paratuberculosis in the herd, animals should be quarantined immediately if they are suspected to be infected by fecal PCR and/or serum ELISA and should be culled after clinical symptoms such as diarrhea have developed. In addition, a diagnostic method for subclinical animals which show no clinical symptoms should be established, and these animals should be isolated from other animals. Also, when introducing a new animal from other herds, quarantine it in a separate area in the ranch for a certain period of time, and should confirm with the serum ELISA and fecal PCR that there is no infection. To prevent vertical infections, infected animals are encouraged to prohibit and cull breeding. Calves should be kept in a clean place and should always be careful not to be contaminated with feces and fluids from infected adult animals. After birth, the calf should be

isolated from the mother immediately and raised in a breeding facility separated from the other animals. Also, management of hygiene in the breeding facility is an important part for prevention of new infections. Therefore, all workers should be taken not to use contaminated clothing or equipment. In addition, colostrum and milk fed to the neonatal calf should be obtained from paratuberculosis free herd. In the herd, the number of livestock, the in and out of animals, and the results of the screening test should be recorded and stored. If there is an infected animal in the herd, the occurrence of clinical symptoms should be observed and recorded. In addition, the risk of disease transmission should be reduced by preventing contamination of feed, water, equipment, and vehicles by feces in the herd.

Many studies have been conducted and several vaccines have been tested but complete protection has not been obtained in the fields against paratuberculosis. Live vaccines which based on mutation of relA, lsr2, and pknG genes known as virulence factors of *Mycobacterim tuberculosis* and *Mycobacterium bovis* were developed using the allelic exchange technique. The ΔrelA mutant was superior to the ΔpknG mutant in attenuation of virulence and defense efficacy (Park *et al.,* 2011; Park *et al.,* 2008). Studies on subunit vaccines are also conducting. Several antigens have been evaluated as vaccine candidates such as heat shock protein 70 (Hsp70), antigen 85 complex proteins (Ag85A, Ag85B, Ag85C), lipoproteins (LprG, MAP0261c), and PPE family proteins (MAP1518, MAP3184) (Huntley *et al.,* 2005; Koets *et al.,* 1999; Shin *et al.,* 2005). Until now, the Hsp70 protein among the vaccine candidates shows highest protection effect in experimentally infected animals (Vrieling *et al.,* 2013).

8. Diagnosis

Various diagnostic methods are available for the detection of paratuberculosis, each has their own advantages and disadvantages (Britton *et al.*, 2016). Diagnostic methods classified into three categories as follows: (1) assays to detect the pathogen in the specimen such as feces, blood, tissue, and milk, (2) assays to detect cellular immune response to MAP infection, (3) assays to detect humoral response to MAP infection. Combination of different diagnostic methods can ensure high sensitivity of the test.

8.1 Assays to detect the pathogen

Assays to detect the MAP in the biological specimen including feces, blood, tissue, and milk are widely used for detection of paratuberculosis. PCR methods have the advantage for detection of subclinically infected animals which shed MAP through feces but does not have antibody to MAP (Britton *et al.*, 2016). The PCR has the advantage of being able to inspect a large number of samples in a short time. However, since PCR detects DNA of MAP, a positive result does not ensure the presence of live MAP bacteria. Also, PCR inhibitors in clinical specimens such as feces, blood, and milk can induce a false negative result. Therefore, various PCR techniques targeting MAP specific genes have been developed to improve the disadvantage of PCR assay (Bhide *et al.*, 2006; Corti and Stephan, 2002). *IS900* targeted PCR method can detect up to 10 to 100 CFU per ml in milk samples,

showing higher sensitivity than culture method. However, the specificity and sensitivity of the sample may be lowered due to the PCR-interfering substances in the sample. Recently, a triplex real-time PCR technique has been developed to increase the efficiency of diagnosis due to its high specificity and sensitivity, and it can detect up to 2.5 X 10^2 MAP per gram of feces (Irenge *et al.,* 2009). In addition, optimization of the DNA extraction method has been conducted by many researchers (Mita *et al.,* 2016; Park *et al.,* 2014a; Timms *et al.,* 2015).

8.2 Assays to detect cellular immune response to MAP infection

The representative diagnostic method based on cell-mediated immune response is the IFN-γ assay (Jungersen *et al.,* 2012; Kalis *et al.,* 2003). IFN-γ is an important mediator of cell-mediated immune response which activates macrophage after exposure of mycobacterial pathogens (Arsenault *et al.,* 2014). Previous studies revealed that level of IFN-γ was up-regulated in MAP-infected cattle which show fecal shedding (Huda *et al.,* 2004; Jungersen *et al.,* 2012). Due to the decreased level of IFN-γ level with the progression of the disease, IFN-γ assay shows low sensitivity in the late stage of MAP infection (Nielsen and Toft, 2008). Therefore, researches focused on improvement of IFN-γ assay have been conducted. Hughes *et al.,* suggest Map-specific proteins, MAP_3651c and MAP_0268c as a candidate for new antigens of IFN-γ assay which show high in sub-clinically infected sheep (Hughes *et al.,* 2017). Also, Dernivoix *et al.,* developed new IFN-γ assay based on three antigens (Ag6, MAP1637c, and MAP0586c) which showed the significantly higher

level of IFN-γ in MAP infected animal than *M. bovis* infected animals (Dernivoix *et al.*, 2017).

8.3 Assays to detect humoral response to MAP infection

ELISA which detects specific antibodies to MAP has been developed as a serological diagnostic method. ELISA is a rapid, low-cost method for screening of MAP-infected animals in the herd (Collins, 1996). ELISA is the useful method for investigation of the infection prevalence in a large herd. ELISA methods show high sensitivity in cattle which have clinical symptoms (50 to 87 %) (Nielsen and Toft, 2008). However, the sensitivity of ELISA method in subclinically infected cattle is relatively low (7 to 22 %) (Nielsen and Toft, 2008). Therefore, many researches have been conducted for improvement of sensitivity and specificity of ELISA. Preabsorption of *Mycobacterium phlei* protein to sample can increase the specificity of the ELISA (Yokomizo *et al.*, 1983). Modification of the ELISA method with formaldehyde-treated MAP antigen can improve the sensitivity and specificity of the test (95% sensitivity and 100% specificity) (Speer *et al.*, 2006). Also, MAP antigen secreted during early to mid-log phase was used for development of ELISA for diagnosis of subclinically infected cattle (Shin *et al.*, 2008).

Biomarkers

1. Definition of biomarkers

Biomarkers are measurable biological characteristics that reflect the severity or presence of various disease states (Strimbu and Tavel, 2010). Generally, a biomarker is the biological markers that can be used as an indicator of a particular disease state or other physiological states of an organism (Mayeux, 2004). Biomarkers include specific cell, enzyme, hormone, protein, metabolite, gene, and gene transcript in a variety of sources such as body fluids and tissues (Jimenez-Luna *et al.,* 2018; Tsuyoshi and Yoshida, 2018; Yang *et al.*, 2018). Because biomarkers appear differently depending on the occurrence and progress of the specific diseases, it can be used for indicator substance in body fluids that allows measurement of physiological change during the progress of the disease (Mayeux, 2004). Therefore, biomarkers have been used for various purposes such as diagnosis of disease, evaluation of prognosis, and prediction of response to therapy (Mayeux, 2004). Especially, biomarkers considered as a non-invasive diagnostic tool for diverse diseases such as cancers, autoimmune diseases, and infectious diseases (Manda *et al.,* 2017; Moyer and Force, 2012; Schmidt *et al.,* 2011; Shirmohammadi *et al.,* 2018). For example, up-regulation of mutation in EGFRγIII protein was found in cerebrospinal fluid (CSF) of glioma patients and investigated for biomarker as an

indicator for glioma (Manda *et al.,* 2017). In addition, the prostate-specific antigen has been used for the diagnosis of prostate cancer since the approval of US FDA in 1986, and it is known to be useful for the screening of prostate cancer though it is controversial issues about overtreatment (Moyer and Force, 2012). CXCL13 is known to increase in cerebrospinal fluid of patients with acute Lyme neuroborreliosis, and diagnosis using level of CXCL13 in CSF shows high sensitivity and specificity for the early diagnosis of atypical neuroborreliosis (Schmidt *et al.,* 2011).

Currently, biomarkers have become widely used due to enhanced knowledge of the pathophysiological mechanism of disease and the development of next-generation sequencing technology.

2. Biomarkers for diagnosis of paratuberculosis

Paratuberculosis is a chronic wasting disease of ruminants which caused by *Mycobacterium avium* subsp. *paratuberculosis* (MAP) and characterized with persistent diarrhea and cachexia (Sweeney, 2011). Because the MAP can survive in the environment for a long time, the spread of the disease is mainly through the ingestion of contaminated feed or water (Whitlock and Buergelt, 1996). In general, infected cattle will undergo a subclinical phase that does not present symptoms for long periods of time. During the subclinical phase, the infected cattle emit MAP through the feces resulting in a continuous circulation of the MAP in the environment and the spread of the disease in the herd (Stabel, 1998). To date, there have been

developed PCR techniques to detect MAP in the feces and ELISA to detect antibodies against MAP in the body, but they show low sensitivity and specificity for detection of subclinically infected animals (Bögli-Stuber *et al.*, 2005; Collins, 2011; Cousins *et al.*, 1999; Englund *et al.*, 2002; Sockett *et al.*, 1992b).

In recent years, studies on host biomarker-based diagnostic methods have been conducted to overcome these problems. Diagnostic methods based on biomarkers can be classified into specific protein assay, transcriptomic analysis, and miRNA analysis depending on the type of the target indicator (Britton *et al.*, 2016). Several studies were conducted for discovery of specific proteins which can discriminate MAP-infected animals and non-infected animals (De Buck *et al.*, 2014; Seth *et al.*, 2009; Stabel and Robbe-Austerman, 2011; You *et al.*, 2012; Zhong *et al.*, 2011). When sera from infected and uninfected individuals were analyzed through protein fingerprinting, sera from infected cattle showed more than two-fold upregulation of six proteins and two-fold downregulation of two proteins (You *et al.*, 2012). They also found proteins with significantly altered expression in infected cattle were involved in iron regulation, leukocyte/lymphocyte directing, apoptosis, coagulation, and complement activation (You *et al.*, 2012). The previous study analyzed serum of unexposed, MAP-vaccinated, and MAP-infected sheep for the discovery of specific biomarkers for ovine paratuberculosis. As a result, they found that transthyretin was significantly reduced in both of vaccinated and infected sheep while alpha hemoglobin was highly increased in the vaccinated sheep and moderately in the MAP-infected sheep compared to unexposed group (Zhong *et al.*, 2011). Seth *et al.*,

found vitamin DBP increased in both *M. bovis* and MAP-infected cattle while cathelicidins increased significantly only in MAP-infected cattle (Seth *et al.,* 2009). These changes are believed to be related to the activation of innate immunity, which shares common changes that occur in humans when infected with *M. tuberculosis*. They also found an increase of transthyretin in MAP-infected cattle, which would increase the transport of vitamin A, resulting in increased differentiation of monocytes and activation of mucosal immunity to inhibit MAP proliferation (Seth *et al.,* 2009). Infection of MAP provokes specific host response in the early stage of infection. Stabel and Robbe-Austerman discovered early immune markers of MAP infection in the experimental infection model. All infected groups maintained a strong IFN-γ response during the study (Stabel and Robbe-Austerman, 2011). T cell activation markers such as CD25, CD26, CD45RO, and CD5 were significantly up-regulated in infected calves as compared to uninfected controls (Stabel and Robbe-Austerman, 2011). De Buck *et al.,* found that concentrations of acetone, citrate, glycerol, and iso-butyrate were significantly changed in infected cattle, indicating increased lipid metabolism in infected cattle (De Buck *et al.,* 2014). Significant changes in amino acid concentrations were also observed in infected cattle, indicating that protein turnover or deficiencies occurred in infected individuals (De Buck *et al.,* 2014).

Recently, studies on microRNA-based diagnostic methods have been carried out for early diagnosis of paratuberculosis. Seven miRNAs were down-regulated in MAP-infected animals compared to unexposed animals, and five and three miRNAs

decreased and increased in the exposed group, respectively, compared to the unexposed group. Six of the differentially expressed miRNAs are associated with an immune response and two are new miRNAs. This result suggests that miRNA expression is influenced by MAP infection and plays a key role in regulating host response to infection (Malvisi *et al.,* 2016). Also, Farrell *et al.,* identified a range of novel miRNA in bovine serum, and shown the utility of small RNA sequencing approaches to explore the potential of miRNA as novel biomarkers for paratuberculosis in cattle (Farrell *et al.,* 2015). Summarized information on biomarker studies for diagnosis of bovine paratuberculosis was listed in Table 1.

Table 1. Biomarkers which identified in research of bovine paratuberculosis

Type of sample	Type of biomarker	Identified biomarkers	Reference
Serum	Protein	Transferrin, gelsolin isoforms α & β, thrombin	(You *et al.*, 2012)
Serum	Protein	Alpha-haemoglobin , transthyretin	(Zhong *et al.*, 2011)
Serum	Protein	Transthyretin, retinol binding proteins, and cathelicidin	(Seth *et al.*, 2009)
Serum	Protein	CD25, CD26, CD45RO, and CD5	(Stabel and Robbe-Austerman, 2011)
Serum	Metabolite	Isobutyrate, acetone, and myo-inositol	(De Buck *et al.*, 2014)
Macrophage	Gene expression	TFRC, CX3CR1, CCNE1, Cox6a2, IRF7, and Gdf15	(Cha *et al.*, 2013)
Spleen	Gene expression	SAA3, complement factor D, and S100a8	(Shin *et al.*, 2015a)
Whole blood	Gene expression	PRR19, IGFLR1, and T2 cadherin	(Shin *et al.*, 2015b)
Whole blood	Gene expression	CD46, ICOS and CEP350	(David *et al.*, 2014a)
Whole blood	Gene expression	BNBD9-Like, S100A9, GPR77, and C5a2	(David *et al.*, 2014b)
Whole blood	Gene expression	TIMP1, HP, SERPINE1, TFRC, MMP9, DEFB1, DEFB10, and S100A8	(Park *et al.*, 2017a)
Whole blood	Gene expression	TTYH3, LOC617313, ZNF467, and IDO1	(Malvisi *et al.*, 2016)
Whole blood	MicroRNA	bta-mir-19b, bta-mir-19b2, bta-mir-301a and bta-mir-32	(Malvisi *et al.*, 2016)
Serum	MicroRNA	miR-205, miR-432	(Farrell *et al.*, 2015)

Transcriptomics

Transcriptomics is the quantitative study of all part of RNAs present in a sample which allow to understanding gene expression at genome-wide level (Mutz *et al.*, 2013). Through whole-transcriptome analysis, the contribution of gene expression to the onset and progression of the disease can be understood in various diseases such as cancer, diabetes, autoimmune disease, and cardiovascular disease (Devaux, 2017; Guffanti *et al.*, 2009; Li *et al.*, 2018; Peck and Nguyen, 2012). Also, biological pathways and molecular mechanisms which regulate cell signaling, cell development, and immune response can be identified through the genome-wide RNA expression with next-generation sequencing technology (Casamassimi *et al.*, 2017; Wang *et al.*, 2009). The transcriptomic approach is widely used in biomarker research in various fields including cancer, autoimmune disease, and infectious disease (Hwang *et al.*, 2018; Kamel and Al-Amodi, 2017; Peck and Nguyen, 2012; Sobhkhez *et al.*, 2017). Transcriptomic analysis of host gene expression analysis can be used to diagnose for specific diseases (Holcomb *et al.*, 2017).

Recently, several studies have been carried out on biomarkers for the early diagnosis of paratuberculosis based on analysis of host transcriptome profile (Cha *et al.*, 2013; David *et al.*, 2014a; David *et al.*, 2014b; Park *et al.*, 2017a; Park *et al.*, 2016; Shin *et al.*, 2015a; Shin *et al.*, 2015b). First, in vitro study showed the transcriptomic changes of mouse macrophages during the time of MAP infection,

and found that the types of genes that were changed during infection were different, and genes showing a steady increase throughout the infection period. Based on this, candidate genes that can be used as biomarkers during infection were selected (Cha *et al.*, 2013). Second, many researchers attempted to identify host biomarkers through the animal models. Shin *et al.*, reported that gene expression profiles that changed at 3 weeks and 6 weeks after MAP infection in mouse were related to metabolic process, cellular process, cell communication and immune system process (Shin *et al.*, 2015a). Also, the gene expression profile of MAP-infected cattle shows that the production and metabolism of reactive oxygen species are decreased and IL-10 signaling, LXR/RXR signaling, and complement system is activated in the subclinical stage. These results demonstrate a balanced response that provides an immune-limiting mechanism during host-defense response (Shin *et al.*, 2015b). Another study showed that increased expression of *CD46*, *ICOS*, and *CEP350* in infected calves, but decreased expression of *CTLA4*, *YARS*, and *PARVB*. In addition, a comparison of seropositive and seronegative infected calves confirmed that IL6ST, gp130, and CD22 play an important role in inducing antibodies to MAP (David *et al.*, 2014a). Also, the gene expression analysis at 6 months after infection, revealed that down-regulation of the neutrophil beta -diphenine-9 peptide (BNBD9-Like), S100 calcium binding protein A9 (s100A9) and G protein coupling receptor 77 (GPR77) or C5a anaphylatoxin chemotactic receptor (C5a2) and down-regulation of BOLA / MHC-I, BNBD9-like and upregulation of CD46 at 3, 6, 9, 12 and 15 months after inoculation was confirmed (David *et al.*, 2014b). In addition, studies are being

conducted to develop a diagnostic method for paratuberculosis using the degree of specific gene expression in the host. Park *et al.,* found that expression of eight genes (*TIMP1*, *HP*, *SERPINE1*, *TFRC*, *MMP9*, *DEFB1*, *DEFB10*, and *S100A8*) was significantly increased in the whole blood of MAP-infected cattle and investigate the diagnostic value of these biomarkers. As a result, four genes (*TIMP1*, *S100A8*, *DEFB1*, and *DEFB10*) showed the highest diagnostic accuracy in the subclinical group (Park *et al.,* 2017a). Also, another study revealed that diagnostic potential of biomarkers for diagnosis of the early stage of MAP infection in cows and their offspring which show positive tissue MAP and negative fecal MAP (Park *et al.*, 2017b). Taken together, many types of researches to identify biomarkers for diagnosis of paratuberculosis at the early stage were conducted.

Chapter I

Gene expression profiles of putative biomarker candidates in *Mycobacterium avium* subsp. *paratuberculosis* infected cattle

Abstract

This study was conducted to analyze gene expression of prognostic potential biomarker candidates using the whole blood of cattle naturally infected with *Mycobacterium avium* subsp. *paratuberculosis* (MAP). We conducted real-time PCR to evaluate 23 potential biomarker candidates. Experimental animals were divided into four groups based on fecal MAP PCR and serum ELISA. Seven (*KLRB1, HGF, MPO, LTF, SERPINE1, S100A8,* and *S100A9*) genes were up-regulated in fecal MAP positive cattle and three (*KLRB1, MPO,* and *S100A9*) were up-regulated in MAP seropositive cattle relative to uninfected cattle. In subclinically infected animals, 17 genes (*TFRC, S100A8, S100A9, MPO, GBP6, LTF, KLRB1, SERPINE1, PIGR, IL-10, CXCR3, CD14, MMP9, ELANE, CHI3L1, HP*, and *HGF*) were up-regulated

compared to the control group. Moreover, six genes (*CXCR3, HP, HGF, LTF, TFRC*, and *GBP6*) showed significant differences between experimental groups. Taken together, our data suggest that six genes (*LTF, HGF, HP, CXCR3*, *GBP6*, and *TFRC*) played essential roles in immune response to MAP during the subclinical stage and might be therefore be useful as prognostic biomarkers.

Key words: Biomarkers, Cattle, MAP, Paratuberculosis, Subclinical stage

Introduction

Mycobacterium avium subsp. *paratuberculosis* (MAP) is the etiologic agent of bovine paratuberculosis, a chronic wasting disease that affects domestic and wild ruminants (Whitlock and Buergelt, 1996). During the subclinical stage, animals still do not have clinical symptoms and; however, they shed low numbers of MAP into environment and MAP can be circulated in the herd and infect other animals (Tiwari *et al.,* 2006). Therefore, it is very important to remove subclinical stage animals to control the disease. However, current diagnostic methods including fecal culture, fecal PCR, and ELISA are insufficient for diagnosis of subclinical stages of disease (Al Hajri and Alluwaimi, 2007; Bögli-Stuber *et al.,* 2005; Englund *et al.,* 2002).

Host biomarkers have been proposed as a diagnostic tool for chronic disease (Li *et al.,* 2008; Pomorska-Mól *et al.,* 2012; Walzl *et al.,* 2011). Many potential biomarkers have been proposed for the detection of MAP infection in previous studies (David *et al.,* 2014a; David *et al.,* 2014b; Seth *et al.,* 2009; Shin *et al.,* 2015a; Shin *et al.,* 2015b; Verschoor *et al.,* 2010). Although several prognostic markers of bovine paratuberculosis have been suggested, there are still barriers preventing the use of effective diagnostic markers from the biomarkers suggested in previous studies. These studies were designed to analyze gene expression in specific type of cells or organ. Whole blood sample is easy to take and can be represent prognosis and severity of disease (Dickinson *et al.,* 2015; Mejias *et al.,* 2013). Therefore, the present study was conducted to identify gene expression of whole blood in MAP

infected cattle in different stages of infection based on the presence of MAP in feces and MAP antibody.

Materials and Methods

Experimental animals

Twenty seven Holstein cows were selected from national farm in the mid-west region of South Korea by detection of MAP-specific antibodies using a commercial ELISA kit (IDEXX Laboratories, Inc., Westbrook, ME, USA) and MAP in feces by PCR (Park *et al.,* 2014a) in 2014. The detection was performed two times with 6 month interval for precise classification of infection status. The animals were divided by based on the results of PCR and ELISA; a control group (n = 5) that was ELISA and PCR negative, Group 1 (n = 7), which was ELISA and PCR positive, Group 2 (n = 6), which was ELISA negative and PCR positive, and Group 3 (n = 9), which was ELISA positive and PCR negative. Also, infected animals (Group 1 to 3; n = 22) were divided into four groups according to the ELISA S/P ratio; EL200 group (n = 3) which was showed S/P ratio ≥ 200, EL100 group (n = 6) which was showed S/P ratio < 200 and ≥ 100, EL45 group (n = 7) which was showed S/P ratio < 100 and ≥ 45, ELneg group (Same as Group 2; n = 6) which was showed S/P ratio <45. Subclinically infected animals defined as MAP antibody negative and MAP positive

in feces (Group 2 and ELneg group). All animal procedures were performed with the permission by the National Institute of Animal Science (2013-046).

Selection of biomarker candidates

Twenty three genes that differed by more than absolute log 2 fold change value ≥ 1.5 and therefore had the potential for use as prognostic markers were selected based on our previous studies (Cha *et al.*, 2013; Shin *et al.*, 2015a; Shin *et al.*, 2015b). The selected prognostic marker candidates are listed in Table 2.

Extraction of total RNA from blood

Peripheral blood from cattle was collected from the tail vein using a PAX gene Blood RNA tube (PreAnalytiX/Qiagen, Hilden, Germany) according to the manufacturer's instructions. Total RNA was extracted using a PAX gene Blood RNA kit (PreAnalytiX/Qiagen, Hilden, Germany) according to the manufacturer's instruction.

Real-time PCR

Total RNA was used to prepare cDNA with random primers using a QuantiTect®

Reverse Transcription Kit (Qiagen Inc., Valencia, CA, USA) according to the manufacturer's instructions. The expression of 23 genes was analyzed by quantitative real time RT-PCR. Real time PCR reactions were conducted with using the Rotor-Gene SYBR Green PCR kit (Qiagen Inc., Valencia, CA, USA). The primers used in this study are listed in Table 3. Each reaction was initiated with 95°C at 10 min, followed by 40 cycles of 95°C for 15 s, 60°C at 45 s. The expression level was determined by the $2^{-\Delta\Delta Ct}$ method using a housekeeping gene, β-actin, as a reference. Up-regulated genes were as defined as log 2 fold change value ≥ 1.0 and down-regulated genes were as defined as log 2 fold change value < 1.0. Differentially expressed genes were as defined as absolute log 2 fold change value ≥ 1.5 according to previous study (Shin *et al.* 2015a).

Statistical analysis

Data were reported as the mean ± standard error of the mean (S.E.M.) of three or more independent experiments. Statistical significance was determined by ANOVA ($p < 0.05$) with post hoc *t*-tests done using the statistical package for social science (SPSS) software version 21. Differences were considered significant at a $p < 0.05$.

Results

Gene expression profile of the experimental groups

In group 1, two genes (*KLRB1* and *MPO*) were up-regulated, while remaining 21 genes were down-regulated. In group 2, 17 genes (*TFRC, S100A8, S100A9, MPO, GBP6, LTF, KLRB1, SERPINE1, PIGR, IL-10, CXCR3, CD14, MMP9, ELANE, CHI3L1, HP*, and *HGF*) were up-regulated, while remaining six genes were down-regulated. Of the up-regulated genes, six genes (*CXCR3, HP, HGF, LTF, TFRC*, and *GBP6*) were showed a significant difference between group 1 and group 2 ($p<0.05$) (Figure 3). Also, two genes (*CXCR3* and *TFRC*) were showed a significant difference between group 1 and group 3 ($p<0.05$) and four genes (*HP, HGF, LTF*, and *GBP6*) were showed a significant difference between group 2 and group 3 (Table 2 and Figure 3). In group 3, eight genes (*CXCL9, KLRB1, PIGR, MPO, GBP6, S100A8, HGF*, and *S100A9*) were up-regulated, while 15 genes were down-regulated. In EL45 group, six genes (*SERPINE1, S100A9, MPO, PIGR, CXCL9*, and *HGF*) were up-regulated while remaining 17 genes were down-regulated. In EL100 group, only two genes (*KLRB1* and *MPO*) were up-regulated while remaining 21 genes were down-regulated. In EL200 group, five genes (*KLRB1, MPO, S100A9, HGF*, and *CXCL9*) were up-regulated while remaining 18 genes were down-regulated. Of the up-regulated genes, only three genes (*GBP6, HGF*, and *LTF*) showed a significant

change between groups (Figure 3). In fecal MAP positive groups, seven genes (*KLRB1, MPO, HGF, LTF, SERPINE1, S100A8,* and *S100A9*) were up-regulated. In MAP seropositive group, three genes (*KLRB1, MPO,* and *S100A9*) were up-regulated (Table 2).

Discussion

Gene expression of whole blood can reflect infection status without reference to primary infection site. For example, distinct whole blood gene expression signature was observed in Crohn's disease and ulcerative colitis patients (Barnes *et al.,* 2015). Likewise, although the MAP is the enteric pathogen, distinct gene expression signature of whole blood was found in previous study (Shin *et al.,* 2015b). In current study, we examined gene expression profiles of MAP-infected cattle which were classified by the results of ELISA and fecal PCR. We found that there were many genes which were expressed differentially between the infected cattle and healthy cattle.

Among the up-regulated genes, 12 genes (*SERPINE1, HGF, LTF, KLRB1, S100A8, S100A9, HP, MPO, TFRC, GBP6, IL10,* and *PIGR*) were differentially expressed in group 2. Of the differentially expressed genes, six genes (*HGF, LTF, HP, TFRC, CXCR3* and *GBP6*) were showed statistically significant change (Figure 3). HGF is known to be a multifunctional protein that includes tissue protection, regeneration, and suppression of chronic inflammation (Nakamura *et al.,* 2011). Significant up-

regulation of the *HGF* in subclinical stage seems to be a response to chronic inflammation due to MAP infection. Lactoferrin inhibit bacterial invasion to epithelial cell by binding to bacterial surface proteins (Valenti and Antonini, 2005). Significant up-regulation of *LTF* in subclinical stage might be associated with bacterial invasion. Haptoglobin was known to inhibit several function of neutrophil such as phagocytosis and respiratory burst (Rossbacher *et al.,* 1999). Also, HP was known to have protective functions in inflammatory bowel disease via inhibition of several cytokine such as IL-17, IFN-γ, TNF, and IL-6 (Vanuytsel *et al.,* 2013). Up-regulation of the *HP* in subclinical stage could be related to anti-inflammatory activity against immune response due to MAP infection. *GBP6* is a member of the IFN-γ-inducible GTPase super family, which is involved in host immune response (Kim *et al.,* 2011). A previous study showed that IFN-γ-inducible GTPase provide protection against intracellular bacteria via oxidative killing and transfer of antimicrobial peptides to autophagolysosomes (Kim *et al.,* 2011). *TFRC* encodes transferring receptors known as surface markers of unmatured phagosome infected with *M. tuberculosis* (Chua *et al.,* 2004; Clemens and Horwitz). Up-regulation of the *TFRC* gene was observed at 6 h p.i. and maintained at 24 and 48 h p.i. in THP cells infected with MAP (Shin *et al.,* 2015c). *TFRC* was up-regulated in Raw 264.7 cells infected with MAP at 6 h p.i. (Cha *et al.,* 2013). Significant up-regulation of *GBP6* and *TFRC* between groups could be related to intracellular killing in early stage of MAP infection.

Although the gene expression of whole blood can reflect biological changes due to

disease, whole blood samples were collected only single time and analyzed in this study. More distinct changes might be observed if we had sampling at the multiple times. Subclinical animals which cannot detected by ELISA excrete low numbers of MAP into feces and subsequently infect other animals in the herd. Six genes (*LTF, HGF, HP, CXCR3, GBP6,* and *TFRC*) which were significantly up-regulated in group 2 might be useful prognostic biomarkers of subclinical stages of JD. These genes should be further evaluated to determine their suitability for diagnosis of subclinical stage JD. Various factors including infection dose, infected age, animal species, and coexistence of other disease might affect the accuracy of these prognostic biomarkers. Accordingly, field studies need to be conducted to determine the adequacy of these prognostic biomarkers for use as a diagnostic tool of subclinical stage of JD.

Table 2. Fold change of selected biomarker candidate genes between experimental groups and control group

Gene group	Accession No.	Gene Symbol	Gene Name	Location	Fold change								
					Group 1 vs. control	Group 2 vs. control	Group 3 vs. control	Fecal MAP positive group vs. control	MAP sero-positive group vs. control	ELneg vs control	EL45 vs control	EL100 vs control	EL200 vs control
Cytokine	NM_002984.2	*CCL4*	Chemokine (C-C motif) ligand 4	Extracellular Space	-1.26	0.48	0.47	-0.37	-0.21	0.48	0.3	-0.05	-2.13
	NM_002985.2	*CCL5*	Chemokine (C-C motif) ligand 5	Extracellular Space	-1.23	0.93	0.60	-0.13	-0.12	0.93	0.45	-0.15	-1.82
	NM_002416.1	*CXCL9*	Chemokine (C-X-C motif) ligand 9	Extracellular Space	-0.08	-1.16	1.16	-0.5	0.75	-1.16	1.06	-0.03	1.36
	NM_001565.3	*CXCL10*	Chemokine (C-X-C motif) ligand 10	Extracellular Space	-0.49	0.88	0.71	0.22	0.24	0.88	0.33	0.19	-0.15
	NM_000619.2	*IFN-γ*	Interferon-gamma	Extracellular Space	-0.76	0.71	0.69	0.12	0.20	0.71	0.77	-0.25	-1.07
	NM_174088	*IL10*	Interleukin 10	Extracellular Space	-0.36	1.58	0.28	0.84	0.16	1.58	0.14	-0.22	0.34
Receptor	NM_003234.2	*TFRC*	Transferrin receptor (p90, CD71)	Plasma membrane	-0.59	1.62	0.65	0.42	0.08	1.62	0.61	-0.18	-0.51
	NM_001011673	*CXCR3*	Chemokine (C-C motif) receptor 3	Plasma membrane	-0.89	1.75	0.73	0.51	0.29	1.75	0.21	0.65	-0.92
	NM_001206636	*KLRB1*	Killer cell lectin-like receptor subfamily B, member 1	Plasma membrane	1.35	3.13	1.06	2.44	1.36	3.13	0.74	1.17	2.17
	XM_003582266	*KLRC1*	NKG2-A/NKG2-B type II integral membrane protein	Plasma membrane	-0.91	0.64	0.78	0.02	0.23	0.64	0.33	0.12	-0.81

	NM_174143	*PIGR*	Polymeric immunoglobulin receptor	Plasma membrane	-0.12	1.98	1.02	0.88	0.48	1.98	1.07	0.34	-0.38
	NM_001174104.1	*CD14*	CD14 molecule	Plasma Membrane	-0.58	1.18	0.34	0.33	-0.00167	1.18	0.13	-0.53	0.43
Enzyme	NM_174744	*MMP9*	Matrix metallopeptidase 9	Extracellular Space	-0.08	1.48	0.55	0.66	-0.40	1.48	-0.16	-0.9	0.34
	NM_000250.1	*MPO*	Myeloperoxidase	Cytoplasm	1.35	2.64	1.39	2.1	1.42	2.64	1.18	1.07	2.95
	NM_001972.2	*ELANE*	Elastase, neutrophil expressed	Extracellular Space	-0.98	1.44	0.62	0.25	-0.05	1.44	0.06	0.79	-2.1
	NM_001276.2	*CHI3L1*	Chitinase 3-like 1	Extracellular Space	0.25	1.26	0.08	0.82	0.21	1.26	0.44	-0.57	0.94
Others	NM_001075995	*GBP6*	Guanylate binding protein family, member 6	Extracellular Space	-1.32	1.79	1.06	0.29	-1.12	1.79	-0.97	-1.27	-1.424
	NM_002343.3	*LTF*	Lactotransferrin	Extracellular Space	0.25	3.67	0.28	2.03	0.33	3.67	0.2	0.79	-2.1
	NM_002964.4	*S100A8*	S100 calcium binding protein A8	Cytoplasm	0.15	2.80	1.31	1.52	0.88	2.8	0.9	0.66	0.88
	NM_002965.3	*S100A9*	S100 calcium binding protein A9	Cytoplasm	0.81	2.69	1.22	1.8	1.09	2.69	1.32	-0.12	2.67
	NM_174137	*SERPINE1*	Serpin peptidase inhibitor	Extracellular Space	0.27	1.88	0.91	1.04	0.63	1.88	1.05	0.66	-0.42
	NM_005143.3	*HP*	Haptoglobin	Extracellular Space	-0.69	1.78	0.19	0.61	-0.11	1.78	-0.03	-0.68	0.4
	NM_001031751	*HGF*	Hepatocyte growth factor	Extracellular Space	0.55	2.4	1	1.54	0.81	2.4	1.26	0.19	1.33

Table 3. Nucleotide sequence of primers used for real-time PCR

Target gene		Primer sequence (5'→3')	PCR product size (base pair)	Reference
β-actin	F	CGCACCACTGGCATTGTCAT	227	(Cortes *et al.*, 2013)
	R	TCCAAGGCGACGTAGCAGAG		
KLRB1	F	AACCAGCATGGATGCTCAAGA	90	Park *et al.*, 2016
	R	TCTCGGATTCGTTTCCAGTGC		
KLRC1	F	ACCCAGGGATTCTGGCATTG	160	Park *et al.*, 2016
	R	ACTGGTCTCTCTGTTGCTTCC		
CCL4	F	TCCACTTGCAAACTACAGATAACA	115	Park *et al.*, 2016
	R	ACCCAACAGCATCCAAACTCA		
CCL5	F	CCCAGCCAGCTGTGGTATTC	177	Park *et al.*, 2016
	R	CTCGGAGCAGCTCAGTTCAA		
CXCL9	F	CTTCTGCCTCCCCATATGCC	72	Park *et al.*, 2016
	R	ACTTCTTCTCTGGGTTGGCG		
CXCL10	F	CTCTGACTGGAGTTCAAGGAGT	141	Park *et al.*, 2016
	R	TCCCTTGGCTGGTGTTGATG		
CXCR3	F	AAGCATGAGTGTGAAGGGCA	90	Park *et al.*, 2016
	R	AGGGAAACCTTGAACAATTGCAG		
IFN-γ	F	ACATAGCCAAGTCGGTCACG	157	Park *et al.*, 2016
	R	CTCGGAACTTGACACCCACA		
MMP9	F	CCCGGATCAAGGATACAGCC	177	Park *et al.*, 2016
	R	GGGCGAGGACCATACAGATG		
SERPINE1	F	CTGCGAAATTCAGGATGCGG	191	Park *et al.*, 2016
	R	GGGTGAGAAAACCACGTTGC		
IL10	F	TCTGCCCTGCGAAAACAAGA	70	Park *et al.*, 2016
	R	CCTCTCTTGGAGCTCACTGAA		
HP	F	GGCCCCCGAGATTGCTAATA	168	Park *et al.*, 2016
	R	GGGCAGCTGTCATCTTCTTCA		
HGF	F	CGACGGGCTCTTTTAGGCTC	186	Park *et al.*, 2016
	R	CTGTCCTTCTGCATAGGGGATG		
PIGR	F	GAGTTTGCCACCACTACCGA	71	Park *et al.*, 2016
	R	TCCTTGGACGACCTCTTTGC		
MPO	F	GCCCTGGAACTTCAGAGAGATG	132	Park *et al.*, 2016
	R	GTCAGCACCACCGAGGTATC		
CD14	F	TGTCTGACAATCCCAGTCTCG	83	Park *et al.*, 2016
	R	CGCTAGATATTGGAGGGCCG		
CHI3L1	F	ATAAGAGAAGCTGGAGGCCCA	141	Park *et al.*, 2016
	R	CCACAAAACCTGTATGAGCCG		
LTF	F	GGAAGCAGATGCCCTGAACT	141	Park *et al.*, 2016
	R	AGGTACCCTTCCGTTGGTCT		
ELANE	F	TTGTCTGAACGGCCTGAACT	92	Park *et al.*, 2016
	R	CTCTGAACATCTGCCGGGTT		
S100A8	F	ATTTTGGGGAGACCTGGTGG	124	Park *et al.*, 2016
	R	ACGGCGTGGTAATTCCCTTT		
S100A9	F	AGGCTACGGGAAGGGCAG	134	Park *et al.*, 2016
	R	GCTGGCCTCCTGATTAGTGG		
TFRC	F	CAAAGTTTCTGCCAGCCCAC	188	Park *et al.*, 2016
	R	AACAGAAAGAGACCGCTGGG		
GBP6	F	GAGTGAAGGACAAGCAGCCT	179	Park *et al.*, 2016
	R	CAGACAGAAACCTCTGTATTCCG		

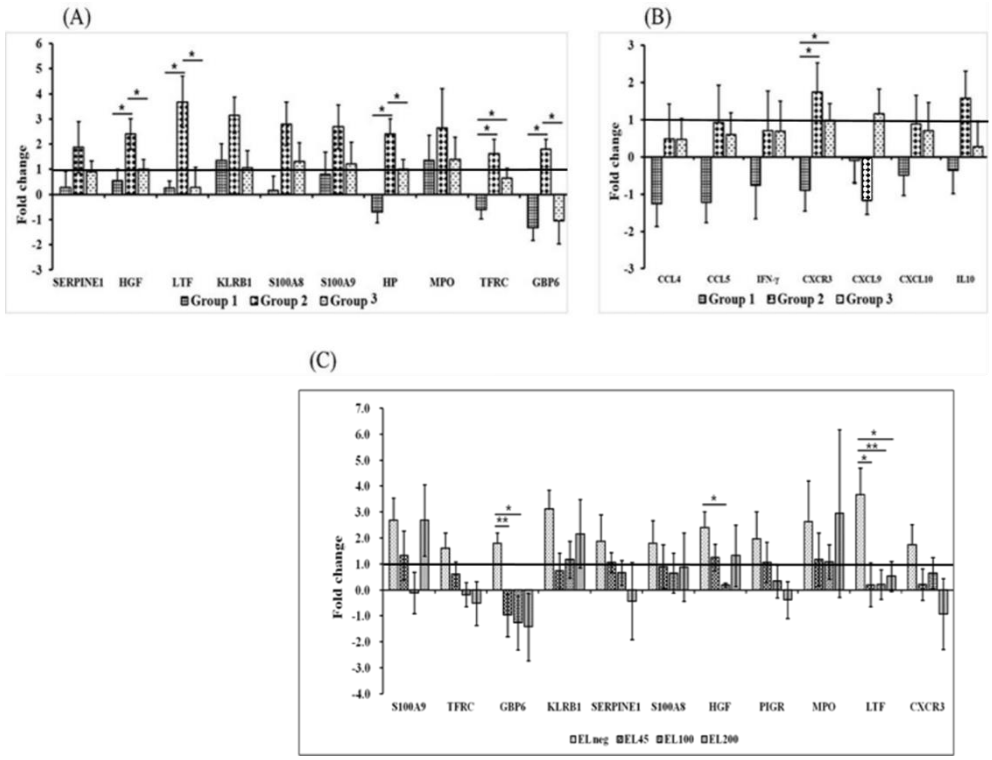

Figure 3. Gene expression profiles of biomarker candidates.

(A) Differentially expressed biomarker genes of cattle infected with *Mycobacterium avium* subspecies *paratuberculosis* in group 2 compared to non-infected cattle. The expression level was normalized by the $2^{-\Delta\Delta CT}$ method in terms of the beta-actin expression level relative to the control group (*, $p<0.05$). (B) Expression of Th1 and Th2 type immune-related genes of cattle infected with *Mycobacterium avium* subspecies *paratuberculosis* compared to non-infected cattle. The expression level was normalized by the $2^{-\Delta\Delta CT}$ method in terms of the beta-actin expression level relative to the control group (*, $p<0.05$). (C) Differentially expressed biomarker genes of cattle infected with *Mycobacterium avium* subspecies *paratuberculosis* in ELneg group compared to non-infected cattle. The expression level was normalized by the $2^{-\Delta\Delta CT}$ method in terms of the beta-actin expression level relative to the control group (*, $p<0.05$ **, $p<0.01$).

Chapter II

Gene expression profiles of immune-regulatory genes in whole blood of cattle with a subclinical infection of *Mycobacterium avium* subsp. *paratuberculosis*

Abstract

Johne's disease (JD) is a chronic wasting disease of ruminants caused by *Mycobacterium avium* subsp. *paratuberculosis* (MAP), resulting in inflammation of intestines and persistent diarrhea. The initial host response against MAP infections is mainly regulated by the Th1 response, which is characterized by the production of IFN-γ. With the progression of disease, MAP can survive in the host through the evasion of the host's immune response by manipulating the host immune response. However, the host response during subclinical phases has not been fully understood. Immune regulatory genes, including Th17-derived cytokines, interferon regulatory factors, and calcium signaling-associated genes, are hypothesized to play an important role during subclinical phases of JD. Therefore, the present study was

conducted to analyze the expression profiles of immune regulatory genes during MAP infection in whole blood. Different expression patterns of genes were identified depending on the infection stages. Downregulation of *IL-17A, IL-17F, IL-22, IL-26*, *HMGB1*, and *IRF4* and upregulation of *PIP5K1C* indicate suppression of the Th1 response due to MAP infection and loss of granuloma integrity. In addition, increased expression of *IRF5* and *IRF7* suggest activation of IFN-α/β signaling during subclinical stages, which induced indoleamine 2, 3-dioxygenase mediated depletion of tryptophan metabolism. Increased expression of *CORO1A* indicate modulation of calcium signaling, which enhanced the survival of MAP. Taken together, distinct host gene expression induced by MAP infection indicates enhanced survival of MAP during subclinical stages.

Keywords: Paratuberculosis, *Mycobacterium avium* subsp. *paratuberculosis*, Johne's disease, Subclinical, Host response, Whole blood

Introduction

Paratuberculosis (PTB) or Johne's disease (JD) is a chronic infectious disease leading to persistent diarrhea, progressive wasting, and cachexia, all of which are caused by *Mycobacterium avium* subsp. *paratuberculosis* (MAP) (Whitlock and Buergelt, 1996). MAP can affect a range of ruminants, including cattle, goats, lamb, and deer (Whitlock and Buergelt, 1996) as well as non-ruminants such as parrots, baboons, tamarins, cavies, lemurs, and wallabies (Münster *et al.,* 2013). The transmission of PTB usually occurs through the ingestion of contaminated materials such as feed, colostrum, water, and soil (Fecteau *et al.,* 2013; Tiwari *et al.,* 2006). After ingesting contaminated materials, intestinal M cells, which are located in Peyer's patches in the ileum, uptake and transfer MAP to macrophages that are distributed in the mesenteric lymph nodes (Rathnaiah *et al.,* 2017). Generally, ingested pathogens are eliminated within the macrophage. However, MAPs can survive in host macrophages by interfering with phagosome maturation (Rumsey *et al.,* 2006). Previous studies have suggested that MAP can inhibit host Rab proteins, which are essential for the phagosome–lysosome fusion following phagocytosis in human and mouse macrophages (Hostetter *et al.,* 2003).

Due to the persistence of MAPs, macrophages form granulomas during subclinical phases of infection in the intestinal lymphoid tissue (Buergelt *et al.,* 1978). Previous studies have suggested immunological changes related to fecal shedding during the progression of disease (Ganusov *et al.,* 2015; Magombedze *et al.,* 2016). Fecal

shedding has been shown to occur with the downregulation of cell-mediated immune response and upregulation of the humoral immune response *in vivo* (Magombedze *et al.*, 2016). In contrast, some infected animals show increased fecal shedding with the activation of cellular immunity (Ganusov *et al.*, 2015). However, specific mechanisms of the immune response that induces fecal shedding are not clear.

In the subclinical stages, infected macrophages with MAP upregulate expression of *CD29, CD56, IL-1α,* and *TRAF1,* resulting in the recruitment of immune cells to the sites of infection (Arsenault *et al.*, 2014). Activated macrophages with MAP move to the local lymph nodes and present an antigen for stimulating naive T cells to induce the Th1 response, which involves the production of interferon gamma and pro-inflammatory cytokines such as IL-6, IL-1α, and IL-2 (Coussens, 2001). Dominance of the Th1 response continue during the subclinical stages, and activated Th1 lymphocytes induce the cell-mediated immune response by producing IL-2, TNF-β, and IFN-γ (Coussens, 2001).

During the late subclinical stages of JD, the Th1 response is gradually diminished and the Th2 response is enhanced, which induces the humoral immune response (Stabel, 2006). With the progression of disease from the subclinical phase to the clinical phase, the cell-mediated immune response totally diminishes, and the humoral immune response, which is characterized by the production of IL-4 and IL-10, becomes prominent (Stabel, 2006). Furthermore, with the shift from the Th1 to Th2 response, clinical signs and lesions become more severe. Therefore, understanding the host response during subclinical phases is critical in identifying

the pathogenesis of JD. We hypothesized that immune regulatory genes play an important role in the subclinical phases of JD during the immunological shift from the Th1 to Th2 response.

The Th17-derived cytokine is known to protect hosts from extracellular bacteria causing respiratory and intestinal tract infections (Dubin and Kolls, 2008). However, several studies have suggested that Th17-derived cytokines may have immune regulatory roles against the infection of intracellular bacteria such as *Salmonella* and *Listeria monocytogenes* (Hamada *et al.,* 2008; Schulz *et al.,* 2008). IL-17 deficient mice show enhanced bacterial numbers in the spleen and liver after an infection by *Salmonella enterica* (Schulz *et al.,* 2008). In addition, with the infection of *Listeria monocytogenes*, bacterial numbers and granuloma formation were increased in the liver (Hamada *et al.,* 2008).

Interferon regulatory factor (IRF) is a transcription factor that has regulatory roles in the immune system (Honda and Taniguchi, 2006). In particular, IRFs regulate the innate immune response via pattern recognition receptor signaling such as TLRs, CLRs, RLRs, and NLRs (Zhao *et al.,* 2015). High mobility group box 1 (HMGB1) is a non-histone nuclear protein that is involved in the regulation of the immune response (Lotze and Tracey, 2005; Scaffidi *et al.,* 2002). PIP5K1C has been known to have an immune-regulatory function via the modulation of neutrophil polarization and infiltration (Xu *et al.,* 2010). In addition, CORO1A have diverse functions, including calcium homeostasis, cytoskeletal dynamics, and maintenance of immune cell diversity and function (Jayachandran and Pieters, 2015).

However, the role of these immune-regulatory genes in JD has not been yet fully understood. Therefore, we analyzed the expression of immune regulatory genes among cattle groups that have different levels of antibodies to MAP and fecal shedding in order to determine the role of immune-regulatory genes during subclinical phases of JD.

Materials and Methods

Animals

The animals were selected from a national farm in the mid-west region of South Korea during 2016 to 2017. In this farm, the presence of infectious diseases, including paratuberculosis, bovine tuberculosis, brucellosis, infectious bovine rhinotracheitis, and bovine viral diarrhea, were investigated two times per year in spring and autumn. In total, 79 Holstein cows were selected for the experiments, according to the results of ELISA performed using a commercial ELISA kit (IDEXX Laboratories, Inc., Westbrook, ME, USA) and fecal detection of MAP by PCR. In brief, fecal DNA was extracted using the mGITC/SC method (Park *et al.*, 2014a) and amplification of *IS900* and *ISMAP02*-targeted real-time PCR was conducted as previously described with slight modification. (Sevilla *et al.*, 2014; Zhang and Zhang, 2011). In total of 20 μl of reaction mixture consisted with 10 μl of 2 × Rotor-Gene Probe PCR master mix (Qiagen, Hilden, Germany), 500 nM primers, 200 nM probes, 4 μl fecal DNA, and 4 μl nuclease free water. Real-time PCR reaction was performed under the following conditions: 1 cycle at 95°C for 5 min, followed by 45 cycles at 95°C for 15 s, and 60°C for 1 min. The fecal sample was regarded to be positive when both *IS900* and *ISMAP02* real-time PCR results were positive. Primers used in real-time PCR were listed in Table 4. For the selection of animals, ELISA and fecal PCR were performed 4 times within a 6-month interval to ensure precise

classification of animals. For evaluation of clinical status of animals, all animals were monitored for two years for the presence of chronic diarrhea and cachexia. This study was carried out in strict accordance with the guidelines of the Institutional Animal Use and Care Committee of the National Institute of Animal Science. The protocol was approved by the Institutional Animal Use and Care Committee of the National Institute of Animal Science (Permit number 2013-046).

Sampling and extraction of total RNA from whole blood

Peripheral blood samples (3 ml) were collected from the tail vein of cattle with the BD Vacutainer® Plus Plastic K_2EDTA Tubes and BD Vacutainer® Plus Plastic Serum Tubes. The extraction of total RNA from whole blood was performed as previously described (Park *et al.*, 2016). In brief, 125 μl of whole blood was mixed with the same volume of RNase-free water and 750 μl of Trizol LS reagent (Ambion, Foster City, CA, USA) and incubated at room temperature for 5 min. Thereafter, 200 μl of chloroform (Sigma-Aldrich, Castle Hill, Australia) was mixed and centrifuged at 13,523 ×g and 4°C for 15 min. The supernatant was collected into a 1.5 ml tube, mixed with the same volume of 70% ethanol, and then transferred to an RNAeasy column (Qiagen, Hilden, Germany) and centrifuged at 8,500 ×g for 15 sec. After the wash steps, 30 μl of RNase-free water was added and centrifuged at 8,500 ×g for 1 min. Eluted RNA was stored at -80°C until use. For the separation of serum, 3 ml of blood samples were centrifuged at 1,500 ×g for 10 min. Separated serum was

transferred to 1.5 ml tube and analyzed for the presence of MAP-specific antibodies using a commercial ELISA kit.

Selection of immune regulatory genes

Eleven genes that are related to immune regulatory function were selected based on previous studies (Khare *et al.*, 2016; Shin *et al.*, 2015a) and classified to three categories as follows; Th17-derived cytokines (*IL-17A*, *IL-17F*, *IL-22*, and *IL-26*), calcium signaling (*HMGB1*, *CORO1A*, and *PIP5K1C*), and interferon regulatory factors (*IRF3*, *IRF4*, *IRF5*, and *IRF7*)(Table 4).

Optimization of real-time PCR conditions

Real-time PCR conditions were optimized with an identical cDNA template for each gene. Five concentrations of both forward and reverse primers ranging from 0.25 μM to 1.25 μM, with a 0.25 μM interval, were tested. In addition, five annealing temperatures from 56°C to 64°C with a two-degree interval were tested. For further experiments, optimal primer concentrations and annealing temperatures that showed the highest fluorescence value were selected for further analysis.

Real-time PCR

The cDNA was synthesized with random primers using a QuantiTect® Reverse Transcription Kit (Qiagen Inc., Valencia, CA, USA) according to the manufacturer's instructions. The expression of eleven immune regulatory genes was identified by quantitative real-time RT-PCR with a Rotor-Gene multiplex PCR kit (Qiagen Inc). Briefly, a total of 18 μl reaction mixture included 10 μl of SYBR master mix, RNase-free water, and 0.5 μM forward and reverse primers. Finally, 2 μl of cDNA template was added to the mixture to a final volume of 20 μl. Specific amplification with primers for each target was identified by a homology search (https://www.ncbi.nlm.nih.gov/tools/primer-blast) and agarose gel electrophoresis. The primers used in this study are shown in Table 4. Real-time PCR was performed with triplicate samples at 95°C for 10 min, followed by 45 cycles of 95°C for 15 s and 60°C for 45 s. A no-template sample was used for the negative control. The gene expression was calculated by the $2^{-\Delta\Delta Ct}$ method with β-actin for the housekeeping gene.

Statistical analysis

Statistical significance was confirmed by ANOVA with Tukey's post hoc test among the experimental groups using the GraphPad Prism software version 7.00 (GraphPad Software, Inc., La Jolla, CA, USA). A *P* value of less than 0.05 ($p < 0.05$) was considered as statistically significant, and all experiments were recorded as the means of biological triplicates.

Results

Animals

The study subject included 79 heifers that were classified into five groups based on the results of the PCR and ELISA. Non-infected group (n = 27) was defined as those that were ELISA- and PCR-negative during the entire examination. Infected animals were classified into four groups according to the ELISA sample to positive (S/P) ratio. The EL Neg group (n = 23) was defined as those with a S/P ratio < 45 and PCR-positive. The EL Low group (n = 9) was defined as those with a S/P ratio <100 and ≥45. The EL Mid group (n = 8) was defined as those with a S/P ratio <150 and ≥100. The EL High group (n = 12) was defined as those with S/P ratio ≥150. All animals did not show chronic diarrhea and cachexia for two years. Furthermore, infected animals were classified into two groups based on the presence of fecal shedding. The FP group (n = 41) was defined as fecal PCR-positive, and the FN group (n = 11) was defined as fecal PCR- negative. The age of animals ranged from 2 to 10 years, and the mean ± SD for the age of the animals for each group was as follows: Non-infected group, 4.92 ± 2.09 years; EL Neg group, 4.69 ± 1.74 years; EL Low group 6.11 ± 1.45 years; EL Mid group 4.87 ± 1.35 years; EL High group 5.16 ± 1.02 years; FP group, 5 year ± 1.61 years; FN group, 5.36 ± 1.28 years. Among these groups, age did not show any significant differences (p > 0.05) (Figure 4).

Detailed characteristics of animals were presented in Table 5.

Optimization of real-time PCR conditions

The optimal concentration of primers and annealing temperature was determined by conducting real-time PCR with three primer concentrations and annealing temperatures. The combination of forward and reverse primers at 0.5 μM and an annealing temperature of 60°C showed the highest florescence and lowest C_T value. The combination of 0.5 μM forward and reverse primers and 60°C of an annealing temperature of were used in further analysis.

Gene expression profiles between the infected groups

The expression of Th17-derived cytokine genes is presented in Figure 5 and 6. *IL-17A* was downregulated in the EL Low, Mid, and High groups compared to the non-infected and EL Neg groups. In addition, *IL-17A* was downregulated in the EL Mid group compared to the EL Low group and upregulated in EL High group compared to the EL Mid group. *IL-22* was downregulated in the EL Mid and High groups compared to the EL Neg group. *IL-26* was downregulated in EL Neg and High groups compared to the non-infected group. Furthermore, *IL-26* was upregulated in the EL Mid group compared to the EL Neg group. When compared with the presence of fecal shedding, 3 genes (*IL-17A*, *IL-17F*, and *IL-26*) were downregulated in the

FP group compared to the non-infected group. In addition, two genes (*IL-17F* and *IL-26*) were downregulated in the FN group compared to the non-infected group. Furthermore, the expression of *IL-17A* was increased in the FN group compared to the FP group.

The expressions of interferon regulatory factors are presented in Figure 7 and 8. *IRF3* was downregulated in the EL Mid and High groups compared to the EL Neg group. On the other hand, *IRF5* was upregulated in the EL Neg, Low, and High groups compared to the non-infected group. The expression of *IRF7* was increased in the EL Neg group compared to the non-infected group. In addition, *IRF7* was downregulated in the EL Mid group compared to the EL Neg group. According to the fecal shedding-based classification, *IRF5* was upregulated in the FP group compared to the non-infected group. In contrast, IRF4 was downregulated in the FP and FN groups compared to the non-infected group.

The expressions of calcium signaling-associated genes are presented in Figure 9 and 10. *HMGB1* was downregulated in the EL Neg, Low, Mid, and High groups compared to the non-infected group. In addition, the expression of *HMGB1* was decreased in the FP and FN groups compared to the non-infected group. The expression of *PIP5K1C* was increased in the FP group compared to the non-infected group and decreased in the FN group compared to the FP group. *CORO1A* was upregulated only in the FP group compared to the non-infected group.

Discussion

Gene expression profiling of whole blood is a useful indicator of the progression of diseases and immune responses in chronic infectious diseases (Mejias *et al.,* 2013; Seok *et al.,* 2013). Although gene expression in whole blood does not completely reflect the immunological changes at the site of infection, alteration of gene expression in peripheral blood may be specific to disease progression and provide useful information for identification of pathophysiology (Andrés-Benito *et al.,* 2017; Li *et al.,* 2017; Smith *et al.,* 2017). Several studies have investigated the host response to MAP infection in whole blood, peripheral blood mononuclear cells (PBMC), and monocyte-derived macrophages (MDM) (Casey *et al.,* 2015; David *et al.,* 2014a; David *et al.,* 2014b; Marino *et al.,* 2017; Park *et al.,* 2016; Shin *et al.,* 2015b; Verschoor *et al.,* 2010). However, the host responses during the immunological shift period between early subclinical to late subclinical stages were not fully understood. Therefore, the present study was conducted to identify the host response during the subclinical stages that revealed different levels of antibodies and the presence of MAP shedding in feces.

The present study suggests a difference in the gene expression profile of non-infected animals and infected animals with subclinical phases with different levels of fecal shedding and antibodies to MAP. The expression of Th17-derived cytokine genes differed between the experimental groups. Although the expression of all

genes was not perfectly matched, Th17-derived cytokine genes were downregulated during the progression of disease. Th17-derived cytokines play an important role in the early stage of mycobacterial infection (Torrado and Cooper, 2010). IL-26 and IL-17F are the main effector cytokines of the Th17 response and are associated with host defense against intracellular bacteria (Coulter *et al.,* 2017; Tengvall *et al.,* 2016). IL-26 induces priming of immune cells and direct killing of pathogens via membrane pore formation (Stephen-Victor *et al.,* 2016). Furthermore, previous studies have revealed that IL-26 upregulates tumor necrosis factor (TNF)-related apoptosis-inducing ligand (TRAIL) expression in human NK cells, which induces the elimination of hepatitis C-infected hepatocytes (Miot *et al.,* 2015). Moreover, IL-17 provides protective immunity against intracellular pathogens by modulation of Th1 response and neutrophilic recruitment (Raffatellu *et al.,* 2008; Umemura *et al.,* 2007). In addition, Robinson et al. analyzed the expression of Th17 cytokines in tissue samples pooled with jejunum, ileocecal valve, and adjacent lymph node of MAP-infected red deer (Robinson *et al.,* 2011). Expression of *IL-17* was not significantly changed in early stage of infection, but was significantly increased at late stage. On the other hand, the expression of *IL-21, IL-22*, and *IL-23* were not significantly changed depending on the stage of infection (Robinson *et al.,* 2011). In this study, the expression of *IL-17A* and *IL-17F* tended to decrease with the progression of disease. This difference may be due to the difference between the host animal (red deer vs cattle) and the sample (jejunum vs whole blood). Park *et al.,* found that the expression of *IL-17, IL-22, IL-23* and *RORC* was upregulated after the stimulation

of MAP in PBMC isolated from cattle infected with MAP (Park *et al.,* 2014b). This suggests that Th17-derived cytokines play an important role in the early stages of JD. Therefore, downregulation of Th17-derived cytokine genes reflects insufficient immune response for eliminating intracellular MAP during all subclinical stages in this study.

Formation of granuloma is an important factor in the pathogenesis of JD (Koets *et al.,* 2015). MAP crosses the intestinal barrier through M cells or enterocytes and subsequently up-taken by macrophages located in the lamina propria. Thereafter, cytokine production by activated macrophages and MAP antigens attracts new monocytes. Finally, multi-nucleated giant cells and epithelioid cells are formed, resulting in the formation of new granuloma (Koets *et al.,* 2015). Formation of granulomas is tightly regulated by immune responses such as TNF-signaling and neutrophil trafficking (Bernut *et al.,* 2016a). Neutrophil recruitment regulated by the TNF/IL-8 axis is essential for the establishment and maintenance of granulomas, which provides protective immunity to the host during mycobacterial infections (Bernut *et al.,* 2016b; Smith *et al.,* 2009). Therefore, impaired recruitment of neutrophil can induce unstable maintenance of granulomas. Th17-derived cytokines, including IL-17, IL-23, and IL-26, enhance granuloma integrity through the modulation of neutrophil recruitment via CXCR3 signaling (Seiler *et al.,* 2003). In addition, *PIP5K1C* encodes protein phosphatidylinositol phosphate kinases, which regulate E-cadherin sorting for degradation, and increased activity of PIP5K1C induced the downregulation of E-cadherin (Schill *et al.,* 2014). A previous study

suggested that E-cadherin is expressed in macrophages if the macrophages fail to eliminate intracellular pathogens, which subsequently contributes to the formation of granulomas (Cronan *et al.,* 2016). Therefore, upregulation of *PIP5K1C* and downregulation of *IL-17A* and *IL-17F* in the whole blood can reflect loss of granuloma integrity, which induces bacterial shedding through feces.

Maturation of phagosomes is an important process in the defense against microbial pathogen (Uribe-Querol and Rosales, 2017). However, intracellular pathogens can survive and replicate in the phagocytes by disrupting phagosome maturation (Queval *et al.,* 2017). *CORO1A* encodes protein coronin 1 in mammalian cells, and is involved in actin dynamics (Rybakin and Clemen, 2005). A recent study revealed that coronin 1 is an essential factor for modulating calcium signaling after the invasion of pathogenic mycobacteria (Jayachandran *et al.,* 2007). Coronin 1 modulates physiological Ca^{2+} fluxes and induces the activation of calcineurin, subsequently blocking phagosome–lysosome fusion (Jayachandran *et al.,* 2007). Moreover, IL-22 activates phagosome maturation via enhancing calgranulin A expression in MDMs infected with *Mycobacterium tuberculosis* (Dhiman *et al.,* 2014). Calgranulin A was upregulated in MAP-infected animals and has been proposed as a diagnostic biomarker for subclinical MAP infections (Park *et al.,* 2016; Verschoor *et al.,* 2010). Thus, upregulation of *CORO1A* and downregulation of *IL-22* indicate enhanced intracellular survival of MAP during subclinical stages.

Expression of interferon regulatory genes was different between experimental groups. First, the expression of *IRF4* was decreased in all infected groups compared

to the non-infected group. IRF4 is an essential factor for the differentiation of T and B cells as well as the generation of plasma cells (Nam and Lim, 2016). In a previous study, *IRF4* knockout mice failed to provoke Th1 immune response against *Listeria monocytogenes* infections (Mahnke *et al.,* 2016). Decreased expression of *IRF4* can induce downregulation of the Th1 immune response, which can enhance the persistent survival of MAP. *HMGB1* expression is upregulated by the IFN-γ that is secreted in activated macrophages (Rendon-Mitchell *et al.,* 2003). During early infections, mycobacterial pathogen can inhibit the activation of macrophages via the induction of anti-apoptotic and anti-inflammatory response (Abendaño *et al.,* 2014; Awuh *et al.,* 2015). This result coincided with a previous study that showed downregulation of a complement immune pathway induced by MAP and consequently enhanced intracellular survival in macrophages (Shin *et al.,* 2015b).

Interferon regulatory factor (IRF) is the transcriptional regulator of IFN genes that regulates the immune response to intracellular pathogen. *IRF5* and *IRF7* have been shown to activate type I interferons including IFN-α, -β, -ω, -ε, -κ, and pro-inflammatory cytokines (Honda and Taniguchi, 2006; McNab *et al.,* 2015). IFN-α/β is the most widely expressed type I IFN, which has diverse effects on innate and adaptive immunity (McNab *et al.,* 2015). In general, IFN-α/β have been shown to protect the host from intracellular pathogens, including *Chlamydia trachomatis*, *Legionella pneumophila*, and *Salmonella* Typhimurium (Bukholm *et al.,* 1984; Ishihara *et al.,* 2005; Schiavoni *et al.,* 2004). More specifically, IFN-α/β inhibit intracellular replication of *Chlamydia trachomatis* through indoleamine 2,3-

dioxygenase (IDO) mediated depletion of L-tryptophan (Ishihara *et al.,* 2005). A previous study showed upregulation of IDO in THP-1 monocytes, PBMCs, and intestinal tissues of MAP-infected animals (Plain *et al.,* 2011). However, IDO-mediated tryptophan depletion also has a detrimental effect on the host. For example, low concentrations of tryptophan inhibit T cell proliferation (Munn *et al.,* 2005). In addition, metabolites of IDO-mediated tryptophan metabolism such as kynurenine, 3-hydroxykynurenine, and 3-hydroxyanthranilic acid can inhibit T cell proliferation via apoptosis and arrest of the cell cycle (Fallarino *et al.,* 2003; Frumento *et al.,* 2002; Terness *et al.,* 2002). Therefore, upregulation of *IRF5* and *IRF7* can result in the inhibition of T cell proliferation via IDO-mediated tryptophan depletion. In another study, expression of *IRF5* was downregulated after 3 weeks of infection with MAP in the spleen of mice (Shin *et al.,* 2015a). These differences are possibly related to different host species or differences in the first infection time and dose. Taken together, whether IFN-α/β is beneficial or detrimental for the host is not clear in MAP infections. Therefore, the specific role of IFN-α/β during subclinical stages of JD should be identified in further studies.

Several studies revealed molecular mimicry between MAP protein and host *IRF5* protein (Bo *et al.,* 2018; Cossu *et al.,* 2015; Mameli *et al.,* 2016). Mameli *et al.,* identified that molecular mimicry between MAP_4027$_{18\text{-}32}$ and IRF5$_{424\text{-}434}$ peptide (Mameli *et al.,* 2016). Also, they found that antibodies to both MAP_4027$_{18\text{-}32}$ and IRF5$_{424\text{-}434}$ peptides were significantly elevated in sera and cerebrospinal fluid of multiple sclerosis patients when compared to healthy individuals (Mameli *et al.,*

2016). Cossu *et al.,* found similar result in sera of multiple sclerosis patients and these two peptides induce activation of the Th1 response in the whole blood while suppressing the Th2 response (Cossu *et al.,* 2015). Recently, Bo *et al.,* analyzed the serum of rheumatoid arthritis patients and suggests exposure to MAP can trigger specific humoral immune response against host IRF5 protein due to molecular mimicry between MAP_4027$_{18\text{-}32}$ and IRF5$_{424\text{-}434}$ peptides in rheumatoid arthritis patients (Bo *et al.,* 2018). Taken together, humoral immune response to IRF5$_{424\text{-}434}$ peptide which induced by exposure to MAP may weaken the Th1 response and activate the Th2 response during subclinical stage of JD.

In conclusion, we propose a novel model for the host response, which enhances the survival of MAP (Figure 11). Downregulation of *IL-17A, IL-17F, IL-26*, and upregulation of *PIP5K1C* induce loss of granuloma integrity results in fecal shedding and dissemination of the pathogen. Downregulation of *IRF4* resulted in impaired Th1 immune response, which decreased expression of *HMGB1* and enhanced the downregulation of the Th1 immune response. In addition, increased expression of *IRF5* and *IRF7* suggest that activation of IFN-α/β signaling during subclinical stages induce IDO-mediated tryptophan metabolism. IDO-mediated depletion of tryptophan indicates an inhibition of T cell proliferation, subsequently leading to an immunosuppressive state. Upregulation of *CORO1A* suggest the possibility of the failure to intracellularly eliminate MAP. Taken together, this model suggests manipulation of host responses for the survival of MAP that occurs during the subclinical phases of JD. However, this model was established based on the gene

expressions of whole blood, which is not specific to individual immune cell subsets. Therefore, more specific roles of the immune regulatory genes during subclinical phases should be identified via interactions between different immune cells in co-culture systems or *in vivo* in further studies.

Table 4. Oligonucleotide sequences of primers and probes used for real-time PCR

Target gene		Primer sequence (5′→3′)	PCR product size (base pair)	Reference
β-actin	F	GCA AGC AGG AGT ACG ATG AG	134	(Park *et al.*, 2017a)
	R	GCC ATG CCA ATC TCA TCT CG		
IL-17A	F	CAC AGC ATG TGA GGG TCA AC	101	In this study
	R	GTG GAG AGT CCA AGG TGA GG		
IL-17F	F	GAG GAA GCA AAA CGG CTG TC	115	In this study
	R	CTG ATC TGC CAT CGG GTC AT		
IL-22	F	CTG TAG GCT CAA CGA GTC CG	150	In this study
	R	CGC TTC GTC ACC TGA TGG AT		
IL-26	F	AAC GAT TCC AGA AGA TCG CA	164	In this study
	R	CCA CAA AGT GCA TTT CCT TGC		
HMGB1	F	CGA ACA TCC TGG CCT GTC TA	150	In this study
	R	TTA GCT CGG TAT GCG GCA AT		
CORO1A	F	ACC CTG ACA CCA ACA TCG TC	166	In this study
	R	TTG TTC ACC TCC AGA CCA CG		
PIP5K1C	F	GAG ATT GTG GTC CCC AAG GA	191	In this study
	R	CTC CTC TCA TCG GTG GGA AA		
IRF3	F	GAA CCC AAA AGC CTC GGA TAC	162	In this study
	R	CCT GGA AGA TGC CGA AAT CC		
IRF4	F	GCA GAG ATC CCG TAC CAG TG	167	In this study
	R	TCG GCA GAC CTT ATG CTT GG		
IRF5	F	AGA CCT CAA AGA CCG CAT GG	154	In this study
	R	TTA CTG CAT GCC AAC TGG GT		
IRF7	F	CGC AAC GCT TTG TGA TGT TG	146	In this study
	R	TGC AGG TGG GGC ATC TTC TA		
IS900	F	ATG ACG GTT ACG GAG GTG GTT	76	(Zhang and Zhang, 2011)
	R	TGC AGT AAT GGT CGG CCT TAC		
	Probe	FAM-CGA CCA CGC CCG CCC AGA-TAMRA		
ISMAP02	F	CGG CTG GAC ACG GAA TG	67	(Sevilla *et al.*, 2014)
	R	CAT GAG CGA CAG TAT CTT TCG AA		
	Probe	JOE-ATC CGT CCC AGT GGC GGA GTC AC-BHQ-1		

Table 5. Basic characteristics of study subjects

Numbers of subjects	**Non-infected (n=27)**		**EL neg (n=23)**		**EL Low (n=9)**		**EL Mid (n=8)**		**EL high (n=12)**		**FP (n=41)**		**FN (n=11)**	
Heifers, n (%)	27 (100)		23 (100)		9 (100)		8 (100)		12 (100)		41 (100)		11 (100)	
Median age (years)	4 (3 to 10)		5 (2 to 8)		7 (3 to 7)		4.5 (4 to 8)		6 (4 to 6)		5 (2 to 8)		6 (3 to 7)	
Breed	Holstein		Holstein		Holstein		Holstein		Holstein		Holstein		Holstein	
	Animal No.	Age (years)	Animal No.	Age (years)	Animal No.	Age (years)	Animal No.	Age (years)	Animal No.	Age (years)	Animal No.	Age (years)	Animal No.	Age (years)
	A01	5	B01	7	C01	5	D01	4	E01	6	B01	7	C02	3
	A02	10	B02	5	C02	3	D02	5	E02	4	B02	5	C03	7
	A03	10	B03	8	C03	7	D03	4	E03	4	B03	8	C04	5
	A04	8	B04	7	C04	5	D04	5	E04	6	B04	7	C05	7
	A05	8	B05	7	C05	7	D05	4	E05	4	B05	7	C07	7
	A06	6	B06	4	C06	7	D06	8	E06	6	B06	4	E07	6
	A07	6	B07	5	C07	7	D07	4	E07	6	B07	5	E08	6
	A08	4	B08	3	C08	7	D08	5	E08	6	B08	3	E09	4
	A09	4	B09	5	C09	7			E09	4	B09	5	E10	6
	A10	4	B10	3					E10	6	B10	3	E11	4
	A11	3	B11	3					E11	4	B11	3	E12	4
	A12	3	B12	4					E12	4	B12	4		
	A13	6	B13	3							B13	3		
	A14	6	B14	3							B14	3		
	A15	5	B15	5							B15	5		
	A16	5	B16	3							B16	3		
	A17	6	B17	5							B17	5		
	A18	4	B18	7							B18	7		
	A19	3	B19	4							B19	4		
	A20	5	B20	5							B20	5		
	A21	4	B21	7							B21	7		
	A22	3	B22	2							B22	2		
	A23	3	B23	3							B23	3		
	A24	3									C01	5		
	A25	3									C06	7		
	A26	3									C08	7		
	A27	3									C09	7		
											D01	4		
											D02	5		
											D03	4		
											D04	5		
											D05	4		
											D06	8		
											D07	4		
											D08	5		
											E01	6		
											E02	4		
											E03	4		
											E04	6		
											E05	4		
											E06	6		

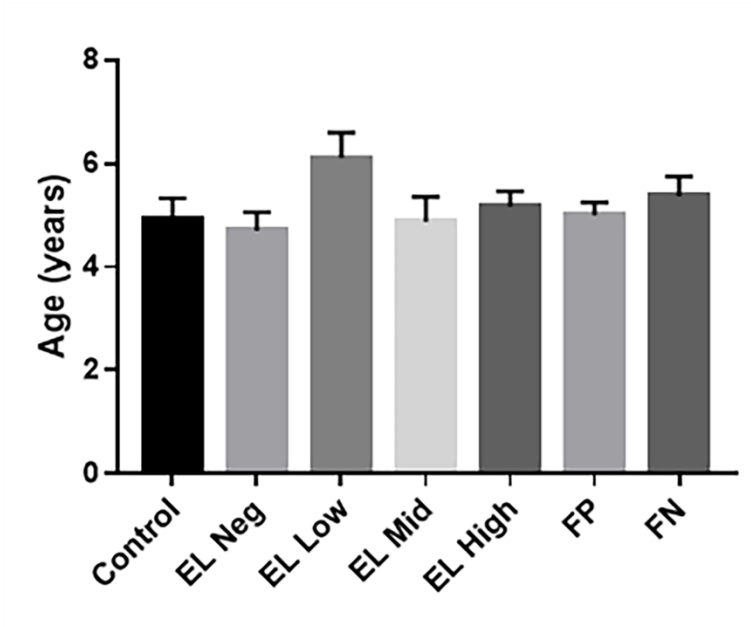

Figure 4. Comparison of mean age among the experimental animals.

The mean age of the experimental animals among the experimental groups was represented with a bar graph. Statistical significance was calculated by ANOVA with Tukey's post hoc test among the experimental groups. A *P* value of less than 0.05 ($p < 0.05$) was considered as statistically significant.

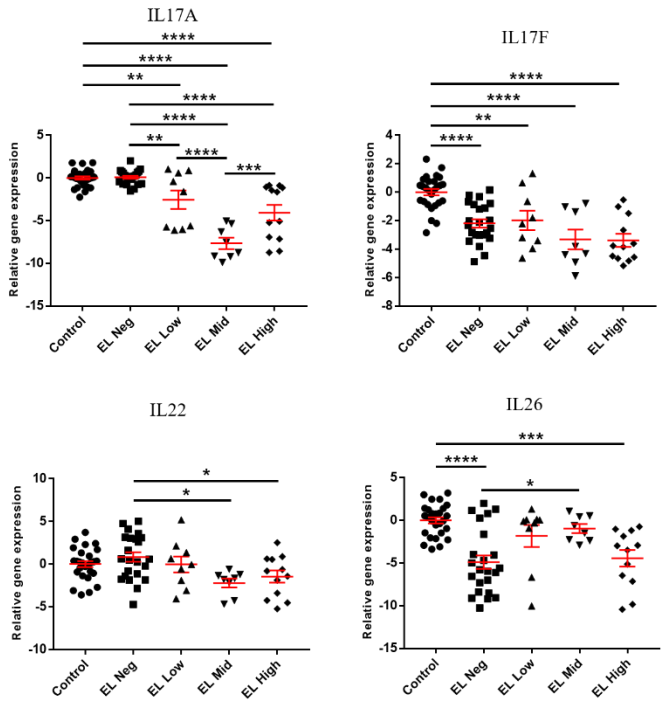

Figure 5. Differences in gene expression levels of Th17-derived cytokine genes of the EL Neg, EL Low, EL Mid, and EL High groups compared to control group.

Scatter plots for each gene represent for each individual animal. Values of relative gene expression were normalized to the reference gene β-actin. * indicates a *p*-value <0.05; ** indicates a *p*-value <0.01; *** indicates a *p*-value <0.001; **** indicates a *p*-value <0.0001. The EL Neg group (*n* = 23) was defined as those with a S/P ratio < 45 and PCR-positive. The EL Low group (*n* = 9) was defined as those with a S/P ratio <100 and ≥45. The EL Mid group (*n* = 8) was defined as those with a S/P ratio <150 and ≥100. The EL High group (*n* = 12) was defined as those with S/P ratio ≥150. Gene expression value of EL Neg, Low, Mid, and High groups were compared to Control group and statistical significance was calculated by ANOVA with Tukey's post hoc test.

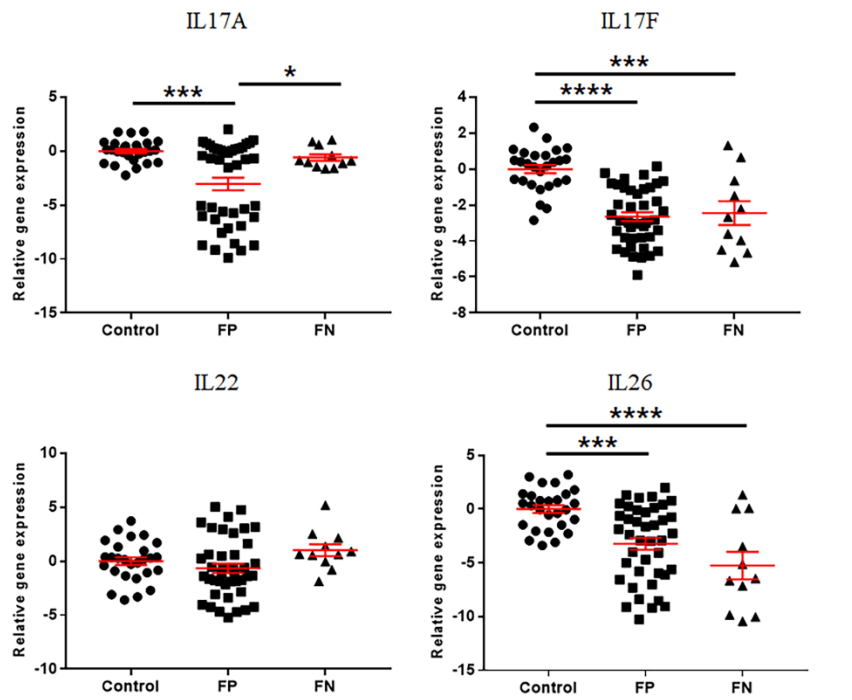

Figure 6. Differences in gene expression levels of Th17-derived cytokine genes of the FP, and FN groups compared to control group.

Scatter plots for each gene represent for each individual animal. Values of relative gene expression were normalized to the reference gene β-actin. * indicates a *p*-value <0.05; ** indicates a *p*-value <0.01; *** indicates a *p*-value <0.001; **** indicates a *p*-value <0.0001. The FP group (n = 41) was defined as fecal PCR positive, and the FN group (n = 11) was defined as fecal PCR- negative. Gene expression value of FP and FN groups were compared to Control group and statistical significance was calculated by ANOVA with Tukey's post hoc test.

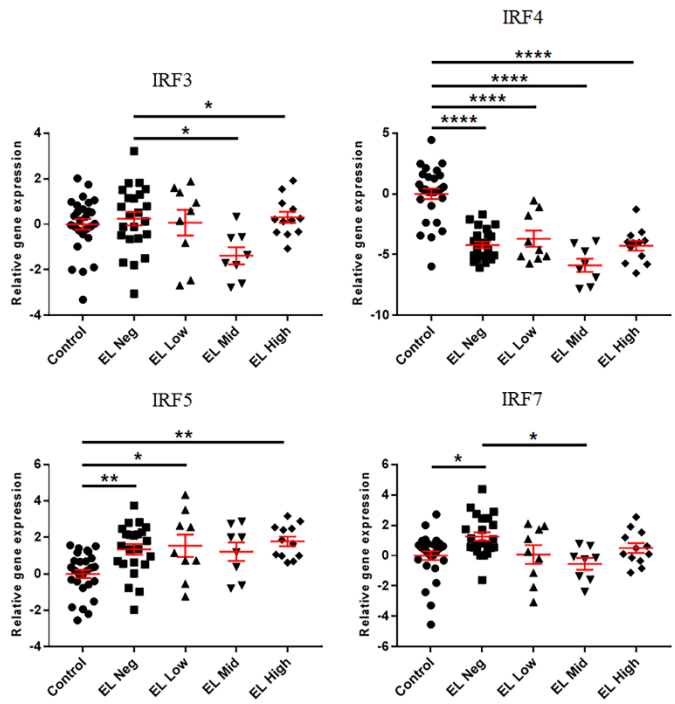

Figure 7. Differences in gene expression levels of interferon regulatory factors of the EL Neg, EL Low, EL Mid, and EL High groups compared to control group.

Scatter plots for each gene represent for each individual animal. Values of relative gene expression were normalized to the reference gene β-actin. * indicates a *p*-value <0.05; ** indicates a *p*-value <0.01; *** indicates a *p*-value <0.001; **** indicates a *p*-value <0.0001. The EL Neg group (n = 23) was defined as those with a S/P ratio < 45 and PCR-positive. The EL Low group (n = 9) was defined as those with a S/P ratio <100 and ≥45. The EL Mid group (n = 8) was defined as those with a S/P ratio <150 and ≥100. The EL High group (n = 12) was defined as those with S/P ratio ≥150. Gene expression value of EL Neg, Low, Mid, and High groups were compared to Control group and statistical significance was calculated by ANOVA with Tukey's post hoc test.

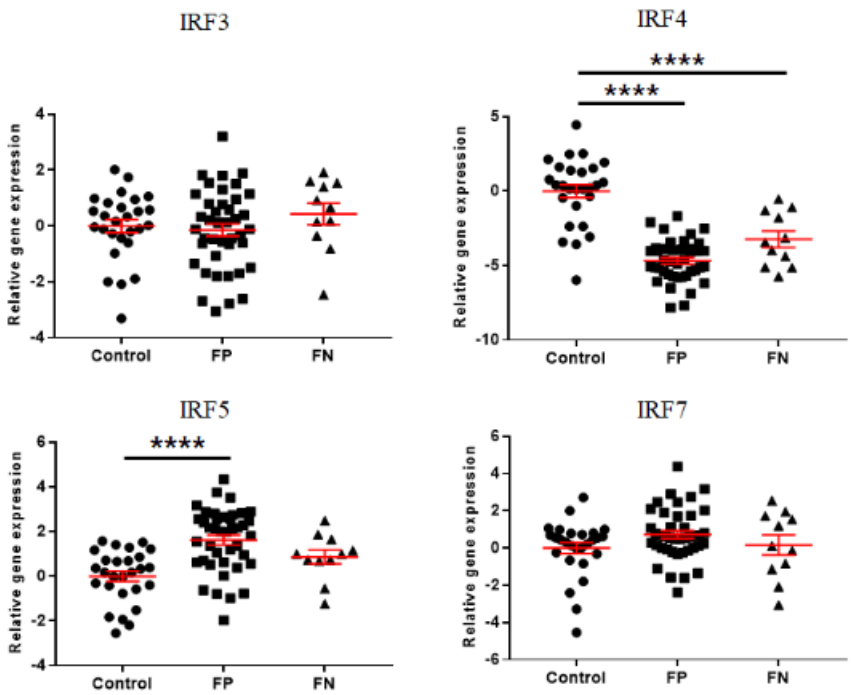

Figure 8. Differences in gene expression levels of interferon regulatory factors of the FP, and FN groups compared to control group.

Scatter plots for each gene represent for each individual animal. Values of relative gene expression were normalized to the reference gene β-actin. * indicates a *p*-value <0.05; ** indicates a *p*-value <0.01; *** indicates a *p*-value <0.001; **** indicates a *p*-value <0.0001. The FP group (n = 41) was defined as fecal PCR positive, and the FN group (n=11) was defined as fecal PCR- negative. Gene expression value of FP and FN groups were compared to Control group and statistical significance was calculated by ANOVA with Tukey's post hoc test.

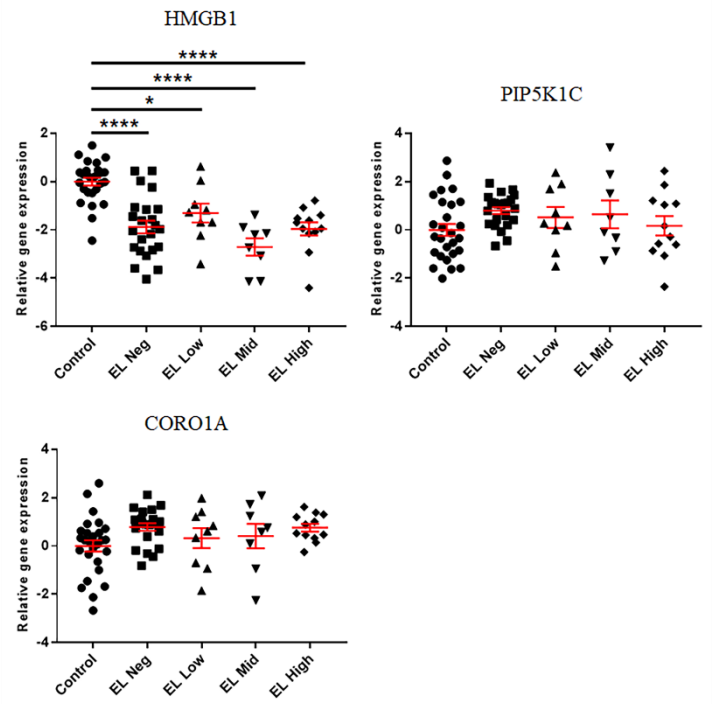

Figure 9. Differences in gene expression levels of calcium signaling-associated genes of the EL Neg, EL Low, EL Mid, and EL High groups compared to control group.

Scatter plots for each gene represent for each individual animal. Values of relative gene expression were normalized to the reference gene β-actin. * indicates a *p*-value <0.05; ** indicates a *p*-value <0.01; *** indicates a *p*-value <0.001; **** indicates a *p*-value <0.0001. The EL Neg group (n = 23) was defined as those with a S/P ratio < 45 and PCR-positive. The EL Low group (n = 9) was defined as those with a S/P ratio <100 and ≥45. The EL Mid group (n = 8) was defined as those with a S/P ratio <150 and ≥100. The EL High group (n = 12) was defined as those with S/P ratio ≥150. Gene expression value of EL Neg, Low, Mid, and High groups were compared to Control group and statistical significance was calculated by ANOVA with Tukey's post hoc test.

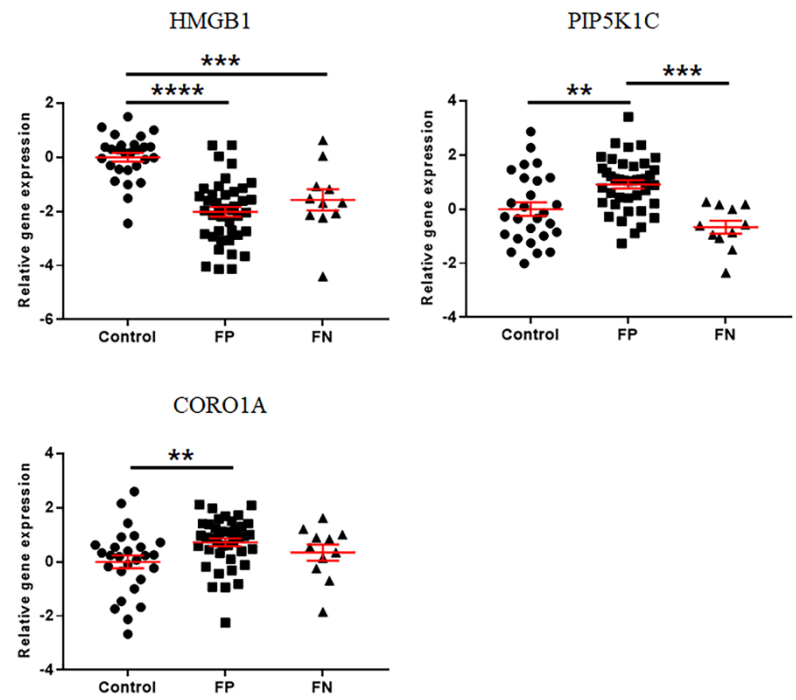

Figure 10. Differences in gene expression levels of calcium signaling-associated genes of the FP, and FN groups compared to control group.

Scatter plots for each gene represent for each individual animal. Values of relative gene expression were normalized to the reference gene β-actin. * indicates a *p*-value <0.05; ** indicates a *p*-value <0.01; *** indicates a *p*-value <0.001; **** indicates a *p*-value <0.0001. The FP group (n = 41) was defined as fecal PCR positive, and the FN group (n = 11) was defined as fecal PCR- negative. Gene expression value of FP and FN groups were compared to Control group and statistical significance was calculated by ANOVA with Tukey's post hoc test.

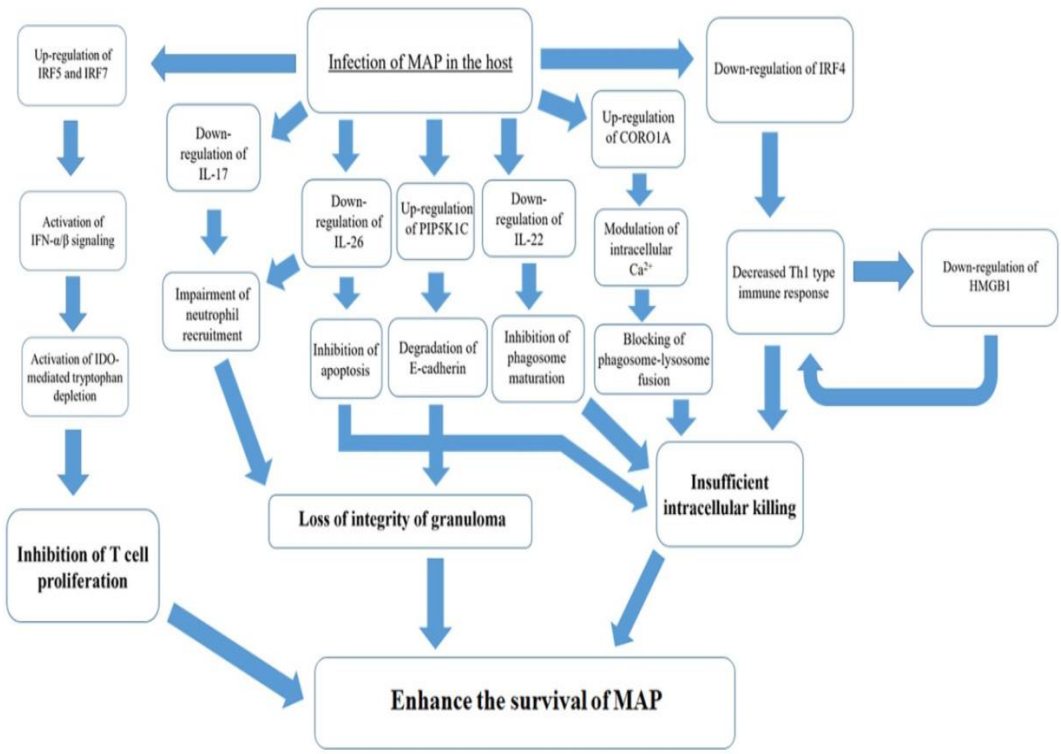

Figure 11. Novel model for the manipulation of host responses by *Mycobacterium avium* subsp. *paratuberculosis* (MAP) for its survival during subclinical stages of Johne's disease.

MAP can manipulate host responses to enhance its survival. Upregulation of *PIP5K1C* and downregulation of *IL-17A*, *IL-17F*, and *IL-26* induces a loss of granuloma integrity, which can result in fecal shedding and dissemination of MAP. In addition, downregulation of *IRF4* and *HMGB1* can impair intracellular elimination of MAP. Upregulation of CORO1A modulates intracellular Ca^{2+}, which can block phagosome–lysosome fusion. Moreover, decreased expression of *IL-22* indicates an inhibition of phagosome maturation. Upregulation of *IRF5* and *IRF7* activates IFN-α/β signaling, which upregulate IDO-mediated tryptophan depletion and subsequently induce the inhibition of T cell proliferation. Taken together, a manipulated host response enhances the survival of MAP during the subclinical phases of JD.

Chapter III

Establishment a real-time reverse transcription PCR based on host biomarkers for the detection of the subclinical cases of *Mycobacterium avium* subsp. *paratuberculosis*.

Abstract

Johne's disease (JD) is a chronic enteric inflammatory disease of cattle caused by *Mycobacterium avium* subsp. *paratuberculosis* (MAP) that causes large economic losses in the dairy industry. Spread of JD is mainly provoked by a long subclinical stage during which MAP is shed into the environment with feces; accordingly, detection of subclinical animals is very important to its control. However, current diagnostic methods are not suitable for detection of subclinical animals. Therefore, the current study was conducted to develop a diagnostic method for analysis of the expression of genes of prognostic potential biomarker candidates in the whole blood

of Holstein cattle naturally infected with MAP. Real-time PCR with nine potential biomarker candidates was developed for the diagnosis of MAP subclinical infection. Animals were divided into four groups based on fecal MAP PCR and serum ELISA. Eight genes (*TIMP1, HP, SERPINE1, TFRC, MMP9, DEFB1, DEFB10*, and *S100A8*) were up-regulated in MAP-infected cattle (p <0.05). Moreover, ROC analysis revealed that eight genes (*TIMP1, HP, SERPINE1, TFRC, MMP9, DEFB1, DEFB10*, and *S100A8*) showed fair diagnostic performance (AUC≥0.8). Four biomarkers (*TIMP1, S100A8, DEFB1*, and *DEFB10*) showed the highest diagnostic accuracy in the PCR positive and ELISA negative group (PN group) and three biomarkers (*TFRC, HP*, and *SERPINE1*) showed the highest diagnostic accuracy in the PCR negative and ELISA positive group (NP group). Moreover, three biomarkers (*S100A8, HP*, and *DEFB10*) were considered the most reliable for the PCR positive and ELISA positive group (PP group). Taken together, our data suggest that real-time PCR based on eight biomarkers (*TIMP1, HP, SERPINE1, TFRC, MMP9, DEFB1, DEFB10*, and *S100A8*) might be useful for diagnosis of JD, including subclinical stage cases.

Keywords: Paratuberculosis, *Mycobacterium avium* subsp. *paratuberculosis*, Johne's disease, Biomarker, Real-time PCR, Diagnosis, Subclinical stage

Introduction

Johne's disease (JD) is a chronic inflammatory disease of the gastrointestinal tract of ruminants with granulomatous lesions that is caused by *Mycobacterium avium* subsp. *paratuberculosis* (MAP) (Whitlock and Buergelt, 1996). Especially, JD causes huge economic losses to dairy industry due to decreased milk production and weight loss (Garcia and Shalloo, 2015). MAP infection in cattle can be divided into four stages depending on the clinical signs and MAP shedding levels including the silent, subclinical, clinical, and advanced clinical stage (Whitlock and Buergelt, 1996). In the silent stage, the infected cattle do not show any clinical sign or excrete MAP into the environment (Tiwari *et al.,* 2006). During the subclinical stage, infected cattle still do not have clinical symptoms; however, they shed low numbers of MAP into environment, which can be circulated in the herd and infect other animals (Tiwari *et al.,* 2006). After subclinical stage, infected cattle enter clinical stage and start to show clinical signs such as gradual weight loss, diarrhea, and decreased milk production (Tiwari *et al.,* 2006). Finally, infected cattle become cachectic and lethargic in advanced clinical stage (Tiwari *et al.,* 2006). Accordingly, it is very important to remove infected cattle in the subclinical stage to control the disease. However, current diagnostic methods are insufficient for diagnosis of subclinical stages of disease (Mortier *et al.,* 2015). Although fecal culture has been considered a gold standard for the diagnosis of MAP (Whittington *et al.,* 2013), this method is time-consuming and shows low sensitivity, especially in subclinical stages

of the disease (Bögli-Stuber *et al.,* 2005; Sockett *et al.,* 1992a). PCR allows rapid detection of MAP in clinical samples such as feces, milk and blood (Sevilla *et al.,* 2014); however, PCR-based methods are also limited in their usefulness for diagnosis of subclinical stages of disease because of the low sensitivity (Wells *et al.,* 2006) and low specificity caused by genetic similarities with other mycobacteria (Cousins *et al.,* 1999; Englund *et al.,* 2002). Although ELISA has been used for detection of antibodies to MAP in clinical samples such as serum and milk, this method is also inadequate for diagnosis of fecal shedders in the subclinical stage, especially in 1–2 year old cattle (Al Hajri and Alluwaimi, 2007). Therefore, new diagnostic tools have been requested to detect MAP-infected animals at early stage of infection.

Biomarkers, which are considered indicators of specific pathogenic conditions or therapeutic responses to treatment (Strimbu and Tavel, 2010), are commonly used as diagnostic tools for various diseases (Dehnad *et al.,* 2016; Goyal *et al.,* 2017; Walker *et al.,* 2016; Waters *et al.,* 2016). Recently, host biomarkers discovered using transcriptomics, metabolomics, and proteomics have been proposed as alternative diagnostic methods for JD (David *et al.,* 2014a; David *et al.,* 2014b; De Buck *et al.,* 2014; You *et al.,* 2012). Biomarkers indicating early stages of MAP-infection were proposed by analyzing gene expression profiles of blood in cattle with experimental MAP infection (David *et al.,* 2014a; David *et al.,* 2014b). A metabolic profiling in cattle with experimental infection of MAP revealed that four metabolites (iso-butyrate, branched chain amino acids, leucine, and isoleucine) were increased in

serum of the MAP-infected cattle while citrate was decreased (De Buck *et al.*, 2014). Moreover, six proteins (transferrin, gelsolin isoforms α & β, complement subcomponent C1r, complement component C3, amine oxidase-copper containing 3, and coagulation factor II) were proposed as biomarkers after they were found to increase by at least 2-fold in MAP-infected cattle, as were two proteins (coagulation factor XIII-B polypeptide, and fibrinogen γ chain and its precursor) that were reduced by nearly two fold in MAP-infected cattle (You *et al.,* 2012). Our previous studies also proposed several biomarkers that were up-regulated in MAP infected macrophages, mice, and cattle (Cha *et al.,* 2013; Shin *et al.*, 2015a; Shin *et al.*, 2015b). Transcriptional profiles of MAP-infected macrophage RAW 264.7 cells and a mouse model suggested five and three genes as prognostic biomarkers, respectively (Cha *et al.,* 2013; Shin *et al.,* 2015b). β-defensins were also suggested as prognostic biomarkers in subclinical animals of MAP-naturally infected cattle (Shin *et al.*, 2015a). However, application of those biomarkers for diagnosis of JD has yet to be investigated. Therefore, we developed a real-time PCR method using the biomarkers for diagnosis of JD by measuring the gene expression level of several biomarkers in whole blood.

Materials and Methods

Experimental design and animals

About 300 Holstein cattle were raised on the national farm in Cheonan city which located in mid-west region of the South Korea. The cattle were regularly tested for absence of JD two times per year using fecal PCR and serum ELISA. A total of three to eight year old forty-four cows were selected for further analysis after detection of MAP-specific antibodies using a commercial ELISA kit (IDEXX Laboratories, Inc., Westbrook, ME, USA) and MAP in the feces by PCR (Park *et al.*, 2016). The detection was performed four times with a 6-month interval to enable accurate classification of infection status. The animals were divided into the following groups based on the results of PCR and ELISA: NN, PCR and ELISA negative; PN, PCR positive and ELISA negative; NP, PCR negative and ELISA positive; PP, PCR positive and ELISA positive. All animal procedures were approved by the National Institute of Animal Science (2013-046). Detailed characteristics of study subjects are shown in Table 6.

Selection of biomarker candidates

Nine genes that were significantly up-regulated in MAP infected macrophages,

mice, and cattle were selected for use as diagnostic biomarkers based on our previous studies (Table 7) (Cha *et al.*, 2013; Park *et al.*, 2016; Shin *et al.*, 2015a; Shin *et al.*, 2015b). All datasets used in selection of the biomarkers are available at Gene Expression Omnibus (GEO) under accession number GSE62836, http://dx.doi.org/10.4014/jmb.1302.02021, and http://dx.doi.org/10.4014/jmb.1408.08059

Extraction of total RNA from blood

Peripheral blood was collected from the tail vein of cattle using a BD Vacutainer® Plus Plastic K_2EDTA Tubes. A total of 125 μl of whole blood was then mixed with 125 μl of RNase-free water and 750 μl of Trizol LS reagent (Ambion, Foster City, CA, USA) and incubated at room temperature for 5 min. Next, 200 μl of chloroform was added to the mixture and it was centrifuged at 13,523 g and 4°C for 15 min. The supernatant was subsequently transferred to an RNAeasy column (Qiagen, Hilden, Germany) and centrifuged at 8,500 g for 15 sec. After washing, RNA was eluted in 30 μl of RNase-free water and immediately stored at -80°C until use.

Optimization of primer and probe concentrations

The optimal concentration of primer and probe concentration was determined with an identical cDNA template for each biomarker gene. Three concentrations (0.5 μM,

0.75 μM, and 1 μM) of both forward and reverse primers with a constant probe concentration were tested. The combination showing the highest fluorescence value was tested at three different concentrations of the probe (0.1 μM, 0. 2μM, and 0.3 μM). For further experiment, primer and probe concentration that showing the highest fluorescence value was selected.

Real-time PCR

Total RNA was employed to prepare cDNA with random primers using a QuantiTect® Reverse Transcription Kit (Qiagen Inc., Valencia, CA, USA) according to the manufacturer's instructions. The expression of nine biomarker genes was measured by quantitative real time RT-PCR, which was conducted using a Rotor-Gene multiplex PCR kit (Qiagen Inc., Valencia, CA, USA). In brief, total of 18 μl reaction mixture was prepared consists of 10 μl Master mix, RNase-free water, 0.5 μM forward and reverse primers, and 0.1 μM probe for each of the biomarker genes. After that, 2 μl of cDNA template was added to a final volume of 20 μl. The specificity of the primers and probes for each biomarker genes was confirmed by homology search (https://www.ncbi.nlm.nih.gov/tools/primer-blast) and agarose gel electrophoresis. The primers and probe used in this study are shown in Table 7. Sensitivity of real-time PCR reactions was confirmed by real-time PCR reaction using the known copy numbers calculated from purified PCR products which serially

diluted from 10^9 to 10^2 copies of the templates. The real-time PCR was conducted for 45 cycles and C_T values were obtained. Negative control was included with no template. Real-time PCR was conducted by subjecting the samples to 95°C for 10 min, followed by 50 cycles of 95°C for 15 s and 60°C for 45 s. The expression level was determined by the $2^{-\Delta\Delta Ct}$ method using the housekeeping gene, β-actin, as a reference.

Statistical analysis

Data were reported as the means ± the standard error of the mean (S.E.M.) of three independent experiments. Statistical significance was determined by ANOVA ($p \leq 0.05$) with Dunnett's post hoc test using the GraphPad Prism software version 7.00 (GraphPad Software, Inc., La Jolla, CA, USA). Receiver operator characteristics (ROC) curve analysis was conducted using the statistical package for social science (SPSS) software version 21.0 (SPSS Inc., Chicago, IL, USA) and the MedCalc Statistical Software version 13.3.3 (MedCalc Software, Ostend, Belgium). Higher AUC scores were considered to show better discriminatory powers as follows: excellent discriminatory power, AUC ≥0.9; good discriminatory power, 0.8≤AUC<0.9; fair discriminatory power, 0.7≤AUC<0.8; poor discriminatory power, AUC<0.7 (Muller *et al.*, 2005). The optimal cutoff values were calculated for each ROC curve while maximizing the Youden Index. Sensitivity and specificity were calculated based on cut-off value which showed highest AUC value in the ROC

curve for each biomarker gene. A p <0.05 was considered to indicate statistical significance.

Results

Specificity of probe and primers

Specificity of primers and probes were confirmed by homology search. Also, to confirm the specificity for each biomarker genes, RT-PCR and agarose gel electrophoresis was performed. Single PCR band were confirmed for each biomarker gene and the β-actin gene and non-specific PCR product was not observed confirmed in the negative control with no cDNA sample (Figure 12).

Sensitivity of real-time PCR reactions

Real-time PCR for the each biomarker gene was performed using the specific primers, probes and the purified PCR products. Amplification plots were presented for biomarker genes with increased template copy numbers from 10^2 to 10^9. Amplification plot shows that fluorescence increase with increased template copy numbers (Figure 13). Also, real-time PCR was highly sensitive to detect low level of gene expression of biomarker genes (about 10^2 copies of the template cDNA) and negative control sample with no template DNA showed no increasing of fluorescence

(Figure 13).

Optimization of primer and probe concentrations

The optimal concentration of primer and probe concentration was determined by conducting real-time PCR with three primer and probe concentrations. The combination of forward and reverse primer at 0.5 μM for biomarker genes and β-actin gene revealed highest florescence and lowest C_T value. With this primer concentration, 0.1 μM of probe showed highest florescence and lowest C_T value. Combination of 0.5 μM forward and reverse primers and 0.1μM probe concentration was used in further analysis.

Gene expression level of biomarkers in MAP infected cattle

Experimental animals were divided into four groups based on the results of fecal PCR and serum ELISA conducted three times with a 6 month interval. When compared with the non-infected NN group, expression of eight genes (*S100A8*, *DEFB1*, *DEFB10*, *MMP9*, *TIMP1*, *HP*, *SERPINE1*, and *TFRC*) showed higher expression in the PN group ($p<0.05$), while higher expression of seven other genes (*TIMP1*, *HP*, *SERPINE1*, *TFRC*, *DEFB1*, *DEFB10*, and *MMP9*) was observed in the NP group ($p <0.05$). Moreover, in the PP group, five genes (*S100A8*, *MMP9*, *HP*, *SERPINE1*, and *TFRC*) showed significantly higher expression in the PP group (*p*

<0.05). Four genes (*TFRC, HP, SERPINE1,* and *MMP9*) were up-regulated in all infected groups, while three genes (*TIMP1, DEFB1,* and *DEFB10*) were up-regulated in the PN group and the NP group, and S100A8 was up-regulated in the PN group and the PP group (Figure 14 and Table 8). The mean fold changes of each biomarker are shown in Table 8.

Discrimination between infected and non-infected animals

The AUC score of biomarkers was calculated during ROC analysis. In the PN group, the AUC scores of eight genes (*TIMP1, DEFB1, TFRC, DEFB10, S100A8, SERPINE1, MMP9,* and *HP*) were ≥0.8. In the NP group, four genes (*HP, TIMP1, TFRC,* and *SERPINE1*) had AUC scores ≥0.8, while six genes (*S100A8, HP, SERPINE1, TFRC, MMP9,* and *DEFB10*) in the PP group had AUC scores ≥0.8 (Figure 15). When the diagnostic accuracies of individual biomarkers were calculated by ROC curve analysis, the most accurate biomarker in the PN group was Timp1, with an AUC value of 0.985, while the most accurate biomarker in the NP group was *HP*, with an AUC value of 0.942. Additionally, the most accurate biomarker in the PP group was *S100A8,* with an AUC value of 0.896 (Figure 15). Similarly, in the PN group, *TIMP1* showed the most accurate diagnostic performance, with a sensitivity of 100% and a specificity of 90.9%. In the NP group, *HP* showed the most accurate diagnostic performance, with a sensitivity of 92.9% and a specificity of 90.9%. Moreover, *S100A8* showed the most accurate diagnostic

performance in the PP group, with a sensitivity of 85.7% and a specificity of 90%. Other details pertaining to the diagnostic performance of biomarkers are shown in Table 8.

Discussion

Early diagnosis of JD is the most important requirement to eradicate it from MAP-infected herds. However, current diagnostic methods are not sufficient for the diagnosis of subclinical stage animals that are actively dispersing MAP into the environment via fecal shedding (Tiwari *et al.,* 2006). Recently, several studies have attempted to diagnose subclinical stages of JD by analyzing host-pathogen interactions, including gene expression, miRNA, protein, and metabolites to MAP infection (David *et al.*, 2014a; David *et al.,* 2014b; De Buck *et al.,* 2014; Malvisi *et al.,* 2016; You *et al.,* 2012). Some of the studies have been conducted to identify prognostic biomarkers of JD by understanding host response to infection during the progression of JD (Cha *et al.,* 2013; Plain *et al.,* 2011; Seth *et al.,* 2009; Verschoor *et al.,* 2010; Wang *et al.,* 2011). However, no attempt has been made to apply biomarkers as diagnostic tools. Therefore, the present study was conducted to diagnose MAP infection using a real-time PCR method based on potential prognostic biomarkers.

In the present study, several biomarkers showed good discriminatory ability

(AUC≥0.8) between MAP-infected cattle and non-infected cattle. Three genes (*HP, SERPINE1,* and *TFRC*) showed good discriminatory ability (AUC≥0.8) in fecal PCR-positive and/or serum ELISA-positive groups (PN, NP, PP). Acute phase proteins are blood proteins that respond to infection and inflammation and have been used as diagnostic and prognostic biomarkers in veterinary medicine (Eckersall and Bell, 2010). *HP* is the major acute phase protein of cattle that responds to infection (Eckersall and Bell, 2010; El-Deeb and Elmoslemany, 2016). Moreover, *HP* is known to exert anti-inflammatory activity by down-regulating neutrophil activity via inhibition of both lipoxygenase and cycloxygenase (Saeed *et al.*, 2007) and to inhibit bacterial growth by interfering with iron acquisition by the host cell (Eaton *et al.*, 1982). Moreover, *HP* inhibits phagocytosis and intracellular killing of pathogens (Rossbacher *et al.*, 1999). This anti-inflammatory response induced by HP might reduce the harmful aspects of inflammation that could be destructive to the host itself. In that regard, up-regulation of *HP* in MAP-infected animals might be a host response to early infection of MAP. *HP* showed highest diagnostic accuracy for the NP group and whole infected animals, with AUC values of 0.942 and 0.901, respectively.

The initial response to MAP infection is dominant cell-mediated immunity, which is characterized by increasing interferon gamma release (Stabel, 2000). *SERPINE1* is known to be an essential element of the fibrinolytic system that is related to blood coagulation (Furie and Furie, 1988). *SERPINE1* also acts as an inflammatory mediator by increasing the level of interferon gamma in blood to eliminate the

pathogen in the early phase of an infectious disease (Lim *et al.,* 2011; Wang *et al.,* 2013). Therefore, increasing gene expression levels of Serpine1 might be related to interferon gamma release due to MAP infection. In addition, expression of *MAP0403* in MAP was increased in infected macrophages and MAC-T cells in recent study (Kugadas *et al.,* 2016). *MAP0403* is kind of serine protease which served as a key element of the stress response network in intraphagosomal survival of MAP (Kugadas *et al.,* 2016). Up-regulation of *SERPINE1* might be a counter response to intraphagosomal survival of MAP in host cells. The diagnostic accuracy of *SERPINE1* was good (AUC≥0.8) in all infected animals (PN, NP, PP group).

Iron is an important nutrient in innate immune response to bacterial pathogen (Johnson and Wessling-Resnick, 2012). *TFRC* is the one of the key elements of the iron metabolism, transfers iron to cells from transferrin protein (Johnson and Wessling-Resnick, 2012). *TFRC* is known to down-regulated in response to intracellular pathogen infection (Cha *et al.,* 2013); however, its expression was significantly increased in all infected animals in the present study. This phenomenon might be related to the alternative iron acquisition system of MAP, which acts in a host-independent manner using mycobactin (Wang *et al.,* 2015), however, further studies are needed to confirm this.

MMP9 is a matrix metalloproteinase related to leukocyte migration to infection sites and tissue destruction if it is secreted in excess amounts (Goetzl *et al.,* 1996). The level of MMP9 was regulated by TIMP1, which inhibits the activity of MMP9 (Goetzl *et al.,* 1996). *MMP9* and *TIMP1* are known to be up-regulated in tuberculosis

infection and have therefore been proposed as biomarkers for diagnosis of tuberculosis (Chen *et al.,* 2017). The simultaneous up-regulation of *MMP9* and *TIMP1* in infected animals might be caused by inflammatory conditions due to the early stages of MAP infection. Two genes (*MMP9* and *TIMP1*) showed good discriminatory ability (AUC≥0.8) in the PN group.

β-defensins exhibit antimicrobial functions, providing first protection against pathogens while playing an immune-modulation role (Meade *et al.,* 2014). Moreover, β-defensins interplay between innate and adaptive immune responses by down-regulating pro-inflammatory cytokines (Allaker, 2008). In the present study, *DEFB1* and *DEFB10* were significantly up-regulated in both the PN group and the NP group. Moreover, *DEFB1* and *DEFB10* showed excellent discriminatory ability (AUC≥ 0.9) in the PN group.

S100A8 and S100A9 are members of a calcium-binding cytosolic protein family that are located in the cytoplasm (Schiopu and Cotoi, 2013). S100A8 and S100A9 form a heterodimer known as calprotectin that induces an inflammatory response via activation of TLR4 signaling (Vogl *et al.,* 2007). Moreover, calprotectin is known to induce leukocyte migration in the early phase of bacterial infection (Achouiti *et al.,* 2012). In previous studies, serum S100A8/A9 have been proposed as prognostic biomarkers for disease progression and therapeutic response in inflammatory bowel diseases (IBD) (Cayatte *et al.,* 2012; Leach *et al.,* 2007). In the present study, *S100A8* showed good discriminatory ability (AUC≥0.8) in the PN and PP groups. However, gene expression of *S100A9* was not significant in all infected animals. Generally,

S100A8 and *S100A9* exist as heterodimers, but they also exist as homodimers (Vogl *et al.,* 2004). The inconsistent gene expression levels between *S100A8* and *S100A9* might be related to the presence of the homodimer form.

An ideal biomarker for diagnosis of JD should be able to discriminate between infected and non-infected animals with high sensitivity and specificity. Our data showed that the response of eight biomarkers (*HP, TIMP1, MMP9, SERPINE1, TFRC, S100A8, DEFB1,* and *DEFB10*) significantly discriminated MAP-infected and non-infected animals. Moreover, eight biomarkers (*HP, TIMP1, MMP9, SERPINE1, TFRC, S100A8, DEFB1,* and *DEFB10*) showed good accuracy (AUC≥ 0.7) for diagnosis of subclinical animals. Additionally, four genes (*TIMP1, S100A8, DEFB1*, and *DEFB10*) showed sensitivity over 80% and specificity over 90%. It is generally very difficult to detect subclinical stages of JD using currently available diagnostic methods such as bacterial culture, fecal PCR and serum ELISA (Mortier *et al.,* 2015). Fecal PCR is a reliable method for diagnosis of MAP infection; however, intermittent shedding of MAP into feces because of immunological changes during the progress of disease can interfere with accurate diagnosis (Mitchell *et al.,* 2015). Moreover, although serum ELISA is a simple, fast and cost-effective method for diagnosis of JD, it is known to have low sensitivity for MAP-infected animals that do not show clinical signs (Nielsen and Toft, 2008). However, our real-time PCR method based on biomarkers showed relatively precise diagnostic results. In that regard, combination of eight biomarker genes (*HP, TIMP1, MMP9, SERPINE1, TFRC, S100A8, DEFB1,* and *DEFB10*) might be used for diagnosis of

JD, including in subclinical stage animals.

In conclusion, a real-time PCR method was developed based on eight biomarkers that can be used as a new diagnostic tool for JD with good diagnostic performance. Moreover, this real-time PCR based on biomarkers might be used for diagnosis of JD, especially in subclinical stage animals that cannot be detected by current diagnostic methods. Although our developed diagnostic method might be applied to field test, this method will be more concreted if possible limitations in our study such as the low number of samples and sampling times would be addressed in future studies by including large scale field investigations.

Table 6. Characteristics of study subjects

Number of subjects		**All (*n*=44)**	**NN group (*n*=11)**	**PN group (*n*=12)**	**NP group (*n*=14)**	**PP group (*n*=7)**
Heifers, n (%)		44 (100)	11 (100)	12 (100)	14 (100)	7 (100)
Median age (Years)		6 (4 to 9)	4 (4 to 7)	6 (4 to 9)	6.5 (4 to 8)	6 (5 to 8)
Serum ELISA	Positive, n (%)	21 (47.7)	0 (0)	0 (0)	14 (100)	7 (100)
	Negative, n (%)	23 (52.3)	11 (100)	12 (100)	0 (0)	0
Fecal PCR	Positive, n (%)	19 (43.2)	0 (0)	12 (100)	0 (0)	7 (100)
	Negative, n (%)	25 (56.8)	11 (100)	0 (0)	14 (100)	0 (0)

Table 7. Oligonucleotide sequences of primers and probes used for real-time PCR

Target gene		Primer sequence (5'→3')	Product size (base pair)	Reference
β-ACTIN	F	GCAAGCAGGAGTACGATGAG	134	Park *et al.*, 2017
	R	GCCATGCCAATCTCATCTCG		
	Probe	FAM-TTCTAGGCGGACTGTTAGCTGCGTTACAC-BHQ1		
MMP9	F	CCCGGATCAAGGATACAGCC	177	Park *et al.*, 2016
	R	GGGCGAGGACCATACAGATG		
	Probe	HEX-AGTTTGGCCACGCGCTGGGCTTAGAT-BHQ1		
SERPINE1	F	CTGCGAAATTCAGGATGCGG	191	Park *et al.*, 2016
	R	GGGTGAGAAAACCACGTTGC		
	Probe	FAM-AGACTTTGGAGTGAAGGTGTTTCAGCAGG-BHQ1		
TIMP1	F	TCTGCAACTCCGATGTCGTC	125	Park *et al.*, 2017
	R	CCTCAAGGCACTGAACCCTT		
	Probe	HEX-GTTCGTGGGGACCGCAGAAGTCAATG-BHQ1		
HP	F	CCAAGTACCAGGACGACACC	131	Park *et al.*, 2017
	R	ACCATACTCAGCCACAGCAC		
	Probe	FAM-ACGACAAGGAAGACGACACCTGGTATGC-BHQ1		
S100A8	F	ATTTTGGGGAGACCTGGTGG	124	Park *et al.*, 2017
	R	ACGGCGTGGTAATTCCCTTT		
	Probe	FAM-TAACTCCCTGATTGACGTCTACCACAAG-BHQ1		
S100A9	F	AGGCTACGGGAAGGGCAG	134	Park *et al.*, 2016
	R	GCTGGCCTCCTGATTAGTGG		
	Probe	HEX-ATGGAGGTCACGGCCACAGCCAC-BHQ1		
TFRC	F	CAAAGTTTCTGCCAGCCCAC	188	Park *et al.*, 2016
	R	AACAGAAAGAGACCGCTGGG		
	Probe	HEX-TATCGGGACAGCAACTGGATCAGCAAAG-BHQ1		
DEFB1	F	CGAATGGAGGCATCTGTTTG	110	Park *et al.*, 2017
	R	CTTCGCCTTCTTTTACCACGA		
	Probe	FAM-TGCCCTGGACACATGATACAGATTGGCA-BHQ1		
DEFB10	F	ATCTAAGCTGCTGGGGGAAT	97	Park *et al.*, 2017
	R	CATTTTACTCGGGGCGCTAA		
	Probe	HEX-GTTTGCTTAACAGGTGCCCTGGAC-BHQ1		

Table 8. Mean fold change of selected biomarker genes between infected animals and non-infected animals

Accession No.	**Gene Symbol**	**Gene Name**	**Location**	**Mean fold change (log2 value)**					
				PN *vs.* NN	**P value**	**NP *vs.* NN**	**P value**	**PP *vs.* NN**	**P value**
NM_003234.2	*TFRC*	Transferrin receptor (p90, CD71)	Plasma membrane	1.6	0.0005	1.3	0.0021	1.9	0.0004
NM_174744	*MMP9*	Matrix metallopeptidase 9	Extracellular Space	2.9	0.008	2.4	0.0342	3.6	0.0052
NM_002964.4	*S100A8*	S100 calcium binding protein A8	Cytoplasm	1.6	0.0039	0.9	0.146	1.7	0.0069
NM_002965.3	*S100A9*	S100 calcium binding protein A9	Cytoplasm	0.4	0.6228	0.6	0.2596	1.1	0.0548
NM_174137	*SERPINE1*	Serpin peptidase inhibitor	Extracellular Space	1.9	0.0041	1.6	0.0183	2.6	0.0009
NM_005143.3	*HP*	Haptoglobin	Extracellular Space	2.3	0.0031	3.2	<0.0001	3.3	0.0003
NM_174471.3	*TIMP1*	Tissue inhibitor of metallopeptidase 1	Extracellular Space	1.7	<0.0001	1.4	0.0002	0.5	0.415
NM_001324544.1	*DEFB1*	Defensin beta 1	Extracellular Space	5.2	0.0009	3.3	0.039	1.8	0.5842
NM_001115084.1	*DEFB10*	Defensin beta 10	Extracellular Space	2.3	0.0017	1.6	0.0313	1.6	0.1009

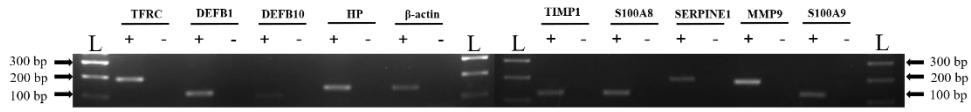

Figure 12. Gel electrophoresis of PCR products of biomarkers genes and β-actin gene. The biomarker genes and β-actin gene expression from bovine whole blood cDNA were confirmed by RT-PCR. A single PCR product was observed with expected size for each biomarker and β-actin gene. No band was observed in the PCR products of negative control without template DNA sample. In the figure (L) indicates 100 bp DNA size marker, (+) indicates PCR product with template cDNA, (-) indicates PCR product without cDNA.

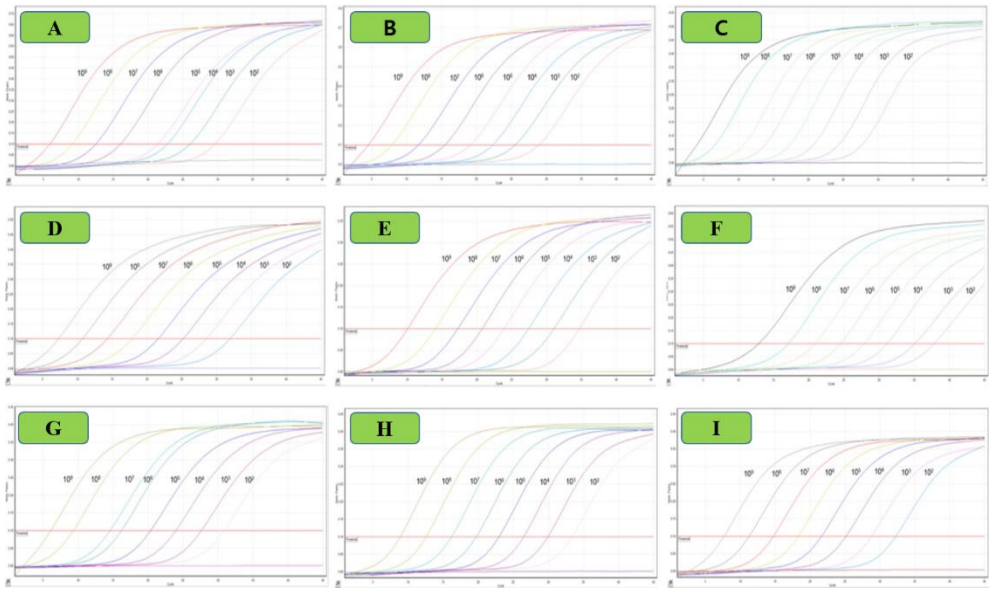

Figure 13. Amplification plots of the biomarker genes in the real-time PCR.

Real-time PCR was conducted with PCR product that serially diluted 10-fold from 10^9 to 10^2 copy numbers. The emission of fluorescence was measured at each cycle numbers and negative control sample with no template DNA showed no increasing of fluorescence. (A) *DEFB1*; (B) *DEFB10*; (C) *HP*; (D) *MMP9*; (E) *S100A8*; (F) *S100A9*; (G) *SERPINE1*; (H) *TFRC*; (I) *TIMP1*

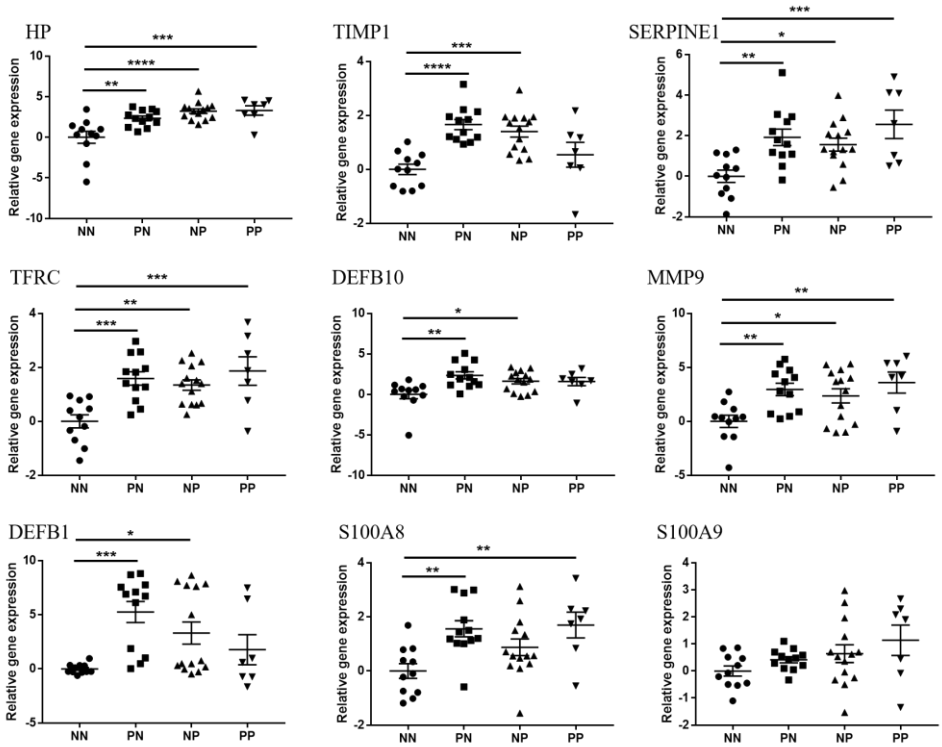

Figure 14. Gene expression level of biomarkers in MAP-infected cattle.

The gene expression level of biomarker genes in cattle infected with *Mycobacterium avium* subspecies *paratuberculosis* compared to non-infected cattle. The data are shown as scatter plots with each dot representing a single animal. (*, $p<0.05$ **, $p<0.01$ ***, $p<0.001$ ****, $p<0.0001$).

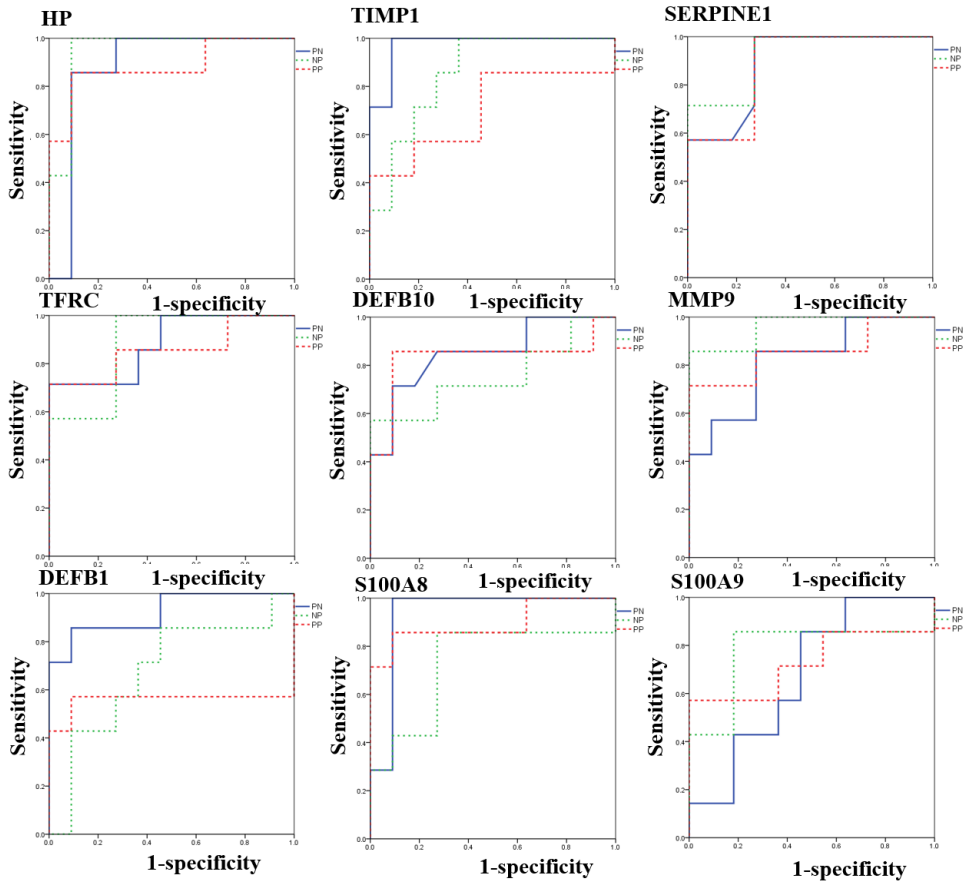

Figure 15. Discriminatory ability of biomarkers between infected animals and control animals.

Receiver operator characteristics curves of biomarker genes in cattle infected with *Mycobacterium avium* subspecies *paratuberculosis* compared to non-infected cattle.

General conclusions

Up to date, it is still far from complete understanding pathogenesis and efficient diagnostic method for the subclinical stage of MAP infection. To development effective diagnostic methods, it is necessary to understand host gene expression as which are involved in the pathogenesis of paratuberculosis. Several biomarkers were identified by gene expression profiling of whole blood was analyzed and the new real-time method was developed using host biomarker. Moreover, expression of immune-regulatory genes in whole blood of the subclinical animal was analyzed. Expression of immune-regulatory genes indicates that manipulation of host response for enhancing the survival of MAP.

1. Six genes (*CXCR3, HP, HGF, LTF, TFRC,* and *GBP6*) showed significant differences between experimental groups based on fecal shedding and ELISA S/P ratio. Taken together, our data suggest that six genes (*LTF, HGF, HP, CXCR3, GBP6*, and *TFRC*) played essential roles in immune response to the MAP during the subclinical stage and might be useful as prognostic biomarkers.

2. Downregulation of Th17 cytokine genes and upregulation of *PIP5K1C* induce loss of granuloma integrity results in fecal shedding and dissemination of the pathogen. Downregulation of *IRF4* resulted in the impaired Th1 immune

response, which decreased expression of *HMGB1* and enhanced the downregulation of the Th1 immune response. In addition, increased expression of *IRF5* and *IRF7* suggest that activation of IFN-α/β signaling during subclinical stages induce IDO-mediated tryptophan metabolism. IDO-mediated depletion of tryptophan indicates an inhibition of T cell proliferation, subsequently leading to an immunosuppressive state. Upregulation of *CORO1A* suggests the possibility of the failure to intracellularly eliminate MAP. Taken together, this model suggests manipulation of host responses for the survival of MAP that occurs during the subclinical phases of JD

3. A real-time PCR method was developed based on eight biomarkers (*HP, TIMP1, MMP9, SERPINE1, TFRC, S100A8, DEFB1,* and *DEFB10*) that can be used as a new diagnostic tool for JD with good diagnostic performance. Moreover, this real-time PCR based on biomarkers might be used for diagnosis of JD, especially in subclinical stage animals that cannot be detected by current diagnostic methods.

On the basis of these results, selected biomarkers and immune-regulatory genes seem to play important role in the pathogenesis of MAP during the subclinical stage. This study provided a deeper understanding of host responses to the MAP during the subclinical stage for the development of alternative diagnostic methods based on biomarkers.

References

Abendaño, N., Tyukalova, L., Barandika, J.F., Balseiro, A., Sevilla, I.A., Garrido, J.M., Juste, R.A., Alonso-Hearn, M., 2014. *Mycobacterium avium* subsp. *paratuberculosis* isolates induce in vitro granuloma formation and show successful survival phenotype, common anti-inflammatory and antiapoptotic responses within ovine macrophages regardless of genotype or host of origin. PLoS ONE, 9(8), e104238.

Achouiti, A., Vogl, T., Urban, C.F., Röhm, M., Hommes, T.J., van Zoelen, M.A., Florquin, S., Roth, J., van't Veer, C., de Vos, A.F., 2012. Myeloid-related protein-14 contributes to protective immunity in gram-negative pneumonia derived sepsis. PLoS Pathogens, 8(10), e1002987.

Adaska, J., Whitlock, R., 2012. Low rate of detectable in utero transmission of *Mycobacterium avium* subspecies *paratuberculosis* in a dairy herd with a low prevalence of Johne's disease. Journal of Veterinary Diagnostic Investigation, 24(1), 153-155.

Al Hajri, S., Alluwaimi, A., 2007. ELISA and PCR for evaluation of subclinical paratuberculosis in the Saudi dairy herds. Veterinary Microbiology, 121(3-4), 384-385.

Allaker, R., 2008. Host defence peptides-a bridge between the innate and adaptive immune responses. Transactions of the Royal Society of Tropical Medicine and Hygiene, 102(1), 3-4.

Andrés-Benito, P., Moreno, J., Domínguez, R., Aso, E., Povedano, M., Ferrer, I., 2017. Inflammatory gene expression in whole peripheral blood at early stages of sporadic

amyotrophic lateral sclerosis. Frontiers in Neurology, 8, 546.

Arsenault, R.J., Maattanen, P., Daigle, J., Potter, A., Griebel, P., Napper, S., 2014. From mouth to macrophage: mechanisms of innate immune subversion by *Mycobacterium avium* subsp. *paratuberculosis*. Veterinary Research, 45, 54.

Awuh, J.A., Haug, M., Mildenberger, J., Marstad, A., Do, C.P.N., Louet, C., Stenvik, J., Steigedal, M., Damås, J.K., Halaas, Ø., 2015. Keap1 regulates inflammatory signaling in *Mycobacterium avium*-infected human macrophages. Proceedings of the National Academy of Sciences of the United States of America, 112(31), E4272-4280.

Ayele, W., Bartos, M., Svastova, P., Pavlik, I., 2004. Distribution of *Mycobacterium avium* subsp. *paratuberculosis* in organs of naturally infected bull-calves and breeding bulls. Veterinary microbiology, 103(3-4), 209-217.

Bannantine, J.P., Bermudez, L.E., 2013. No holes barred: invasion of the intestinal mucosa by *Mycobacterium avium* subsp. *paratuberculosis*. Infection and Immunity, 81(11), 3960-3965.

Barnes, E.L., Liew, C.-C., Chao, S., Burakoff, R., 2015. Use of blood based biomarkers in the evaluation of Crohn's disease and ulcerative colitis. World Journal of Gastrointestinal Endoscopy, 7(17), 1233-1237.

Bates, A., O'Brien, R., Liggett, S., Griffin, F., 2018. The effect of sub-clinical infection with *Mycobacterium avium* subsp. *paratuberculosis* on milk production in a New Zealand dairy herd. BMC Veterinary Research, 14(1), 93.

Benedictus, G., Kalis, C., 2003. Paratuberculosis: eradication, control and diagnostic methods. Acta Veterinaria Scandinavica, 44(3-4), 231-241.

Bermudez, L.E., Petrofsky, M., Sommer, S., Barletta, R.G., 2010. Peyer's patch-deficient

mice demonstrate that *Mycobacterium avium* subsp. *paratuberculosis* translocates across the mucosal barrier via both m cells and enterocytes but has inefficient dissemination. Infection and Immunity, 78(8), 3570-3577.

Bernut, A., Nguyen-Chi, M., Halloum, I., Herrmann, J.-L., Lutfalla, G., Kremer, L., 2016. *Mycobacterium abscessus*-induced granuloma formation is strictly dependent on tnf signaling and neutrophil trafficking. PLoS Pathogens, 12(11),. e1005986.

Bhide, M., Chakurkar, E., Tkacikova, L., Barbuddhe, S., Novak, M., Mikula, I., 2006. IS900-PCR-based detection and characterization of *Mycobacterium avium* subsp. *paratuberculosis* from buffy coat of cattle and sheep. Veterinary Microbiology, 112(1), 33-41.

Bo, M., Erre, G., Niegowska, M., Piras, M., Taras, L., Longu, M., Passiu, G., Sechi, L., 2018. Interferon regulatory factor 5 is a potential target of autoimmune response triggered by Epstein-Barr virus and *Mycobacterium avium* subsp. *paratuberculosis* in rheumatoid arthritis: investigating a mechanism of molecular mimicry. Clinical and Experimental Rheumatology, 36(3), 376-381.

Bögli-Stuber, K., Kohler, C., Seitert, G., Glanemann, B., Antognoli, M., Salman, M., Wittenbrink, M., Wittwer, M., Wassenaar, T., Jemmi, T., 2005. Detection of *Mycobacterium avium* subspecies *paratuberculosis* in Swiss dairy cattle by real-time PCR and culture: a comparison of the two assays. Journal of Applied Microbiology, 99(3), 587-597.

Britton, L., Cassidy, J., O'Donovan, J., Gordon, S., Markey, B., 2016. Potential application of emerging diagnostic techniques to the diagnosis of bovine Johne's disease (paratuberculosis). Veterinary Journal, 209, 32-39.

Buergelt, C., Hall, C., McEntee, K., Duncan, J., 1978. Pathological evaluation of

paratuberculosis in naturally infected cattle. Veterinary Pathology, 15(2), 196-207.

Bukholm, G., Berdal, B., Haug, C., Degré, M., 1984. Mouse fibroblast interferon modifies *Salmonell*a typhimurium infection in infant mice. Infection and Immunity, 45(1), 62-66.

Bull, T., McMinn, E., Sidi-Boumedine, K., Skull, A., Durkin, D., Neild, P., Rhodes, G., Pickup, R., Hermon-Taylor, J., 2003. Detection and verification of *Mycobacterium avium* subsp. *paratuberculosis* in fresh ileocolonic mucosal biopsy specimens from individuals with and without Crohn's disease. Journal of Clinical Microbiology, 41(7), 2915-2923.

Carter, M., 2012. Prevalence and prevention of paratuberculosis in North America. The Japanese Journal of Veterinary Research, 60, Suppl:S9-18.

Casamassimi, A., Federico, A., Rienzo, M., Esposito, S., Ciccodicola, A., 2017. Transcriptome profiling in human diseases: new advances and perspectives. International Journal of Molecular Sciences, 18(8), E1652.

Casey, M.E., Meade, K.G., Nalpas, N.C., Taraktsoglou, M., Browne, J.A., Killick, K.E., Park, S.D., Gormley, E., Hokamp, K., Magee, D.A., 2015. Analysis of the bovine monocyte-derived macrophage response to *Mycobacterium avium* subspecies *paratuberculosis* infection using RNA-seq. Frontiers in Immunology, 6, 23.

Cayatte, C., Joyce-Shaikh, B., Vega, F., Boniface, K., Grein, J., Murphy, E., Blumenschein, W.M., Chen, S., Malinao, M.-C., Basham, B., 2012. Biomarkers of therapeutic response in the IL-23 pathway in inflammatory bowel disease. Clinical and Translational Gastroenterology, 3, e10.

Cha, S., Yoo, A., Park, H., Sung, K., Shin, M., Yoo, H., 2013. Analysis of transcriptional profiles to discover biomarker candidates in *Mycobacterium avium* subsp.

paratuberculosis-infected macrophages, RAW 264.7. Journal of Microbiology and Biotechnology, 23(8), 1167-1175.

Charavaryamath, C., Gonzalez-Cano, P., Fries, P., Gomis, S., Doig, K., Scruten, E., Potter, A., Napper, S., Griebel, P.J., 2013. Host responses to persistent *Mycobacterium avium* subspecies *paratuberculosis* infection in surgically isolated bovine ileal segments. Clinical and Vaccine Immunology, 20(2), 156-165.

Chase, CC., Hurley, DJ., Reber, AJ., 2008. Neonatal immune development in the calf and its impact on vaccine response. The Veterinary Clinics of North America Food Animal Practice, 24(1), 87-104.

Chen, X., Ba, Y., Ma, L., Cai, X., Yin, Y., Wang, K., Guo, J., Zhang, Y., Chen, J., Guo, X., 2008. Characterization of microRNAs in serum: a novel class of biomarkers for diagnosis of cancer and other diseases. Cell Research, 18(10), 997-1006.

Chen, Y., Wang, J., Ge, P., Cao, D., Miao, B., Robertson, I., Zhou, X., Zhang, L., Chen, H., Guo, A., 2017. Tissue inhibitor of metalloproteinases 1, a novel biomarker of tuberculosis. Molecular Medicine Reports, 15(1), 483-487.

Cheville, N., Hostetter, J., Thomsen, B., Simutis, F., Vanloubbeeck, Y., Steadham, E., 2001. Intracellular trafficking of *Mycobacterium avium* subsp. *paratuberculosis* in macrophages. Deutsche Tierarztliche Wochenschrift, 108(6), 236-243.

Chua, J., Vergne, I., Master, S., Deretic, V., 2004. A tale of two lipids: *Mycobacterium tuberculosis* phagosome maturation arrest. Current Opinion in Microbiology, 7(1), 71-77.

Clemens, D.L., Horwitz, M.A., 1995. Characterization of the *Mycobacterium tuberculosis* phagosome and evidence that phagosomal maturation is inhibited. Journal of Experimental Medicine, 181(1), 257-270.

Collins, M., Sockett, D., Goodger, W., Conrad, T., Thomas, C., Carr, D., 1994. Herd prevalence and geographic distribution of, and risk factors for, bovine paratuberculosis in Wisconsin. Journal of the American Veterinary Medical Association, 204(4), 636-641.

Collins, M., 1996. Diagnosis of paratuberculosis. The Veterinary Clinics of North America. Food Animal Practice, 12(2), 357-371.

Collins, M., 2011. Diagnosis of paratuberculosis. The Veterinary Clinics of North America. Food Animal Practice, 27(3), 581-591.

Cortes, Y., Ojeda, M., Araya, D., Dueñas, F., Fernández, M.S., Peralta, O.A., 2013. Isolation and multilineage differentiation of bone marrow mesenchymal stem cells from abattoir-derived bovine fetuses. BMC Veterinary Research, 9, 133.

Corti, S., Stephan, R., 2002. Detection of *Mycobacterium avium* subspecies *paratuberculosis* specific *IS900* insertion sequences in bulk-tank milk samples obtained from different regions throughout Switzerland. BMC Microbiology, 2, 15.

Cossu, D., Mameli, G., Galleri, G., Cocco, E., Masala, S., Frau, J., Marrosu, M., Manetti, R., Sechi, L., 2015. Human interferon regulatory factor 5 homologous epitopes of Epstein-Barr virus and *Mycobacterium avium* subsp. *paratuberculosis* induce a specific humoral and cellular immune response in multiple sclerosis patients. Multiple Sclerosis, 21(8), 984-995.

Coulter, F., Parrish, A., Manning, D., Kampmann, B., Mendy, J., Garand, M., Lewinsohn, D.M., Riley, E.M., Sutherland, J.S., 2017. IL-17 Production from T Helper 17, mucosal-associated invariant T, and γδ cells in tuberculosis infection and disease. Frontiers in Immunology, 8, 1252.

Cousins, D., Whittington, R., Marsh, I., Masters, A., Evans, R., Kluver, P., 1999.

Mycobacteria distenct from *Mycobacterium avium* subsp. *paratuberculosis* isolated from the faeces of ruminants possess *IS900*-like sequences detectable *IS900* polymerase chain reaction: implications for diagnosis. Molecular and Cellular Probes, 13(6), 431-442.

Coussens, P., 2001. *Mycobacterium paratuberculosis* and the bovine immune system. Animal Health Research Reviews, 2(2), 141-161.

Coussens, P.M., 2004. Model for immune responses to *Mycobacterium avium* subspecies *paratuberculosis* in cattle. Infection and Immunity, 72(6), 3089-3096.

Coussens, P.M., Verman, N., Coussens, M.A., Elftman, M.D., McNulty, A.M., 2004. Cytokine gene expression in peripheral blood mononuclear cells and tissues of cattle infected with *Mycobacterium avium* subsp. *paratuberculosis*: evidence for an inherent proinflammatory gene expression pattern. Infection and Immunity, 72(3), 1409-1422.

Cronan, M., Beerman, R., Rosenberg, A., Saelens, J., Johnson, M., Oehlers, S., Sisk, D., Jurcic, S.K., Medvitz, N., Miller, S., 2016. Macrophage epithelial reprogramming underlies mycobacterial granuloma formation and promotes infection. Immunity, 45(4), 861-876.

Dargatz, D., Byrum, B., Hennager, S., Barber, L., Kopral, C., Wagner, B., Wells, S., 2001. Prevalence of antibodies against *Mycobacterium avium* subsp. *paratuberculosis* among beef cow-calf herds. Journal of the American Veterinary Medical Association, 219(4), 497-501.

David, J., Barkema, H., Mortier, R., Ghosh, S., Guan, l.L., De Buck, J., 2014a. Gene expression profiling and putative biomarkers of calves 3 months after infection with *Mycobacterium avium* subspecies *paratuberculosis*. Veterinary Immunology and

Immunopathology, 160(1-2), 107-117.

David, J., Barkema, H.W., Le Luo Guan, J.D.B., 2014b. Gene-expression profiling of calves 6 and 9 months after inoculation with *Mycobacterium avium* subspecies *paratuberculosis*. Veterinary Research, 45, 96.

De Buck, J., Shaykhutdinov, R., Barkema, H.W., Vogel, H.J., 2014. Metabolomic profiling in cattle experimentally infected with *Mycobacterium avium* subsp. *paratuberculosis*. PLoS ONE, 9(11), e111872.

Dehnad, A., Ravindran, R., Subbian, S., Khan, I., 2016. Development of immune-biomarkers of pulmonary tuberculosis in a rabbit model. Tuberculosis, 101, 1-7.

Dernivoix, K., Roupie, V., Welby, S., Roelandt, S., Viart, S., Letesson, J., Wattiez, R., Huygen, K., Govaerts, M., 2017. Field performance of six *Mycobacterium avium* subsp. *paratuberculosis* antigens in a 20h interferon gamma release assay in Belgium. Veterinary Immunology and Immunopathology, 189, 17-27.

Devaux, Y., 2017. Transcriptome of blood cells as a reservoir of cardiovascular biomarkers. Biochimica et Biophysica Acta, 1864(1), 209-216.

Dhiman, R., Venkatasubramanian, S., Paidipally, P., Barnes, P.F., Tvinnereim, A., Vankayalapati, R., 2014. Interleukin 22 inhibits intracellular growth of mycobacterium tuberculosis by enhancing calgranulin a expression. The Journal of Infectious Diseases, 209(4), 578-587.

Dickinson, P., Smith, C.L., Forster, T., Craigon, M., Ross, A.J., Khondoker, M.R., Ivens, A., Lynn, D.J., Orme, J., Jackson, A., 2015. Whole blood gene expression profiling of neonates with confirmed bacterial sepsis. Genomics Data, 3, 41-48.

Doecke, J., Laws, S., Faux, N., Wilson, W., Burnham, S., Lam, C., Mondal, A., Bedo, J., Bush, A., Brown, B., 2012. Blood-based protein biomarkers for diagnosis of

Alzheimer disease. Archives of Neurology, 69(10), 1318-1325.

Donaghy, J., Linton, M., Patterson, M., Rowe, M., 2007. Effect of high pressure and pasteurization on *Mycobacterium avium* subsp. *paratuberculosis* in milk. Letters in Applied Microbiology, 45(2), 154-159.

Dubin, P., Kolls, J., 2008. Th17 cytokines and mucosal immunity. Immunological Reviews, 226, 160-171.

Eaton, J., Brandt, P., Mahoney, J., Lee Jr, J., 1982. Haptoglobin: a natural bacteriostat. Science, 215(4533), 691-693.

Eckersall, P., Bell, R., 2010. Acute phase proteins: Biomarkers of infection and inflammation in veterinary medicine. Veterinary Journal, 185(1), 23-27.

El-Deeb, W., Elmoslemany, A., 2016. Acute phase proteins as biomarkers of urinary tract infection in dairy cows: diagnostic and prognostic accuracy. The Japanese Journal of Veterinary Research, 64(1), 57-66.

Englund, S., Bölske, G., Johansson, K., 2002. An *IS900*-like sequence found in a *Mycobacterium* sp. other than *Mycobacterium avium* subsp. *paratuberculosis*. FEMS Microbiology Letters, 209(2), 267-271.

Fallarino, F., Grohmann, U., Vacca, C., Orabona, C., Spreca, A., Fioretti, M., Puccetti, P., 2003. T cell apoptosis by kynurenines. Advances in Experimental Medicine and Biology, 527, 183-190.

Farrell, D., Shaughnessy, R.G., Britton, L., MacHugh, D.E., Markey, B., Gordon, S.V., 2015. The identification of circulating miRNA in bovine serum and their potential as novel biomarkers of early *Mycobacterium avium* subsp *paratuberculosis* infection. PLoS ONE, 10(7), e0134310.

Fecteau, M., Hovingh, E., Whitlock, R., Sweeney, R., 2013. Persistence of *Mycobacterium*

avium subsp. *paratuberculosis* in soil, crops, and ensiled feed following manure spreading on infected dairy farms. The Canadian Veterinary Journal, 54(11), 1083-1085.

Feller, M., Huwiler, K., Stephan, R., Altpeter, E., Shang, A., Furrer, H., Pfyffer, G., Jemmi, T., Baumgartner, A., Egger, M. 2007. *Mycobacterium avium* subspecies *paratuberculosis* and Crohn's disease: a systematic review and meta-analysis. Lancet Infectius Disease, 7(9), 607-613.

Florou, M., Leontides, L., Kostoulas, P., Billinis, C., Sofia, M., Kyriazakis, I., Lykotrafitis, F., 2008. Isolation of *Mycobacterium avium* subspecies *paratuberculosis* from non-ruminant wildlife living in the sheds and on the pastures of Greek sheep and goats. Epidemiology and Infection, 136(5), 644-652.

Fratti, R., Chua, J., Deretic, V., 2003. Induction of p38 mitogen-activated protein kinase reduces early endosome autoantigen 1 (EEA1) recruitment to phagosomal membranes. The Journal of Biological Chemistry, 278(47), 46961-46967.

Frumento, G., Rotondo, R., Tonetti, M., Damonte, G., Benatti, U., Ferrara, G.B., 2002. Tryptophan-derived catabolites are responsible for inhibition of T and natural killer cell proliferation induced by indoleamine 2, 3-dioxygenase. The Journal of Experimental Medicine, 196(4), 459-468.

Furie, B., Furie, B., 1988. The molecular basis of blood coagulation. Cell, 53(4), 505-518.

Ganusov, V.V., Klinkenberg, D., Bakker, D., Koets, A.P., 2015. Evaluating contribution of the cellular and humoral immune responses to the control of shedding of *Mycobacterium avium* subsp. *paratuberculosis* in cattle. Veterinary Research, 46, 62.

Garcia, A., Shalloo, L., 2015. Invited review: The economic impact and control of

paratuberculosis in cattle. Journal of Dairy Science, 98(8), 5019-5039.

Gilmour, N., Gardiner, A., 1968. Detection of antibodies to *Mycobacterium johnei* by immunofluorescence. Journal of Comparative Pathology, 78(1), 107-113.

Goetzl, E., Banda, M., Leppert, D., 1996. Matrix metalloproteinases in immunity. Journal of Immunology, 156(1), 1-4.

Goyal, N., Kashyap, B., Singh, N., Kaur, I., 2017. Neopterin and oxidative stress markers in the diagnosis of extrapulmonary tuberculosis. Biomarkers, 22(7), 648-653

Groenendaal, H., Galligan, D., 2003. Economic consequences of control programs for paratuberculosis in midsize dairy farms in the United States. Journal of the American Veterinary Medical Association, 223(12), 1757-1763.

Guffanti, A., Iacono, M., Pelucchi, P., Kim, N., Soldà, G., Croft, L.J., Taft, R.J., Rizzi, E., Askarian-Amiri, M., Bonnal, R.J., 2009. A transcriptional sketch of a primary human breast cancer by 454 deep sequencing. BMC Genomics, 10, 163.

Guirado, E., Schlesinger, L.S., Kaplan, G. 2013. Macrophages in tuberculosis: friend or foe. Seminars in Immunopathology, 35(5), 563-583.

Hamada, S., Umemura, M., Shiono, T., Tanaka, K., Yahagi, A., Begum, M.D., Oshiro, K., Okamoto, Y., Watanabe, H., Kawakami, K., 2008. IL-17A produced by γδ T cells plays a critical role in innate immunity against *Listeria monocytogenes* infection in the liver. Journal of Immunology, 181(5), 3456-3463.

Holcomb, Z., Tsalik, E., Woods, C., McClain, M., 2017. Host-based peripheral blood gene expression analysis for diagnosis of infectious diseases. Journal of Clinical Microbiology, 55(2), 360-368.

Honda, K., Taniguchi, T., 2006. IRFs: master regulators of signalling by Toll-like receptors and cytosolic pattern-recognition receptors. Nature Reviews Immunology, 6(9),

644-658.

Hostetter, J., Steadham, E., Haynes, J., Bailey, T., Cheville, N., 2003. Phagosomal maturation and intracellular survival of *Mycobacterium avium* subspecies *paratuberculosis* in J774 cells. Comparative Immunology, Microbiology and Infectious Diseases, 26(4), 269-283.

Huda, A., Jungersen, G., Lind, P., 2004. Longitudinal study of interferon-gamma, serum antibody and milk antibody responses in cattle infected with *Mycobacterium avium* subsp. *paratuberculosis*. Veterinary Microbiology, 104(1-2), 43-53.

Hughes, V., McNair, J., Strain, S., Barry, C., McLuckie, J., Nath, M., Caldow, G., Stevenson, K., 2017. Gamma interferon responses to proteome-determined specific recombinant proteins in cattle experimentally-and naturally-infected with paratuberculosis. Research in Veterinary Science, 114, 244-253.

Huntley, J.F., Stabel, J.R., Bannantine, J.P., 2005. Immunoreactivity of the *Mycobacterium avium* subsp. *paratuberculosis* 19-kDa lipoprotein. BMC Microbiology, 5, 3.

Hwang, J., Markkandan, K., Kwon, M., Seo, J., Yoo, S., Hwang, S., Son, M., Park, J., 2018. Transcriptome analysis of olive flounder (*Paralichthys olivaceus*) head kidney infected with moderate and high virulent strains of infectious viral hemorrhagic septicaemia virus (VHSV). Fish & Shellfish Immunology, 76, 293-304.

Irenge, L., Walravens, K., Govaerts, M., Godfroid, J., Rosseels, V., Huygen, K., Gala, J., 2009. Development and validation of a triplex real-time PCR for rapid detection and specific identification of *Mycobacterium. avium* subsp. *paratuberculosis* in faecal samples. Veterinary Microbiology, 136(1-2), 166-172.

Ishihara, T., Aga, M., Hino, K., Ushio, C., Taniguchi, M., Iwaki, K., Ikeda, M., Kurimoto, M., 2005. Inhibition of chlamydia trachomatis growth by human interferon-alpha:

mechanisms and synergistic effect with interferon-gamma and tumor necrosis factor-alpha. Biomedical Research, 26(4), 179-185.

Jayachandran, R., Pieters, J., 2015. Regulation of immune cell homeostasis and function by coronin 1. International Immunopharmacology, 28(2), 825-828.

Jayachandran, R., Sundaramurthy, V., Combaluzier, B., Mueller, P., Korf, H., Huygen, K., Miyazaki, T., Albrecht, I., Massner, J., Pieters, J., 2007. Survival of mycobacteria in macrophages is mediated by coronin 1-dependent activation of calcineurin. Cell, 130(1), 37-50.

Jimenez-Luna, C., Torres, C., Ortiz, R., Dieguez, C., Martinez-Galan, J., Melguizo, C., Prados, J.C., Caba, O., 2018. Proteomic biomarkers in body fluids associated with pancreatic cancer. Oncotarget, 9(23), 16573-16587.

Johnson, E.E., Wessling-Resnick, M., 2012. Iron metabolism and the innate immune response to infection. Microbes and Infection, 14(3), 207-216.

Jungersen, G., Mikkelsen, H., Grell, S., 2012. Use of the johnin PPD interferon-gamma assay in control of bovine paratuberculosis. Veterinary Immunology and Immunopathology, 148(1-2), 48-54.

Kalis, C., Collins, M., Hesselink, J., Barkema, H., 2003. Specificity of two tests for the early diagnosis of bovine paratuberculosis based on cell-mediated immunity: the Johnin skin test and the gamma interferon assay. Veterinary Microbiology, 97(1-2), 73-86.

Kamel, H.F.M., Al-Amodi, H.S.A.B., 2017. Exploitation of gene expression and cancer biomarkers in paving the path to era of personalized medicine. Genomics. Proteomics & Bioinformatics, 15(4), 220-235.

Kaur, P., Filia, G., Singh, S., Patil, P., Ravi, K.G., Sandhu, K., 2011. Molecular epidemiology of *Mycobacterium avium* subspecies *paratuberculosis*: *IS900* PCR identification

and *IS1311* polymorphism analysis from ruminants in the Punjab region of India. Comparative Immunology. Microbiology and Infectious Diseases, 34(2), 163-169.

Keane, R.W., Dietrich, W.D., de Rivero Vaccari, J.P., 2018. Inflammasome proteins as biomarkers of multiple sclerosis. Frontiers in Neurology, 9, 135.

Keown, D.A., Collings, D.A., Keenan, J.I., 2012. Uptake and persistence of *Mycobacterium avium* subsp. *paratuberculosis* in human monocytes. Infection and Immunity, 80(11), 3768-3775.

Khare, S., Drake, K.L., Lawhon, S.D., Nunes, J.E., Figueiredo, J.F., Rossetti, C.A., Gull, T., Everts, R.E., Lewin, H.A., Adams, L.G., 2016. Systems analysis of early host gene expression provides clues for transient *Mycobacterium avium* subsp. *avium* vs. persistent *Mycobacterium avium* subsp. *paratuberculosis* intestinal infections. PLoS ONE, 11(9), e0161946.

Kim, B., Shenoy, A., Kumar, P., Das, R., Tiwari, S., MacMicking, J., 2011. A family of IFN-γ-inducible 65-kD GTPases protects against bacterial infection. Science, 332(6030), 717-721.

Kim, J., Ahn, J., Woo, S., Jo, D., Jo, Y., Park, J., Yoon, Y., Chang, G., 1994. A survey of paratuberculosis by immunological methods in dairy and Korean native cattle. Korean Journal of Veterinary Research, 34(1), 93-97..

Kim, J., Ku, B., Lee, H., Hwang, I., Jang, Y., Kim, J., Hyun, B., Jung, S., 2013. *Mycobacterium avium paratuberculosis* in wild boars in Korea. Journal of Wildlife Diseases, 49(2), 413-417.

Koets, A., Rutten, V., Hoek, A., Bakker, D., van Zijderveld, F., Müller, K., van Eden, W., 1999. Heat-shock protein-specific T-cell responses in various stages of bovine paratuberculosis. Veterinary Immunology and Immunopathology, 70(1-2), 105-115.

Koets, A.P., Eda, S., Sreevatsan, S., 2015. The within host dynamics of *Mycobacterium avium* subsp. *paratuberculosis* infection in cattle: where time and place matter. Veterinary Research, 46, 61.

Koo, H C., Park, Y H., Hamilton, M J., Barrington, G M., Davies, C J., Kim, J B., Dahl, J L., Waters, W R., Davis, W C., 2004. Analysis of the immune response to *Mycobacterium avium* subsp. *paratuberculosis* in experimentally infected calves. Infection and Immunity, 72(12), 6870-6883

Koul, A., Herget, T., Klebl, B., Ullrich, A., 2004. Interplay between mycobacteria and host signalling pathways. Nature Reviews. Microbiology, 2(3), 189-202.

Kugadas, A., Lamont, E., Bannantine, J., Shoyama, F., Brenner, E., Janagama, H., Sreevatsan, S., 2016. A *Mycobacterium avium* subsp. *paratuberculosis* predicted serine protease is associated with acid stress and intraphagosomal survival. Frontiers in Cellular and Infection Microbiology, 6, 85.

Lamont, E.A., O'Grady, S.M., Davis, W.C., Eckstein, T., Sreevatsan, S., 2012. Infection with *Mycobacterium avium* subsp. *paratuberculosis* results in rapid interleukin-1β release and macrophage transepithelial migration. Infection and Immunity, 80(9), 3225-3235.

Leach, S., Yang, Z., Messina, I., Song, C., Geczy, C., Cunningham, A., Day, A., 2007. Serum and mucosal S100 proteins, calprotectin (S100A8/S100A9) and S100A12, are elevated at diagnosis in children with inflammatory bowel disease. Scandinavian Journal of Gastroenterology, 42(11), 1321-1341.

Lee, K., Jung, B., 2009. Seroprevalence of *Mycobacterium avium* subspecies *paratuberculosis* in cattle in Korea. The Veterinary Record, 165(22), 661-662.

Lee, K., Jung, B., Moon, O., Yang, D., Lee, S., Kim, J., Kweon, C., 2006. Seroprevalence of

Mycobacterium avium subspecies *paratuberculosis* in Korean black goats (*Capra hircus aegagrus*). The Journal of Veterinary Medical Science, 68(12), 1379-1381.

Li, H., Hong, G., Lin, M., Shi, Y., Wang, L., Jiang, F., Zhang, F., Wang, Y., Guo, Z., 2017. Identification of molecular alterations in leukocytes from gene expression profiles of peripheral whole blood of Alzheimer's disease. Scientific Reports 7(1), 14027.

Li, X., Conklin, L., Alex, P., 2008. New serological biomarkers of inflammatory bowel disease. World Journal of Gastroenterology, 14(33), 5115-24.

Li, X., Lin, Z., Zhan, X., Gao, J., Sun, L., Cao, Y., Qiu, H., 2018. RNA-seq analysis of the transcriptome of the liver of cynomolgus monkeys with type 2 diabetes. Gene, 651, 118-125.

Lim, J.H., Woo, C.-H., Li, J.-D., 2011. Critical role of type 1 plasminogen activator inhibitor (PAI-1) in early host defense against nontypeable *Haemophilus influenzae* infection. Biochemical and Biophysical Research Communications 414(1), 67-72.

Lombard, J., 2011. Epidemiology and economics of paratuberculosis. The Veterinary clinics of North America. Food Animal Practice 27(3), 525-535.

Lombard, J., Gardner, I., Jafarzadeh, S., Fossler, C., Harris, B., Capsel, R., Wagner, B., Johnson, W., 2013. Herd-level prevalence of *Mycobacterium avium* subsp. *paratuberculosis* infection in United States dairy herds in 2007. Preventive Veterinary Medicine, 108(2-3), 234-238

Lotze, M., Tracey, K., 2005. High-mobility group box 1 protein (HMGB1): nuclear weapon in the immune arsenal. Nature Reviews. Immunology, 5(4), 331-342.

Magombedze, G., Eda, S., Koets, A., 2016. Can immune response mechanisms explain the fecal shedding patterns of cattle infected with *Mycobacterium avium* subspecies *paratuberculosis*? PLoS ONE, 11(1), e0146844.

Mahnke, J., Schumacher, V., Ahrens, S., Käding, N., Feldhoff, L.M., Huber, M., Rupp, J., Raczkowski, F., Mittrücker, H.-W., 2016. Interferon regulatory factor 4 controls TH1 cell effector function and metabolism. Scientific Reports 6, 35521.

Malvisi, M., Palazzo, F., Morandi, N., Lazzari, B., Williams, J.L., Pagnacco, G., Minozzi, G., 2016. Responses of bovine innate immunity to *Mycobacterium avium* subsp. *paratuberculosis* Infection revealed by changes in gene expression and levels of microRNA. PLoS ONE, 11(10), e0164461.

Mameli, G., Cocco, E., Frau, J., Marrosu, M.G., Sechi, L.A., 2016. Epstein Barr virus and *Mycobacterium avium* subsp. *paratuberculosis* peptides are recognized in sera and cerebrospinal fluid of MS patients. Scientific Reports 6, 22401.

Manda, S., Kataria, Y., Tatireddy, B., Ramakrishnan, B., Ratnam, B., Lath, R., Ranjan, A., Ray, A., 2017. Exosomes as a biomarker platform for detecting epidermal growth factor receptor-positive high-grade gliomas. Journal of Neurosurgery, 128(4), 1091-1101.

Marino, R., Capoferri, R., Panelli, S., Minozzi, G., Strozzi, F., Trevisi, E., Snel, G., Ajmone-Marsan, P., Williams, J., 2017. Johne's disease in cattle: an in vitro model to study early response to infection of *Mycobacterium avium* subsp. *paratuberculosis* using RNA-seq. Molecular Immunology, 91, 259-271.

Mayeux, R., 2004. Biomarkers: potential uses and limitations. Journal of the American Society for Experimental NeuroTherapeutics, 1(2), 182-188.

McNab, F., Mayer-Barber, K., Sher, A., Wack, A., O'Garra, A., 2015. Type I interferons in infectious disease. Nature Reviews Immunology, 15(2), 87-103.

Meade, K., Cormican, P., Narciandi, F., Lloyd, A., O'Farrelly, C., 2014. Bovine β-defensin gene family: opportunities to improve animal health? Physiological Genomics,

46(1), 17-28.

Mejias, A., Dimo, B., Suarez, N.M., Garcia, C., Suarez-Arrabal, M.C., Jartti, T., Blankenship, D., Jordan-Villegas, A., Ardura, M.I., Xu, Z., 2013. Whole blood gene expression profiles to assess pathogenesis and disease severity in infants with respiratory syncytial virus infection. PLoS Medicine, 10(11), e1001549.

Mercier, P., Freret, S., Laroucau, K., Gautier, M., Brémaud, I., Bertin, C., Rossignol, C., Souriau, A., Guilloteau, L., 2016. A longitudinal study of the *Mycobacterium avium* subspecies *paratuberculosis* infection status in young goats and their mothers. Veterinary Microbiology, 195, 9-16

Minnikin, D., Minnikin, S., Parlett, J., Goodfellow, M., Magnusson, M., 1984. Mycolic acid patterns of some species of *Mycobacterium*. Archives of Microbiology, 139(2-3), 225-31.

Miot, C., Beaumont, E., Duluc, D., Le Guillou-Guillemette, H., Preisser, L., Garo, E., Blanchard, S., Hubert, F.I., Créminon, C., Lamourette, P., 2015. IL-26 is overexpressed in chronically HCV-infected patients and enhances TRAIL-mediated cytotoxicity and interferon production by human NK cells, Gut 64(9), 1466-1475.

Mita, A., Mori, Y., Nakagawa, T., Tasaki, T., Utiyama, K., Mori, H., 2016. Comparison of fecal pooling methods and DNA extraction kits for the detection of *Mycobacterium avium* subspecies *paratuberculosis*. MicrobiologyOpen, 5(1), 134-142.

Mitchell, R.M., Schukken, Y., Koets, A., Weber, M., Bakker, D., Stabel, J., Whitlock, R.H., Louzoun, Y., 2015. Differences in intermittent and continuous fecal shedding patterns between natural and experimental *Mycobacterium avium* subspecies *paratuberculosis* infections in cattle. Veterinary Research 46, 66.

Momotani, E., Whipple, D., Thiermann, A., Cheville, N., 1988. Role of M cells and

macrophages in the entrance of *Mycobacterium paratuberculosis* into domes of ileal Peyer's patches in calves. Veterinary Pathology. 25(2), 131-7.

Momotani, E., 2012. Epidemiological situation and control strategies for paratuberculosis in Japan. The Japanese Journal of Veterinary Research 60, Suppl, S19-29.

Mortier, R., Barkema, H., De Buck, J., 2015. Susceptibility to and diagnosis of *Mycobacterium avium* subspecies *paratuberculosis* infection in dairy calves: A review. Preventive Veterinary Medicine, 121(3-4), 189-198.

Moyer, V., Force, U.P.S.T., 2012. Screening for prostate cancer: US preventive services task force recommendation statement. Annals of Internal Medicine, 157(2), 120-134.

Münster, P., Fechner, K., Völkel, I., von Buchholz, A., Czerny, C., 2013. Distribution of *Mycobacterium avium* subsp. *paratuberculosis* in a German zoological garden determined by *IS900* semi-nested and quantitative real-time PCR. Veterinary Microbiology, 163(1-2), 116-123.

Muller, M., Tomlinson, G., Marrie, T., Tang, P., McGeer, A., Low, D., Detsky, A., Gold, W., 2005. Can routine laboratory tests discriminate between severe acute respiratory syndrome and other causes of community-acquired pneumonia? Clinical Infectious Diseases, 40(8), 1079-1086.

Munn, D., Sharma, M., Baban, B., Harding, H., Zhang, Y., Ron, D., Mellor, A., 2005. GCN2 kinase in T cells mediates proliferative arrest and anergy induction in response to indoleamine 2, 3-dioxygenase. Immunity, 22(5), 633-42.

Mutz, K., Heilkenbrinker, A., Lönne, M., Walter, J., Stahl, F., 2013. Transcriptome analysis using next-generation sequencing. Current Opinion in Biotechnology, 24(1), 22-30.

Nakamura, T., Sakai, K., Nakamura, T., Matsumoto, K., 2011. Hepatocyte growth factor twenty years on: Much more than a growth factor. Journal of Gastroenterology and

Hepatology, 26 Suppl 1, 188-202.

Nam, S., Lim, J., 2016. Essential role of interferon regulatory factor 4 (IRF4) in immune cell development. Archives of Pharmacal Research, 39(11), 1548-1555.

Nielsen, S., Hansen, K., Kvist, L., Kostoulas, P., 2016. Dam's infection progress and within-herd prevalence as predictors of *Mycobacterium avium* subsp. *paratuberculosis* ELISA response in Danish Holstein cattle. Preventive Veterinary Medicine, 125, 54-58.

Nielsen, S., Toft, N., 2008. Ante mortem diagnosis of paratuberculosis: a review of accuracies of ELISA, interferon-gamma assay and faecal culture techniques. Veterinary Microbiology, 129(3-4), 217-35.

Nielsen, S., Toft, N., 2009. A review of prevalences of paratuberculosis in farmed animals in Europe. Preventive Veterinary Medicine, 88(1), 1-14.

Okuni, J.B., Dovas, C.I., Loukopoulos, P., Bouzalas, I.G., Kateete, D.P., Joloba, M.L., Ojok, L., 2012. Isolation of *Mycobacterium avium* subspecies *paratuberculosis* from Ugandan cattle and strain differentiation using optimised DNA typing techniques. BMC Veterinary Research, 8, 99.

Ott, S.L., Wells, S.J., Wagner, B.A., 1999. Herd-level economic losses associated with Johne's disease on US dairy operations. Preventive Veterinary Medicine, 40(3-4), 179-92.

Ozturk, D., Pehlivanoglu, F., Tok, A., Gunlu, S., Guldali, Y., Turutoglu, H., 2010. Seroprevalence of paratuberculosis in the Burdur province (Turkey), in dairy cattle using the enzyme linked immunosorbent assay (ELISA). Israel Journal of Veterinary Medicine, 65(2), 53-57.

Pak, S., Kim, D., Salman, M., 2003. Estimation of paratuberculosis prevalence in dairy cattle

in a province of Korea using an enzyme-linked immunosorbent assay: application of Bayesian approach. Journal of Veterinary Science, 4(1), 51-56.

Park, H E., Shin, M., Park, H., Jung, M., Cho, Y., Yoo, H., 2016. Gene expression profiles of putative biomarker candidates in *Mycobacterium avium* subsp. *paratuberculosis*-infected cattle. Pathogens and Disease, 74(4), ftw022.

Park, H E., Park, H.T., Jung, Y.H., Yoo, H.S., 2017. Establishment a real-time reverse transcription PCR based on host biomarkers for the detection of the subclinical cases of *Mycobacterium avium* subsp. *paratuberculosis*. PLoS ONE, 12(5), e0178336.

Park, H.T., Shin, M.K., Sung, K.Y., Park, H.E., Cho, Y.I., Yoo, H.S., 2014. Effective DNA extraction method to improve detection of *Mycobacterium avium* subsp. *paratuberculosis* in bovine feces. Korean Journal of Veterinary Research, 54, 55-57.

Park, H.T., Park, H.E., Cho, Y.I., Kim, E.H., Jung, M., Shin, S.W., Lee, S.-H., Kim, D.-Y., Yoo, H.S., 2017. Potential biomarkers as an indicator of vertical transmission of Johne's disease in a Korean native cattle farm. Journal of Veterinary Science, 18(S1), 343-349.

Park, K.T., Allen, A.J., Bannantine, J.P., Seo, K.S., Hamilton, M.J., Abdellrazeq, G.S., Rihan, H.M., Grimm, A., Davis, W.C., 2011. Evaluation of two mutants of *Mycobacterium avium* subsp. *paratuberculosis* as candidates for a live attenuated vaccine for Johne’s disease. Vaccine, 29(29-30), 4709-4719.

Park, K.T., Allen, A.J., Barrington, G.M., Davis, W.C., 2014b. Deletion of relA abrogates the capacity of *Mycobacterium avium paratuberculosis* to establish an infection in calves. Frontiers in Cellular and Infection Microbiology 4, 64.

Park, K.T., Dahl, J.L., Bannantine, J.P., Barletta, R.G., Ahn, J., Allen, A.J., Hamilton, M.J., Davis, W.C., 2008. Demonstration of allelic exchange in the slow-growing

bacterium *Mycobacterium avium* subsp. *paratuberculosis*, and generation of mutants with deletions at the pknG, relA, and lsr2 loci. Applied and Environmental Microbiology, 74(6), 1687-1695.

Payne, J., Rankin, J.D., 1961. A comparison of the pathogenesis of experimental Johne's disease in calves and cows. Research in Veterinary Science, 2, 175-179

Peck, A., Nguyen, C., 2012. Transcriptome analysis of the interferon-signature defining the autoimmune process of sjögren's syndrome. Scandinavian Journal of Immunology, 76(3), 237-45.

Plain, K.M., de Silva, K., Earl, J., Begg, D.J., Purdie, A.C., Whittington, R.J., 2011. Indoleamine 2, 3-dioxygenase, tryptophan catabolism, and *Mycobacterium avium* subsp. *paratuberculosis*: a model for chronic mycobacterial infections. Infection and Immunity, 79(9), 3821-3832.

Plattner, B.L., Doyle, R.T., Hostetter, J.M., 2009. Gamma–delta T cell subsets are differentially associated with granuloma development and organization in a bovine model of mycobacterial disease. International Journal of Experimental Pathology, 90(6), 587-97.

Pomorska-Mól, M., Markowska-Daniel, I., Pejsak, Z., 2012. Acute phase protein response during subclinical infection of pigs with H1N1 swine influenza virus. Veterinary Microbiology, 159(3-4), 499-503.

Premanandan, C., Storozuk, C., Clay, C., Lairmore, M., Schlesinger, L., Phipps, A., 2009. Complement protein C3 binding to *Bacillus anthracis* spores enhances phagocytosis by human macrophages. Microbial Pathogenesis, 46(6), 306-314.

Queval, C., Brosch, R., Simeone, R., 2017. The Macrophage: A disputed fortress in the battle against *Mycobacterium tuberculosis*. Frontiers in Microbiology, 8, 2284.

Raffatellu, M., Santos, R.L., Verhoeven, D.E., George, M.D., Wilson, R.P., Winter, S.E., Godinez, I., Sankaran, S., Paixao, T.A., Gordon, M.A., 2008. Simian immunodeficiency virus–induced mucosal interleukin-17 deficiency promotes Salmonella dissemination from the gut. Nature Medicine, 14(4), 421-8.

Raizman, E.A., Habteselassie, M.Y., Wu, C.C., Lin, T.L., Negron, M., Turco, R.F., 2011. Leaching of *Mycobacterium avium* subsp *paratuberculosis* in soil under in vitro conditions. Veterinary Medicine International, 2011, 506239.

Rathnaiah, G., Zinniel, D.K., Bannantine, J.P., Stabel, J.R., Gröhn, Y.T., Collins, M.T., Barletta, R.G., 2017. Pathogenesis, molecular genetics, and genomics of *Mycobacterium avium* subsp. *paratuberculosis*, the etiologic agent of Johne's disease. Frontiers in Veterinary Science, 4, 187.

Rendon-Mitchell, B., Ochani, M., Li, J., Han, J., Wang, H., Yang, H., Susarla, S., Czura, C., Mitchell, R., Chen, G., 2003. IFN-gamma induces high mobility group box 1 protein release partly through a TNF-dependent mechanism. Journal of Immunology, 170(7), 3890-3897.

Rhodes, G., Henrys, P., Thomson, B., Pickup, R., 2013. *Mycobacterium avium* subspecies *paratuberculosis* is widely distributed in British soils and waters: implications for animal and human health. Environmental Microbiology, 15(10), 2761-2774.

Robinson, M., O'Brien, R., Mackintosh, C., Clark, R., Griffin, J., 2011. Immunoregulatory cytokines are associated with protection from immunopathology following *Mycobacterium avium* subspecies *paratuberculosis* infection in red deer. Infection and Immunity, 79(5), 2089-2097.

Rohde, R., Shulaw, W., 1990. Isolation of *Mycobacterium paratuberculosis* from the uterine flush fluids of cows with clinical paratuberculosis. Journal of the American

Veterinary Medical Association, 197(11), 1482-1483.

Rohde, R., Shulaw, W., Hueston, W., Bech-Nielsen, S., Haibel, G., Hoffsis, G., 1990. Isolation of *Mycobacterium paratuberculosis* from washed bovine ova after in vitro exposure. American Journal of Veterinary Research, 51(5), 708-710.

Rossbacher, J., Wagner, L., Pasternack, M., 1999. Inhibitory effect of haptoglobin on granulocyte chemotaxis, phagocytosis and bactericidal activity. Scandinavian Journal of Immunology, 50(4), 399-404.

Rossiter, C., Burhans, W., 1996. Farm-specific approach to paratuberculosis (Johne's disease) control. The Veterinary clinics of North America. Food Animal Practice, 12(2), 383-415.

Rumsey, J., Valentine, J., Naser, S., 2006. Inhibition of phagosome maturation and survival of *Mycobacterium avium* subspecies *paratuberculosis* in polymorphonuclear leukocytes from Crohn's disease patients. Medical Science Monitor, 12(4), BR130-9.

Rybakin, V., Clemen, C., 2005. Coronin proteins as multifunctional regulators of the cytoskeleton and membrane trafficking. BioEssays, 27(6), 625-632.

Saeed, S., Ahmad, N., Ahmed, S., 2007. Dual inhibition of cyclooxygenase and lipoxygenase by human haptoglobin: its polymorphism and relation to hemoglobin binding. Biochemical and Biophysical Research Communications, 353(4), 915-920.

Salem, M., Heydel, C., El-Sayed, A., Ahmed, S., Zschöck, M., Baljer, G., 2013. *Mycobacterium avium* subspecies *paratuberculosis*: an insidious problem for the ruminant industry. Tropical Animal Health and Production, 45(2), 351-366.

Scaffidi, P., Misteli, T., Bianchi, M., 2002. Release of chromatin protein HMGB1 by necrotic cells triggers inflammation. Nature, 418(6894), 191-195.

Schiavoni, G., Mauri, C., Carlei, D., Belardelli, F., Pastoris, M., Proietti, E., 2004. Type I IFN protects permissive macrophages from Legionella pneumophila infection through an IFN-gamma-independent pathway. Journal of Immunology, 173(2), 1266-1275.

Schill, N.J., Hedman, A.C., Choi, S., Anderson, R.A., 2014. Isoform 5 of PIPKIγ regulates the endosomal trafficking and degradation of E-cadherin. Journal of Cell Science, 127(Pt 10), 2189-2203.

Schiopu, A., Cotoi, O.S., 2013. S100A8 and S100A9: DAMPs at the Crossroads between Innate Immunity, Traditional Risk Factors, and Cardiovascular Disease. Mediators of Inflammation, 2013, 828354.

Schmidt, C., Plate, A., Angele, B., Pfister, H., Wick, M., Koedel, U., Rupprecht, T., 2011. A prospective study on the role of CXCL13 in Lyme neuroborreliosis. Neurology, 76(12), 1051-1058.

Schulz, S., Köhler, G., Holscher, C., Iwakura, Y., Alber, G., 2008. IL-17A is produced by Th17, gammadelta T cells and other CD4-lymphocytes during infection with *Salmonella enterica* serovar Enteritidis and has a mild effect in bacterial clearance. International Immunology, 20(9), 1129-1138.

Seiler, P., Aichele, P., Bandermann, S., Hauser, A., Lu, B., Gerard, N., Gerard, C., Ehlers, S., Mollenkopf, H., Kaufmann, S., 2003. Early granuloma formation after aerosol *Mycobacterium tuberculosis* infection is regulated by neutrophils via CXCR3-signaling chemokines. European Journal of Immunology, 33(10), 2676-2686.

Seok, J., Warren, H.S., Cuenca, A.G., Mindrinos, M.N., Baker, H.V., Xu, W., Richards, D.R., McDonald-Smith, G.P., Gao, H., Hennessy, L., 2013. Genomic responses in mouse models poorly mimic human inflammatory diseases. Proceedings of the National Academy of Sciences of the United States of America, 110(9), 3507-3512.

Seth, M., Lamont, E.A., Janagama, H.K., Widdel, A., Vulchanova, L., Stabel, J.R., Waters, W.R., Palmer, M.V., Sreevatsan, S., 2009. Biomarker discovery in subclinical mycobacterial infections of cattle. PLoS ONE, 4(5), e5478.

Sevilla, I., Singh, S., Garrido, J., Aduriz, G., Rodríguez, S., Geijo, M., Whittington, R., Saunders, V., Whitlock, R., Juste, R., 2005. Molecular typing of *Mycobacterium avium* subspecies *paratuberculosis* strains from different hosts and regions. Revue Scientifique et Technique, 24(3), 1061-1066.

Sevilla, I.A., Garrido, J.M., Molina, E., Geijo, M.V., Elguezabal, N., Vázquez, P., Juste, R.A., 2014. Development and evaluation of a novel multicopy-element-targeting triplex PCR for detection of *Mycobacterium avium* subsp. *paratuberculosis* in feces. Applied and Environmental Microbiology, 80(12), 3757-3768.

Shin, M., Park, H., Shin, S.W., Jung, M., Lee, S.-H., Kim, D.-Y., Yoo, H.S., 2015a. Host transcriptional profiles and immunopathologic response following *Mycobacterium avium* subsp. *paratuberculosis* infection in mice. PLoS ONE, 10(10), e0138770.

Shin, M., Park, H., Shin, S., Jung, M., Im, Y., Park, H., Cho, Y., Yoo, H., 2015b. Whole-blood gene-expression profiles of cows infected with *Mycobacterium avium* subsp. *paratuberculosis* reveal changes in immune response and lipid metabolism. Journal of Microbiology and Biotechnology, 25(2), 255-67.

Shin, M., Shin, S., Jung, M., Park, H., Park, H., Yoo, H., 2015c. Host gene expression for *Mycobacterium avium* subsp. *paratuberculosis* infection in human THP-1 macrophages. Pathogens and Disease, 73(5), ftv031.

Shin, S.J., Chang, C.-F., Chang, C.-D., McDonough, S.P., Thompson, B., Yoo, H.S., Chang, Y.-F., 2005. In vitro cellular immune responses to recombinant antigens of *Mycobacterium avium* subsp. *paratuberculosis*. Infection and Immunity, 73(8),

5074-85.

Shin, S.J., Cho, D., Collins, M.T., 2008. Diagnosis of bovine paratuberculosis by a novel enzyme-linked immunosorbent assay based on early secreted antigens of *Mycobacterium avium* subsp. *paratuberculosis*. Clinical and Vaccine Immunology, 15(8), 1277-1281.

Shirmohammadi, K., Sohrabi, S., Samani, Z.J., Effatpanah, H., Yadegarazari, R., Saidijam, M., 2018. Evaluation of altered expression of miR-9 and miR-106a as an early diagnostic approach in gastric cancer. Journal of Gastrointestinal Oncology, 9(1), 46-51.

Sigurethardóttir, O., Valheim, M., Press, C., 2004. Establishment of *Mycobacterium avium* subsp. *paratuberculosis* infection in the intestine of ruminants. Advanced Drug Delivery Reviews, 56(6), 819-34.

Singh, S., Sohal, J., Singh, P., Singh, A., 2009. Genotype profiles of *Mycobacterium avium* subspecies *paratuberculosis* isolates recovered from animals, commercial milk, and human beings in North India. International Journal of Infectious Diseases, 13(5), e221-227.

Smith, A.M., Rahman, F.Z., Hayee, B.H., Graham, S.J., Marks, D.J., Sewell, G.W., Palmer, C.D., Wilde, J., Foxwell, B.M., Gloger, I.S., 2009. Disordered macrophage cytokine secretion underlies impaired acute inflammation and bacterial clearance in Crohn's disease. The Journal of Experimental Medicine, 206(9), 1883-1897.

Smith, S.G., Kleinnijenhuis, J., Netea, M.G., Dockrell, H.M., 2017. Whole blood profiling of bacillus calmette–guérin-induced trained innate immunity in infants identifies epidermal growth factor, IL-6, platelet-derived growth factor-ab/bb, and natural killer cell activation. Frontiers in Immunology, 8, 644.

Sobhkhez, M., Krasnov, A., Chang, C.J., Robertsen, B., 2017. Transcriptome analysis of plasmid-induced genes sheds light on the role of type I IFN as adjuvant in DNA vaccine against infectious salmon anemia virus. PLoS ONE, 12(11), e0188456.

Sockett, D., Carr, D., Collins, M., 1992a. Evaluation of conventional and radiometric fecal culture and a commercial DNA probe for diagnosis of *Mycobacterium paratuberculosis* infections in cattle. Canadian Journal of Veterinary Research, 56(2), 148-153.

Sockett, D., Conrad, T., Thomas, C., Collins, M., 1992b. Evaluation of four serological tests for bovine paratuberculosis. Journal of Clinical Microbiology, 30(5), 1134-1139.

Sonawane, G., Narnaware, S., Tripathi, B., 2016. Molecular epidemiology of *Mycobacterium avium* subspecies *paratuberculosis* in ruminants in different parts of India. International Journal of Mycobacteriology, 5(1), 59-65.

Speer, C., Scott, M.C., Bannantine, J.P., Waters, W.R., Mori, Y., Whitlock, R.H., Eda, S., 2006. A novel enzyme-linked immunosorbent assay for diagnosis of *Mycobacterium avium* subsp. *paratuberculosis* infections (Johne's Disease) in cattle. Clinical and Vaccine Immunology, 13(5), 535-540.

Stabel, J., 1998. Johne's disease: a hidden threat. Journal of Dairy Science, 81(1), 283-288.

Stabel, J., 2000. Transitions in immune responses to *Mycobacterium paratuberculosis*. Veterinary Microbiology, 77(3-4), 465-473.

Stabel, J., 2006. Host responses to *Mycobacterium avium* subsp. *paratuberculosis*: a complex arsenal. Animal Health Research Reviews, 7(1-2), 61-70.

Stabel, J., 2008. Pasteurization of colostrum reduces the incidence of paratuberculosis in neonatal dairy calves. Journal of Dairy Science, 91(9), 3600-3606.

Stabel, J., Palmer, M., Harris, B., Plattner, B., Hostetter, J., Robbe-Austerman, S., 2009.

Pathogenesis of *Mycobacterium avium* subsp. *paratuberculosis* in neonatal calves after oral or intraperitoneal experimental infection. Veterinary Microbiology, 136(3-4), 306-313.

Stabel, J., Robbe-Austerman, S., 2011. Early immune markers associated with *Mycobacterium avium* subsp. *paratuberculosis* Infection in a neonatal calf model. Clinical and Vaccine Immunology, 18(3), 393-405.

Stanescu, I., Calenic, B., Dima, A., Gugoasa, L., Balanescu, E., van Staden, R., Baicus, C., Badita, D., Greabu, M., 2018. Salivary biomarkers of inflammation in systemic lupus erythematosus. Annals of Anatomy, S0940-9602(18), 30034-30037.

Stephen-Victor, E., Fickenscher, H., Bayry, J., 2016. IL-26: An emerging proinflammatory member of the IL-10 cytokine family with multifaceted actions in antiviral, antimicrobial, and autoimmune responses. PLoS Pathogens, 12(6), e1005624.

Strimbu, K., Tavel, J.A., 2010. What are biomarkers? Current Opinion in HIV and AIDS, 5(6), 463–466.

Sweeney, R., 1996. Transmission of paratuberculosis. The Veterinary clinics of North America. Food Animal Practice, 12(2), 305-312.

Sweeney, R., 2011. Pathogenesis of paratuberculosis. The Veterinary clinics of North America. Food Animal Practice, 27(3), 537-546.

Sweeney, R., Uzonna, J., Whitlock, R., Habecker, P., Chilton, P., Scott, P., 2006. Tissue predilection sites and effect of dose on *Mycobacterium avium* subsp. *paratuberculosis* organism recovery in a short-term bovine experimental oral infection model. Research in Veterinary Science, 80(3), 253-259.

Tengvall, S., Che, K., Lindén, A., 2016. Interleukin-26: An emerging player in host defense and inflammation. Journal of Innate Immunity, 8(1), 15-22.

Terness, P., Bauer, T.M., Röse, L., Dufter, C., Watzlik, A., Simon, H., Opelz, G., 2002. Inhibition of allogeneic T cell proliferation by indoleamine 2, 3-dioxygenase–expressing dendritic cells: mediation of suppression by tryptophan metabolites. The Journal of Experimental Medicine, 196(4), 447-457.

Thompson, B., Clark, R., Mackintosh, C., 2007. Intra-uterine transmission of *Mycobacterium avium* subsp *paratuberculosis* in subclinically affected red deer (Cervus elaphus). New Zealand Veterinary Journal, 55(6), 308-13.

Timms, V., Mitchell, H., Neilan, B., 2015. Optimisation of DNA extraction and validation of PCR assays to detect *Mycobacterium avium* subsp. *paratuberculosis*. Journal of Microbiological Methods, 112, 99-103.

Timms, V.J., Daskalopoulos, G., Mitchell, H.M., Neilan, B.A., 2016. The association of *Mycobacterium avium* subsp. *paratuberculosis* with inflammatory bowel disease. PLoS ONE, 11(2), e0148731.

Tiwari, A., VanLeeuwen, J.A., McKenna, S.L., Keefe, G.P., Barkema, H.W., 2006. Johne's disease in Canada: part I: clinical symptoms, pathophysiology, diagnosis, and prevalence in dairy herds. The Canadian Veterinary Journal, 47(9), 874-882.

Torrado, E., Cooper, A.M., 2010. IL-17 and Th17 cells in tuberculosis. Cytokine & Growth Factor Reviews, 21(6), 455-462.

Tsuyoshi, H., Yoshida, Y., 2018. Molecular biomarkers for uterine leiomyosarcoma and endometrial stromal sarcoma. Cancer Science, 109(6), 1743-1752.

Umemura, M., Yahagi, A., Hamada, S., Begum, M., Watanabe, H., Kawakami, K., Suda, T., Sudo, K., Nakae, S., Iwakura, Y., 2007. IL-17-mediated regulation of innate and acquired immune response against pulmonary *Mycobacterium bovis* bacille Calmette-Guerin infection. Journal of Immunology, 178(6), 3786-3796.

Unver, N., McAllister, F., 2018. IL-6 family cytokines: key inflammatory mediators as biomarkers and potential therapeutic targets. Cytokine & Growth Factor Reviews, 41, 10-17

Uribe-Querol, E., Rosales, C., 2017. Control of phagocytosis by microbial pathogens. Frontiers in Immunology, 8, 1368.

Valenti, P., Antonini, G., 2005. Lactoferrin: an important host defence against microbial and viral attack. Cellular and Molecular Life Science, 62, 2576-2587.

Vanuytsel, T., Vermeire, S., Cleynen, I., 2013. The role of Haptoglobin and its related protein, Zonulin, in inflammatory bowel disease. Tissue Barriers, 1(5), e27321.

Verschoor, C., Pant, S., You, Q., Kelton, D., Karrow, N., 2010. Gene expression profiling of PBMCs from Holstein and Jersey cows sub-clinically infected with *Mycobacterium avium* subsp. *paratuberculosis*. Veterinary Immunology and Immunopathology, 137(1-2), 1-11.

Vogl, T., Ludwig, S., Goebeler, M., Strey, A., Thorey, I., Reichelt, R., Foell, D., Gerke, V., Manitz, M., Nacken, W., 2004. MRP8 and MRP14 control microtubule reorganization during transendothelial migration of phagocytes. Blood, 104(13), 4260-4268.

Vogl, T., Tenbrock, K., Ludwig, S., Leukert, N., Ehrhardt, C., van Zoelen, M., Nacken, W., Foell, D., van der Poll, T., Sorg, C., 2007. Mrp8 and Mrp14 are endogenous activators of Toll-like receptor 4, promoting lethal, endotoxin-induced shock. Nature Medicine, 13(9), 1042-9.

Vrieling, M., Santema, W., Vordermeier, M., Rutten, V., Koets, A., 2013. Hsp70 vaccination-induced primary immune responses in efferent lymph of the draining lymph node. Vaccine, 31(42), 4720-4727.

Walker, S.J., Beavers, D.P., Fortunato, J., Krigsman, A., 2016. A putative blood-based biomarker for autism spectrum disorder-associated ileocolitis. Scientific Reports, 6, 35820.

Walzl, G., Ronacher, K., Hanekom, W., Scriba, T., Zumla, A., 2011. Immunological biomarkers of tuberculosis. Nature Reviews. Immunology, 11(5), 343-354.

Wang, J., Moolji, J., Dufort, A., Staffa, A., Domenech, P., Reed, M., Behr, M., 2015. Iron acquisition in *Mycobacterium avium* subsp. *paratuberculosis*. Journal of Bacteriology, 198(5), 857-866.

Wang, X., Wang, H., Shu, Y., Momotani, Y., Nagata, R., Mori, Y., Momotani, E., 2011. Decreased expression of matrix metalloproteinase-9 and increased expression of tissue inhibitors of matrix metalloproteinase-1 in paratuberculosis-infected cattle in the ELISA-negative subclinical stage. Animal Biotechnology, 22(1), 44-49.

Wang, Z., Gerstein, M., Snyder, M., 2009. RNA-Seq: a revolutionary tool for transcriptomics. Nature Reviews Genetics, 10(1), 57-63.

Wang, Z., Zhao, Q., Han, Y., Zhang, D., Zhang, L., Luo, D., 2013. PAI-1 and IFN-γ in the regulation of innate immune homeostasis during sublethal yersiniosis. Blood cells, Molecules & Diseases, 50(3), 196-201.

Waters, W.R., Maggioli, M.F., Palmer, M.V., Thacker, T.C., McGill, J.L., Vordermeier, H.M., Berney-Meyer, L., Jacobs Jr, W.R., Larsen, M.H., 2016. Interleukin-17A as a biomarker for bovine tuberculosis. Clinical and Vaccine Immunology, 23(2), 168-180.

Weiss, D.J., Evanson, O.A., Moritz, A., Deng, M.Q., Abrahamsen, M.S., 2002. Differential responses of bovine macrophages to *Mycobacterium avium* subsp. *paratuberculosis* and *Mycobacterium avium* subsp. *avium*. Infection and Immunity, 70(10), 5556-

5561.

Wells, S.J., Collins, M.T., Faaberg, K.S., Wees, C., Tavornpanich, S., Petrini, K.R., Collins, J.E., Cernicchiaro, N., Whitlock, R.H., 2006. Evaluation of a rapid fecal PCR test for detection of *Mycobacterium avium* subsp. *paratuberculosis* in dairy cattle. Clinical and Vaccine Immunology, 13(10), 1125-1130.

Whitlock, R., Buergelt, C., 1996. Preclinical and clinical manifestations of paratuberculosis (including pathology). The Veterinary clinics of North America. Food Animal Practice, 12(2), 345-356.

Whittington, R.J., Whittington, A.-M., Waldron, A., Begg, D.J., de Silva, K., Purdie, A.C., Plain, K.M., 2013. Development and validation of a liquid medium (M7H9C) for routine culture of *Mycobacterium avium* subsp. *paratuberculosis* to replace modified bactec 12B medium. Journal of Clinical Microbiology, 51(12), 3993-4000.

Wolf, R., Clement, F., Barkema, H., Orsel, K., 2014. Economic evaluation of participation in a voluntary Johne's disease prevention and control program from a farmer's perspective--The Alberta Johne's Disease Initiative. Journal of Dairy Science, 97(5), 2822-2834.

Wong, D., Bach, H., Sun, J., Hmama, Z., Av-Gay, Y., 2011. *Mycobacterium tuberculosis* protein tyrosine phosphatase (PtpA) excludes host vacuolar-H+–ATPase to inhibit phagosome acidification. Proceedings of the National Academy of Sciences of the United States of America, 108(48), 19371-19376.

Xu, W., Wang, P., Petri, B., Zhang, Y., Tang, W., Sun, L., Kress, H., Mann, T., Shi, Y., Kubes, P., 2010. Integrin-induced PIP5K1C kinase polarization regulates neutrophil polarization, directionality, and in vivo infiltration. Immunity, 33(3), 340-350.

Yan, L., Deng, Y., Zhou, J., Zhao, H., Wang, G., Group, C.H.-R.F.A.R., 2018. Serum YKL-

40 as a biomarker for liver fibrosis in chronic hepatitis B patients with normal and mildly elevated ALT. Infection, 46(3), 385-393.

Yang, M.X., Coates, R.F., Ambaye, A., Cortright, V., Mitchell, J.M., Buskey, A.M., Zubarik, R., Liu, J.G., Ades, S., Barry, M.M., 2018. NKX2. 2, PDX-1 and CDX-2 as potential biomarkers to differentiate well-differentiated neuroendocrine tumors. Biomarker Research 6, 15.

Yokomizo, Y., Merkal, R., Lyle, P., 1983. Enzyme-linked immunosorbent assay for detection of bovine immunoglobulin G1 antibody to a protoplasmic antigen of *Mycobacterium paratuberculosis*. American Journal of Veterinary Research, 44(11), 2205-2207.

You, Q., Verschoor, C., Pant, S., Macri, J., Kirby, G., Karrow, N., 2012. Proteomic analysis of plasma from Holstein cows testing positive for *Mycobacterium avium* subsp. *paratuberculosis* (MAP). Veterinary Immunology and Immunopathology, 148(3-4), 243-251.

Zhang, M., Zhang, S., 2011. An efficient DNA extraction method for polymerase chain reaction-based detection of *Mycobacterium avium* subspecies *paratuberculosis* in bovine fecal samples. Journal of Veterinary Diagnostic Investigation, 23(1), 41-48.

Zhao, G., Jiang, D., Li, H., 2015. Interferon regulatory factors: at the crossroads of immunity, metabolism, and disease. Biochimica et Biophysica Acta, 1852(2), 365-378.

Zhong, L., Taylor, D., Begg, D., Whittington, R., 2011. Biomarker discovery for ovine paratuberculosis (Johne's disease) by proteomic serum profiling. Comparative Immunology, Microbiology and Infectious Diseases, 34(4), 315-326.

국문초록

Mycobacterium avium subspecies *paratuberculosis*에 의한 소의 준임상형 감염 단계에서의 숙주 유전자 발현 분석을 통한 진단용 생물학적 표지자의 규명

박 현 의

(지도교수: 유한상, D.V.M., Ph.D.)

서울대학교 대학원
수의학과 병인생물학및예방수의학 전공

요네병은 *Mycobacterium avium* subsp. *paratuberculosis* (MAP)에 의해 야기되는 반추 동물의 만성 소모 질환이다. 요네병은 전세계 낙농 산업에 심각한 경제적 손실을 초래하며 주로 분변에 오염된 사료, 물, 우유와 같은 물질의 섭취를 통해 감염된다. 감염이 일어난 이후, 초기 단계에서 동물은 임상 증상을 나타내지 않으나 분변을 통해 요네병균을 체외로 배출하여 환경을 오염시키고 요네병 전파의 근원이 된다. 따라서 질병을 근절하기 위해 감염된 동물을 감염 초기에 진단하여 제거하는 것이 질병

의 근절에 매우 중요하다고 할 수 있다. 그러나 분변 내의 균을 검출하는 PCR이나 배양법, 혈청 내의 요네병균에 특이적인 항체를 검출하는 ELISA 등과 같은 현재의 진단 방법은 임상증상을 나타내지 않는 준임상형 개체의 진단에 적합하지 못하다. 따라서 준임상형 개체를 탐지할 수 있는 진단 기법이 필요한 실정이다.

본 연구에서는 먼저 요네병에 감염된 소의 전혈에서의 유전자 발현 양상을 분석하여 바이오마커 후보들을 평가하였다. 준임상 소의 집단에서 다음 6개의 유전자(*LTF, HGF, HP, CXCR3, GBP6*, 및 *TFRC*)의 발현이 유의적으로 증가하였으며, 이들 유전자는 준임상형 단계에서 요네병균의 병인기전과 관련이 있는 것으로 생각되며, 준임상형 소를 진단하기 위한 바이오마커로 사용될 수 있을 것으로 여겨진다.

둘째로 본 연구에서는 준임상형 소의 전혈 내에서 면역 조절 관련 기능을 가진 유전자들의 발현을 분석하였다. *IL-17A, IL-17F, IL-22, IL-26, HMGB1* 및 *IRF4* 유전자들의 발현의 감소 및 PIP5K1C의 발현의 증가는 Th1 반응의 억제를 유도하는 것으로 생각된다. 또한, *IRF5* 및 *IRF7* 유전자의 발현 증가는 준임상형 단계에서 인터페론 알파/베타 신호체계의 활성화를 암시하며, 이는 indoleamine 2,3-dioxygenase에 의한 트립토판 대사의 감소를 유도하여 T cell의 증식을 억제하는 것으로 여겨진다. *CORO1A* 유전자의 증가 된 발현은 칼슘 신호 전달의 조절

을 통하여 MAP의 숙주 내에서의 생존을 강화시킬 것으로 생각된다. 종합해보면, MAP 감염에 의해 유도된 면역조절 관련 유전자 발현이 준임상형 단계에서 MAP의 생존을 증가 시킨다는 것으로 예상된다.

세번째로 8종류의 숙주 바이오마커 (*HP, TIMP1, MMP9, SERPINE1, TFRC, S100A8, DEFB1, DEFB10*)를 이용하여 준임상형 소를 진단하기 위한 Real-time PCR 기법을 개발하였다. 이들 8종의 바이오마커는 준임상형 개체의 진단에 좋은 정확도 (AUC≥0.7)를 보였다. 또한 그 중 4종의 유전자 (*TIMP1, S100A8, DEFB1, DEFB10*)는 80 % 이상의 민감도와 90 % 이상의 특이도를 보였다.

결론적으로 이러한 결과들은 바이오마커 기반의 진단기법을 통해 요네병 준임상형 개체를 진단할 수 있는 가능성을 보여주었다. 그러므로 본 연구 결과는 현재 사용되고 있는 진단법을 대체할 만한 바이오마커 기반의 진단법의 개발에 공헌할 것으로 생각된다.

핵심어: 요네병 원인균, 바이오마커, 준임상형, 진단